THREE DIMENSIONAL MICROFABRICATION AND MICROMOULDING

THIAN CHEN HAI STANLEY

NATIONAL UNIVERSITY OF SINGAPORE

2008

THREE DIMENSIONAL MICROFABRICATION AND MICROMOULDING

THIAN CHEN HAI STANLEY
(B.Eng.), NUS

A THESIS SUBMITTED

FOR THE DEGREE OF MASTER OF ENGINEERING

DEPARTMENT OF MECHANICAL ENGINEERING

NATIONAL UNIVERSITY OF SINGAPORE

Acknowledgements

"Oh give thanks unto the God; for he is good; for his mercy endureth for ever. I love the LORD, because he hath heard my voice and my supplications (Ps.136:1, 116:1)"

The author would like to express his heartfelt gratitude and appreciation to the following people for their guidance and advice throughout the course of this project:

- Prof Jerry Fuh, Supervisor, National University of Singapore, Department of Mechanical Engineering, Division of Manufacturing, for his continuous support throughout these years.

- Assoc. Prof Loh Han Tong, Co-supervisor, National University of Singapore, Department of Mechanical Engineering, Division of Manufacturing, for his guidance and advice.

- Prof Wong Yoke San, National University of Singapore, Department of Mechanical Engineering, Division of Manufacturing, for his contributions and suggestions during meetings.

- Dr Tang Yaxin, for his guidance and advice throughout my master course work.

Not to leave out the followings staffs from Advanced Manufacturing Lab (AML) and Work Shop 2 (WS2):

- Mr. Tan Choon Huat, lab tech, from AML, for his technical and ordering assistance.

- Mr. Nelson Yeo, lab tech, from AML, for his fast response for machining of my substrates.

- Mr Lim Soon Cheong, lab tech, from AML, for his fast response for machining many small components on short notice.

- Mr Ho Yan Chee, lab tech, from AML, for his advice in ordering and help in machining.

- Mr Lee Chiang Soon, lab tech, from WS2, for machining many of the components involved in this research work.

Table of Contents

Summary

Many microdevices such as MEMS, pressure sensors, accelerometers, gyroscopes, micromechanical sensors and actuators have been fabricated by conventional micromachining techniques such as surfacing / bulk machining, lithography, electro-discharge machining and etching etc. Although more complex micron-scale structures needed in MEMS can be fabricated by LIGA and wafer bondings, these techniques, however, are not capable of making complex 3D micron-scale structures (e.g. photonic crystals) as they utilize sequential planar process. In addition, they are also not able to produce high aspect ratio objects, and are also very tedious. This is a shortcoming as many applications in precision engineering and electronic devices require high aspect ratio structures.

Lithography is a standard silicon based technique used in the semiconductor industry for fabricating IC chips (ICs) and printed circuit boards (PCBs). The complexity of these subtractive techniques can be described by their photomask count. i.e. the more complex, the more the number of photomask needed.

In this research work, a novel process based on Rapid Prototyping (RP) principles of layer-by-layer, for fabricating three-dimensional micron-scale structures with micromoulds via vacuum casting / electro-deposition processes was performed. The process consists of photomask (pattern) preparation and excimer (UV) laser lithography, and vacuum casting / electro-deposition. With the ultra-fine material solidification capability of the excimer (UV) laser and the high replicating accuracy of vacuum casting,

3D micron-scale structures have been fabricated. Using NOA 60 and SL5510 photopolymer as well as SU8 photoresists, a 3-layered 500 μm diameter micron-scale structure was fabricated, thereby demonstrating that this technique has the potential of fabricating complex 3D micron-scale structures.

Instead of using typical silicon wafer as substrate, metal brass substrates machined to a nano surface finishing by diamond turning machine were employed. Together with pulse electro-deposition in nickel solution, a nickel micromould was fabricated. This technique helps to eliminate the time and money needed to deposit seed layer on a typical silicon substrate in order for electro-deposition to take place.

Another technique, using vacuum casting with silicone rubber in the micromould fabrication, can produce the micromoulds in a single step by doing away with the fabrication of the mould insert, thus giving a competitive advantage over many existing techniques.

A total of ten silicone rubber micromoulds were also fabricated and evaluated for its repeatability. The small deviation among the ten micromoulds themselves, as well as small deviation from the master pattern, demonstrated that this technique is suitable for mass productions.

List of Tables

List of Figures

List of Symbols

µCP	Micro Contact Printing
µTM	Micro transfer molding
3D	Three-dimensional
CAD	Computer aided design
CCD	Charge coupled device
DARPA	Defense Advanced Research Projects Agency
DMD	Digital mirror devices
DRIE	Deep reactive ion etching
EBM	Electron Beam Melting
EFAB	Electrochemical fabrication
fs	Femtoseconds, 10^{-15}
HCL	Hydrochloric acid
ICs	Integrated circuits
IPA	Isopropyl Alcohol
IR	Infrared
KrF	krypton fluorine
LASIK	Laser in *s*itu *K*eratomileusis
LCD	Liquid crystal display
LED	Light emitting diode
LIGA	Lithographie Galvanoformung Abformung
LZH	Laser Zentrum Hannover e.V.
MEMS	Micro-Electro-Mechanical-System
MIMIC	Micromolding in capillaries
MW	Mega watts
Nd:YAG	Neodymium-doped yttrium aluminum garnet
NOA	Norland Optical Adhesive
ns	Nanoseconds, 10^{-9}
PCB	Printed circuit board
PDMS	Poly(dimethylsiloxane)
PEB	Post exposure bake
PIM	Powder injection moulding
REM	Replica molding
RIE	Reactive ion etching
RM	Rapid manufacturing
RP	Rapid prototyping
SAMIM	Solvent-assisted micromolding
SB	Soft bake or prebake
SEM	Scanning Electron Microscope
SF_6	Sulphur hexafluoride
SFF	Solid free form fabrication
SLM	Spatial Light Modulator

SLM	Selective Laser Melting
SLS	Selective laser sintering
TFTs	Tin film transistors
Ti	Titanium
TPA	Two photon absorption
USC	University of Southern California
UV	Ultra violet
WLI	White light interferometer
μSLA	Microstereolithography
µm	Micrometers
µWEDM	Micro wire electric discharge machining

1. INTRODUCTION

1.1 Background

Microfabrication processes have been widely used for producing miniature components such as pressure sensors, accelerometers and micro-structured orifices for ink-jet printing and fuel injection applications. Such technologies originate from the microelectronics industry, and the devices are commonly made on silicon substrates (wafers) even though glass, plastic and many other substrates are becoming more widespread. Microfabricated devices include integrated circuits (ICs), microsensors (e.g. air bag sensors), inkjet nozzles and flat panel displays, etc.

The miniaturisation of devices is gaining importance especially with the growing demands of rapidly advancing technologies such as medical technology, biotechnology, microelectronics and drive technology. Minimisation through microfabrication is necessary as it not only improves performance, increases integration of Micro-Electro-Mechanical-System (MEMS) devices, but more importantly, it reduces per unit cost with volume manufacturing.

Microfabrication of such micro-components is actually a collection of technologies which are utilised in making microdevices. Some of them, like lithography or etching, have very old origins that were not connected to manufacturing. Polishing was borrowed from optics manufacturing, and many of the vacuum techniques come from 19th century

research in physics. Electroplating is also a 19th century technique adapted to produce micrometer scale structures, as are various stamping and embossing methods.

To fabricate a microdevice, often many processes must be performed, one after another, with repeated steps. Typically, in the fabrication of a memory chip, there are approximately 30 lithography steps, 10 oxidation steps, 20 etching steps, 10 doping steps, and many additional sub-processes.

Established microfabrication methods such as lithography and surface / bulk micromaching commonly used in MEMS, use *subtractive* methods to create micron-scale structures. Over the past decade, new manufacturing technologies that build parts on a layer-by-layer basis have emerged. These time-saving technologies are known as rapid prototyping (RP) [1]. This term simply suggests 'speedy fabrication' of sample parts for demonstration, evaluation or testing. These consist of numerous manufacturing processes by which a solid physical model of a part is fabricated from a three-dimensional (3D) computer aided design (CAD) data part file. Materials such as liquid resins or powders are cured or sintered using laser to build the part required. Examples of typical applications include micro pump propellers and micro valves [2]. The term RP is interchangeable with the term 'solid free form fabrication' (SFF).

Unlike conventional machining which uses subtractive methods, RP, is an *additive* process of building up 3D structures by adding material layer-by-layer. RP is widely used for part fabrication in the macro (or normal) scale. This report introduces a

microfabrication technique using the RP principle, where layered manufacturing is combined with mask-based microlithography, a method usually used in the semiconductor industry. As there is a need to explore more novel methods to achieve structures of micron to sub-micron dimensions to remain competitive, therefore, integrating lithography to the RP concept is one area worth exploring.

Due to the increasing demands of advancing microtechnology, the RP process has also recently branched into microfabrication. The most successful RP process is the microstereolithography (μSLA), invented by Professor Ikuta in 1993 [2]. Another successful RP-like process is the two photon absorption (TPA) microlithography which was first developed by Maruo [3].

Laymen treat any object (cube, box, container etc) with length, width, and breadth as 3-dimensional. However, in the eyes of RP, object such as a cube, is only considered as 2.5D. 2.5D refers to the projection of a planar surface into the third dimension – thereby creating an object that is 3-dimensional.

A true complex 3D microfabricated object should be freely manipulated, i.e. can be fabricated without any necessary attachments to substrates. An example of a real 3D object can be seen in Fig.1.1. Real 3D micron-scale structures have huge application in the area of photonics such as waveguides.

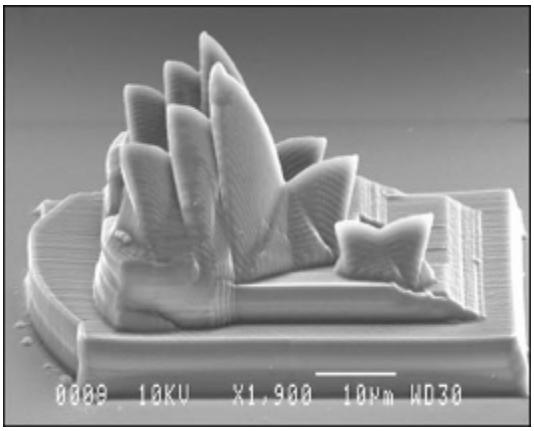

Fig. 1.1: SEM image of microscale model of Sydney opera house [4]

It is difficult for many of the existing microfabrication techniques to create real complex 3D micron-scale structures (See Fig.1.2) and even if they can, the required numbers of processing steps will be numerous.

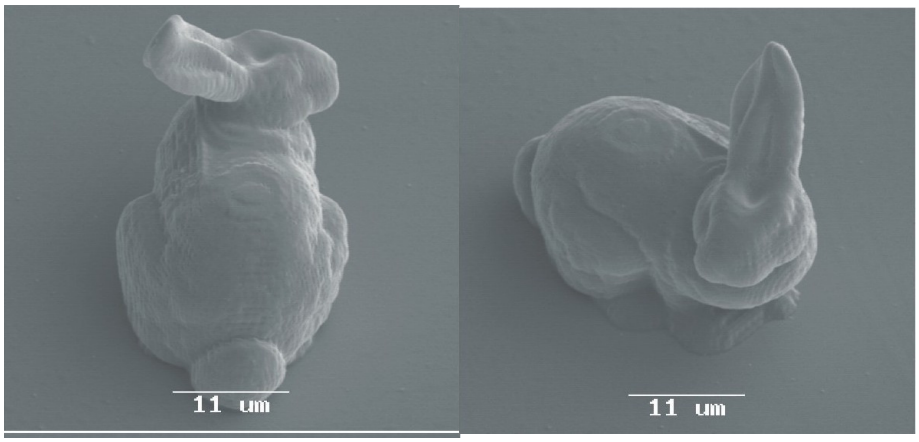

Fig. 1.2: SEM image of Micro-bunny [5]

1.2 Objectives

This research project aims to develop a novel process for fabricating 3D micrometer scale parts using the layered manufacturing mechanism similar to those used in RP technologies. The objective of this research work is to:

- develop a novel method to fabricate complex 3D micron-scale structures and
- develop an alternative moulding method that is simple to implement, has fewer processing steps, and reduces cost and lead time compared to existing moulding methods

1.3 Organisation

Chapter 1 covers the background information of 3D microfabrication as well as the objectives of this research study. Chapter 2 will cover the literature review of existing 3D fabrication methods and the SU8 photoresists, while Chapter 3 will describe the experimental setup and procedure. Chapter 4 will discuss the outcome of the lithography experiments and micromoulds fabrication which will be followed by conclusions and recommendations in Chapter 5 and 6 respectively. A list of papers published from this research work will also be reported.

2. LITERATURE REVIEW

2.1 Introduction to 3D Microfabrication Methods

The 3D microfabrication technique is broadly classified into 2 categories: direct and indirect methods. The following sections below will briefly describe the reported 3D microfabrication methods and the SU8 photoresist used in many microfabrication techniques.

2.2 Direct 3D Microfabrication Methods

The direct method system consists of an automated translation stage which moves a pattern generation device such as ink jet head or laser writing optics [6]. The term 'direct-write' describes fabrication methods that employ a computer-controlled translation stage, which moves a pattern-generating device, e.g. ink deposition nozzle or laser writing optics, to create materials with controlled architecture and composition [7]. Several direct-writing techniques capable of patterning materials in 3D will be mentioned in the following sections.

2.2.1 Lithography

Lithography (also known as photolithography), is one of the most established processes used in microfabrication to selectively remove parts of a thin film or the bulk of a substrate. The process begins with using an UV lamp (which was later advanced to UV laser) to transfer a geometric pattern through a photomask to a light sensitive chemical (photoresists) that is spin-coated on the substrate. The substrate is usually silicon wafer, to make integrated chips or copper coated board for printed circuit board (PCBs) in the semi-conductor industries. Lithography is used because it affords precise control over the shape and size of the objects it creates, and can create patterns over an entire surface simultaneously. It is a very established process but the main disadvantage, is that it requires clean room conditions and a very flat substrate to start with, which can very expensive to build, depending on the class type of the clean room.

2.2.2 Laser

Using laser instead of UV lamp (in the early lithography) as the energy source to expose various materials such as photopolymer, powders and photoresists, those materials that are compatible with the wavelength of the selected laser will be polymerized (for photopolymer and photoresists) or sintered (for powders). Two RP techniques, selective laser sintering (SLS) and sterolithography (SLA), use lasers as their energy source. The main difference between them is the wavelength of the laser and their material type, i.e. SLS uses metal and thermoplastic powder while SLA uses liquid photopolymer. SLA is the most accurate process among the RP techniques and it is the only RP technique that

has been extended to micron-scale fabrication. A new method of using UV LED (light emitting diode) lamp to replace UV laser in SLA was first attempted by Loose, K., Nakagawa, T. and Niino, T. [8]. The advantage is that this process costs much less as compared to the UV laser, since no maintenance is needed for UV LED lamp. However, the resolutions would not be as fine as the laser and the diversion of the LED is not as narrow as laser.

2.2.2.1 Micro Sterolithography (μSLA)

Many μSLA use UV light together with liquid crystal display (LCD) or Spatial Light Modulator (SLM) Technology (Fig.2.1a) as a dynamic mask generator to generate the cross section of each layer. The advantages of this method is that complex shapes (Fig. 2b) can be built and the time to build one layer is the same regardless of what the pattern may be, but the resolution is limited by the pixel of the LCD. Furthermore, only a certain range of UV is suitable for this method due to the limitation of the LCD [9].

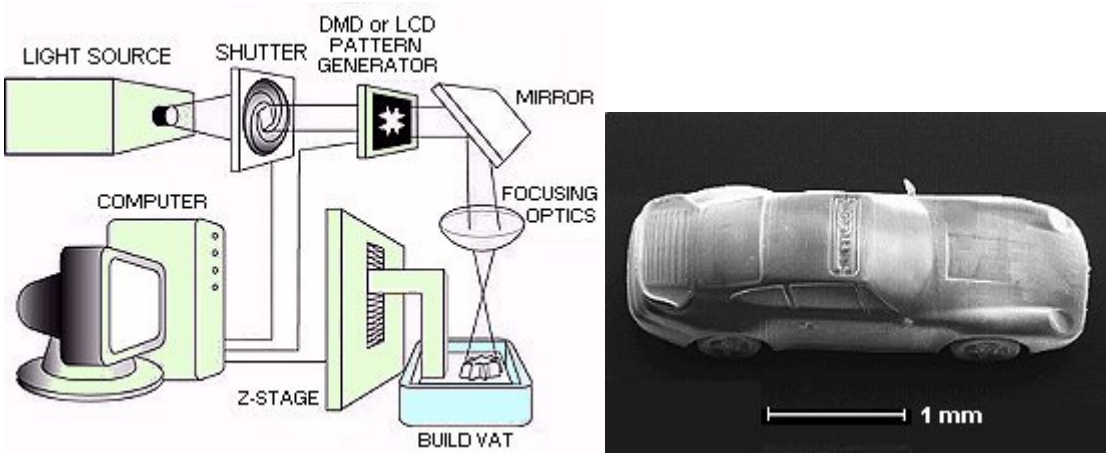

Fig. 2.1: a) Schematic diagram of the μSLA using dynamic mask generator b) micro car

Central Microstructure Facility uses digital mirror devices (DMD) to control the laser beam [10]. In this technique (See Fig. 2.2), uniform UV light is modulated by switching individual micromirrors, where a reduction lens reflects a pattern which is then projected onto the surface of the UV photopolymer. The cost of this DMD is high and the control of it is much more complicated since there are thousands of individual small mirrors in the DMD.

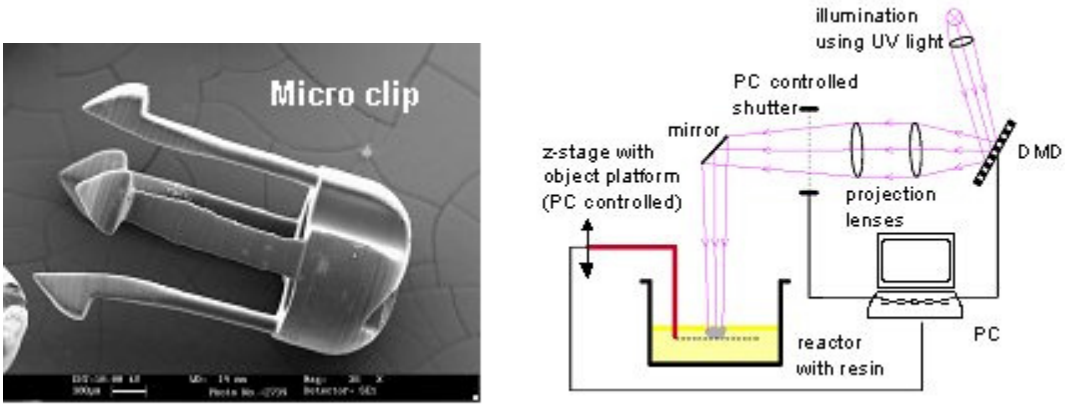

Fig. 2.2: Micro clip fabricated by this μSLA using DMD

This process is greatly dependent on the properties of the materials and many efforts have been made on the material research to suit the wavelength of the energy source as well as the required properties of the material. One such example is the ceramic teapot (Fig. 2.3) fabricated by μSLA [11].

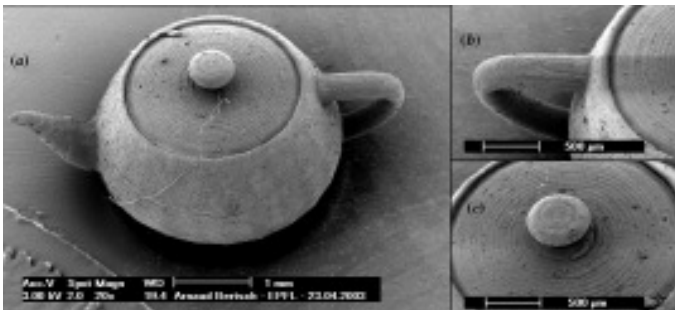

Fig. 2.3: Micro ceramic components [11]

A high-resolution prototype machine (Fig.2.4) that allows the production of microparts in small and medium-sized series was developed at the Laser Zentrum Hannover e.V. (LZH). Their machine (Fig. 2.4) is capable of building a movable micromechanic [12], as shown in Fig. 2.5 below.

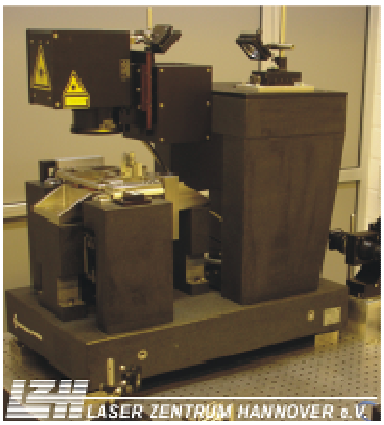

Fig. 2.4: Prototype µSLA by LZH

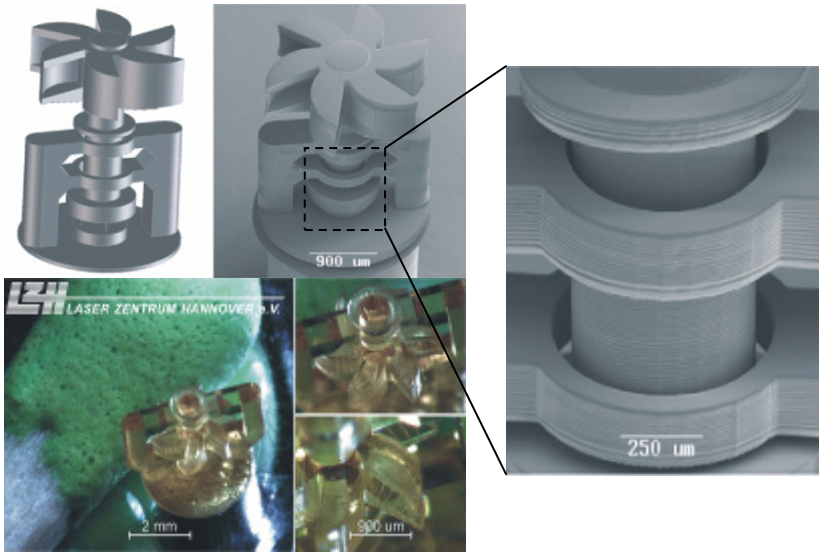

Fig. 2.5: Movable micromechanic manufactured by LZH [12]

A good compilation of information on µSLA can be found in [2].

2.2.3 Electron Beam

Electron beam melting (EBM) uses electron beam as the energy source to melt metal powder in a layer-by-layer process.

In this technique, a vacuum environment is required in the EBM machine to maintain the chemical composition of the material and to provide an excellent environment for building parts with reactive materials such as titanium alloys.

The high power of the electron beam ensures a high rate of deposition and an even temperature distribution within the part, which gives excellent mechanical and physical properties.

Since this technique can fabricate titanium alloys, it is being used for the rapid manufacturing (RM) of medical implants and a range of products for the Aerospace and Automotive industries [13]. Another related RP recently developed that can fabricate titanium and chromium-cobalt is Selective Laser Melting (SLM) but it uses laser instead of electron beam [14].

2.2.4 Proton Beam

Protons are more massive than electrons and therefore have deeper penetrations in materials while maintaining a straight path. This enables proton beam writing to fabricate 3D, high aspect ratio structures with vertical, smooth sidewalls and low line-edge roughness. By using suitable energy of proton beam for direct writing, micro stonehenge

on SU8 photoresist (Fig.2.6a) and silicon (Fig. 2.6b), can be achieved. Many published journals papers and details of using proton beam by NUS Physics Department can be found in [15]. The diameter of the stonehenge pillar is 80 µm.

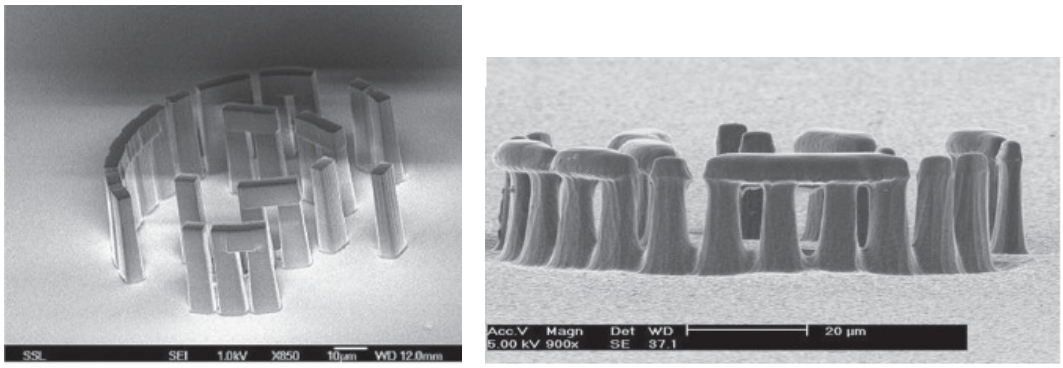

Fig. 2.6: Microstructure by proton beam a) SU8 photoresist b) silicon

No other energy source can fabricate 3D micron-scale structure in silicon. However, generating a proton beam requires a synchrotron, (Fig. 2.7) which is very costly to build and maintain. The control of the proton beam is also much more difficult when compared to laser. This technique was reported in [16].

Fig. 2.7: Schematic layout of a synchrotron source

This break through technique was reported in [16]

2.2.5 Ink Writing Techniques

Ink writing techniques rely on the deposition of materials (colloid-, nanoparticle-, or organic-based inks) to create structures layer-by-layer and can be divided into two approaches; droplet-based (Fig.2.8a) or continuous (filamentary) inks (Fig. 2.8b). The material requirement of this technique is usually a low viscosity fluid (otherwise a high force will be needed) that must be removed by absorption and evaporation or wax-based inks that are heated during droplet formation and then solidified upon impact cooling.

The fluid dynamics involved in drop formation, wetting, and spreading play a vital, but also limiting, role in defining the surface roughness and minimum size of the features deposited by ink-jet printing. This technique is not suitable to build structures that need support structures and the mechanical properties of the built artifacts are not as good due to the nature of the material used.

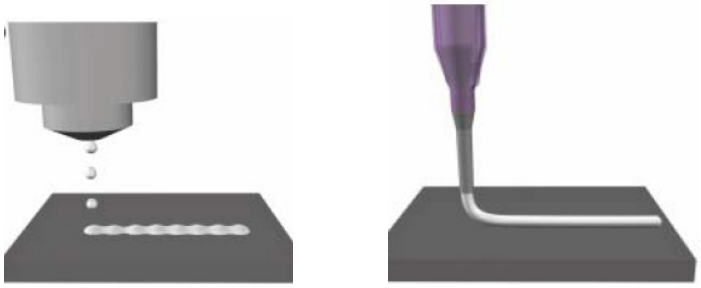

Fig. 2.8: Ink writing techniques a) demand based b) continuous

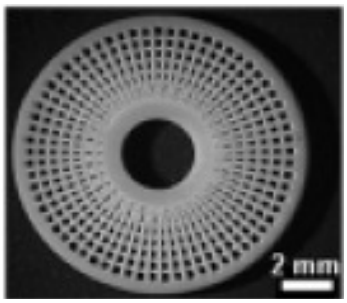

Fig. 2.9: Optical image of 3D radial array assembled by robotic deposition

However, robotic deposition techniques offer new opportunities for 3D patterning of materials at finer length scales. Inks are extruded through a fine cylindrical nozzle to create a filamentary element that is patterned layer-by-layer. By controlling the ink rheology, 3D structures that consist of continuous solids and high aspect ratio e.g. parallel walls or spanning features can be constructed. Fig. 2.9 above is an example build by this technique. [7]. More information on ink jet printing of different materials can be found in [7] and [17].

2.2.6 Two Photon Absorption (TPA)

TPA is the simultaneous absorption of two photons of identical or different frequencies in order to excite a molecule from its ground state to an excited state. Its principle is somewhat similar to the μSLA technique, but TPA provides much better structural resolution and quality.

UV photopolymer materials are highly absorptive in the UV range but are transparent in the IR (infrared) region. As a result, TPA can initiate polymerisation *only at the focal point* due to nonlinear nature of the excitation (See Fig. 2.10) and fabricate 3D micron-

scale structures, whereas with UV laser radiation, due to single photon absorption, polymerization occurs at the surface. Therefore, µSLA is a planar technology, with layer-by-layer polymerization steps, whereas TPA is a truly 3D high-resolution technology. Hence, TPA is very attractive for fabricating complex 3D micron-scale structures. The main system-level distinction between the TPA and µSLA technologies is that TPA uses ultrafast near IR laser (Ti:sapphire) instead of UV laser.

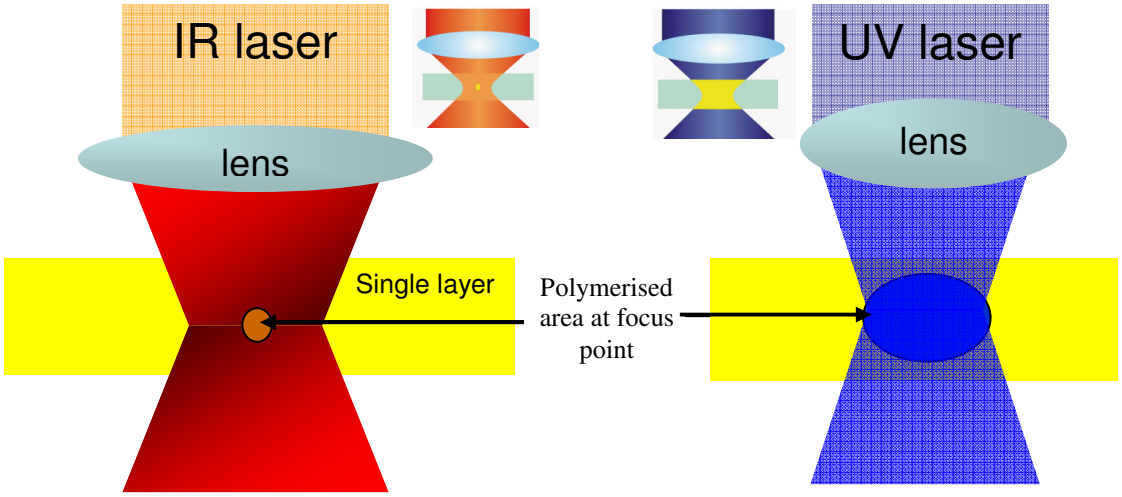

Fig. 2.10: Difference between TPA (left) and 1PA (right)

Using ultrafast IR laser, a group of Japanese scientists managed to directly fabricate a microbull (made of a commercially available resin called SCR 500) that is smaller than the size of a red blood cell (See Fig. 2.11). This outstanding result was first reported in the Nature journal [18, 19].

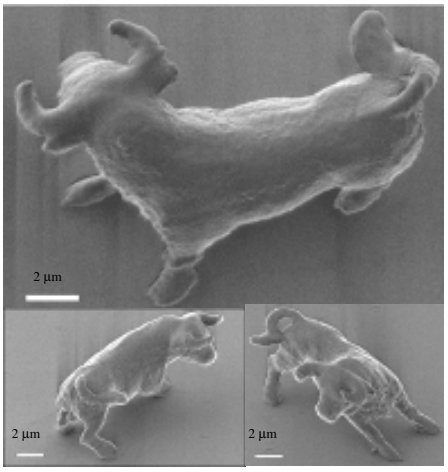

Fig. 2.11: Microbull fabricated by TPA [18]

A spin-off company of the German research lab, LZH, Micreon GmbH, is the first commercial company to use ultra short pulse lasers for the manufacture of highly-precise components. Many materials can be processed by ultra short pulse lasers without any damage, and, in addition, precision of one micrometer can be achieved. The designer glasses for a fly shown below (Fig.2.12) was fabricated by LZH.

Fig. 2.12: Designer glasses for a fly by LZH

By using a specially designed material called ORMOCER (trademark of Fraunhofer-Gesellschaft) [20], LZH can fabricate even more complex micron-scale structure as shown below [21]. The manufacture process of ORMOCER can be found in [22].

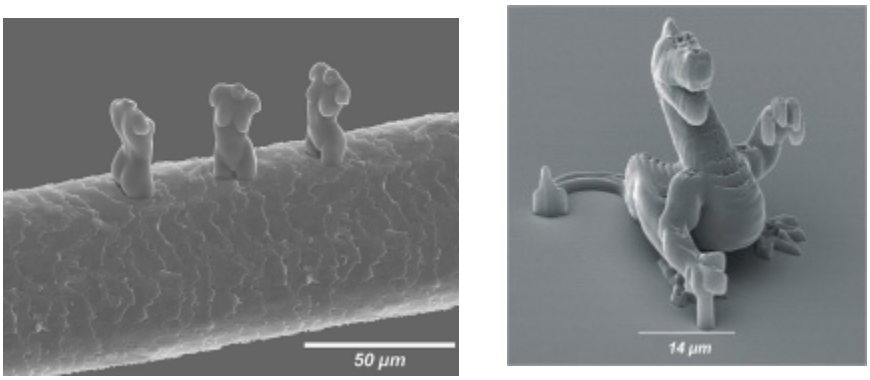

Fig. 2.13: Microdevices by LZH a) micro venus on a human hair b) micro dragon

However, this technique requires an expensive ultrafast laser as compared to the UV laser, as the common µSLA materials have weak sensitivity to TPA excitation and therefore require high laser intensities and exposure duration. In addition, the condition to keep ultrafast laser stable is also much more difficult than other common lasers.

As a result, several research groups [24, 25, 26, 27, 28] have started to design new materials that have large TPA absorption cross section so that these photopolymers can be processed by common lasers. Two common lasers used are Nd:YAG and CO_2 laser.

One French group has designed new stable materials that are sensitive to the Nd:YAG laser [26], thereby, allowing this technique to be extended to the industry. Fig. 2.14 below is one example of the micron-scale structures fabricated by them.

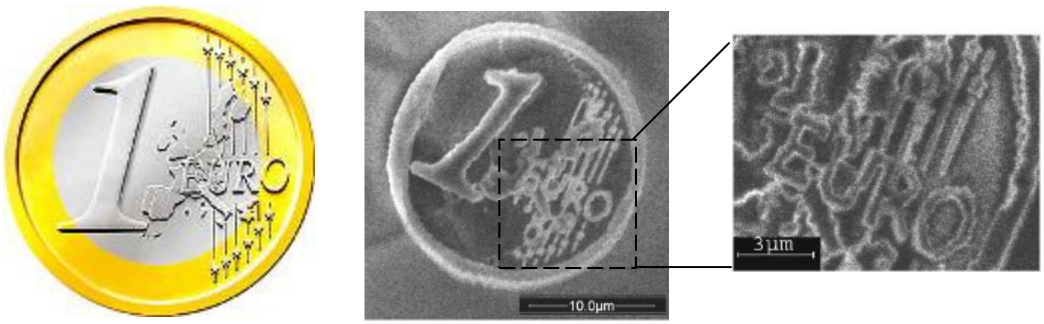

Fig. 2.14: 1 Euro coin a) illustration b) SEM image c) enlarged view

The principle of TPA have already been applied to optical 3D data storage [25, 29,30,31] and TPA microscopy [32] where 3D optical data storage is the term given to any form of optical data storage in which information can be recorded and/or read with 3D resolution. More information on TPA theory and principle can be found in [33, 34, 35].

2.3 Indirect 3D Microfabrication Methods

Moulds are generally used to mass produce components, which must consistently produced dimensional that are very close to the master pattern. This is even more critical in the case of micron-scale parts. The most commonly used substrates are glass and silicon wafer. Regardless of the material of the substrates, many of these fabricated moulds still need to be integrated into the injection moulding machine for mass production.

Powder injection moulding (PIM) [36] has emerged as a viable method for producing complex shaped parts at a competitive cost. The PIM process, which consists of feedstock preparation, injection moulding, debinding and sintering, uses a combination of powder metallurgy and plastic injection moulding technologies to produce net-shape

metal, ceramic or hard materials components. By using fine powders such as ceramic microcomponents of alumina (Al_2O_3), and a modified feedstock and injection process, PIM can also be applied to micron-scale structures and microcomponents (μPIM) [37]. It is one of the common methods employed to mass-produce microparts. Hence, many different types of micromaching techniques have been developed in an attempt to mass-produce microparts through the microinjection molding process. Some of the techniques are laser ablation [38], micro wire electric discharge machining (μWEDM) [39], deep reactive ion etching (DRIE) [40], Lithographie Galvanoformung Abformung (LIGA) process [41], the 'poor man' LIGA process: UV-LIGA process [42], Electrochemical fabrication (EFAB) [43], soft lithography [44] and electroplating [45].

However, many of these techniques possess certain limitations pertaining to the fabrication of micromoulds and often require two discrete steps: making the micromould insert and integrating the insert into a moulding machine.

Vacuum casting, on the other hand, is able to produce the micromoulds in a single step by doing away with the fabrication of the mould insert, thus giving it a competitive advantage over many existing techniques. Hence, it is able to derive savings in resources and lead time, by combining two discrete steps into one.

2.3.1 Laser ablation

The process of laser ablation, also known as laser machining, works on the principle that a high frequency pulsed laser can ablate material by removing it directly in the form of vapor or fine particles from a substrate, without melting. When the laser beam is focused onto the substrate surface, the temperature is raised rapidly and the polymer is vaporised. By moving either the laser or the material in a controlled fashion, laser ablation is capable of machining the desired microcavities precisely into the substrate [38]. Lasers like neodymium-doped yttrium aluminium garnet (Nd:YAG) and krypton fluorine (KrF) excimer allow for the rapid manufacturing of microstructured mould inserts made of plastics, steel, cemented carbide or ceramics [46, 47].

Once the desired microstructure is machined into the polymer substrate, a sacrificial metallic seed layer is then deposited onto the polymer. Electrodeposition is then carried out on that seed layer. Once the desired thickness is met, the seed layer is etched away and the polymer substrate is removed to form the metallic mould insert.

While laser ablation has the potential to be a useful tool for the production of precise microcavities for use in micromoulds, it still has some limitations. For example, conventional long pulse (nanosecond) solid-state laser ablation results in collateral heating and shock-wave damage (e.g. heat affected zone) to the surrounding area (Fig 2.15). The only way to overcome this is to employ ultrafast (picoseconds and femtosecond) pulses laser [48], but this type of laser is very much more expensive and the requirement to keep the laser stable is also a lot more stringent.

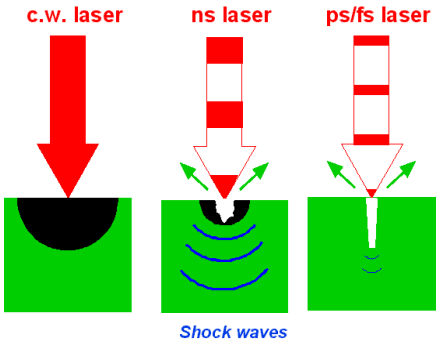

Fig. 2.15: Effect of various pulse width laser on substrate

2.3.2 Surface / bulk micromachining

These are some of the earliest methods for fabricating micron-scale structures and are still being used today to fabricate MEMS.

Surface micromachining starts typically with a silicon wafer and grows layers on top, based on the deposition. These layers are selectively etched by photolithography, either by a wet etch involving an acid or a dry etch involving an ionised gas, or plasma. Dry etching can combine chemical etching with physical etching, or ion bombardment of the material. As the structures are built on top of the substrate and not inside it, the substrate's properties are not as important as in bulk micromachining. Therefore, expensive silicon wafers can be replaced by cheaper substrates, such as glass or even plastic. As a result, the size of the substrates can also be much larger than a silicon wafer, and is used to produce thin film transistors (TFTs) on large area glass substrates for flat panel displays. This technology can also be used for the manufacture of thin film solar cells, which can be deposited on glass, PET substrates or other non-rigid materials.

Bulk micromachining also starts with a silicon wafer but instead of growing layers by deposition, it defines micron-scale structures by selectively etching inside a substrate. Similar to surface micromachining, bulk micromachining can be performed with wet or dry etches, although the most common etch in silicon is the anisotropic wet etch. Because the silicon has a crystal structure, certain planes have weaker bonds and are more susceptible to etching. The etch results in pits that have angled walls, with the angle being a function of the crystal orientation of the substrate. This type of etching is inexpensive and gives a very precise angle. Chun-Jung Chiu *et al* [49] demonstrated the feasibility of fabricating 3D micron-scale structures by using a combined silicon mould insert and micro hot embossing process.

2.3.3 Micro Wire Electric Charge Machining (μWEDM)

The operating concept of μWEDM is similar to that of laser ablation. However, instead of a laser, it employs a series of electrical discharges to melt and remove material from the surface of a conductive work piece. μWEDM is able to produce microcavities of 3D micron-scale structures [39] by slicing the 3D structure and cutting out the negative image of each slice in a metal plate. By assembling the metal plates, a microcavity bearing the negative form of the original structure was obtained. The metal plates were subsequently mounted in an injection moulding machine to produce the micron-scale structures.

One limitation of μWEDM is that the accuracy of the microcavities formed in the micro mould inserts is highly dependent on the control system as well as the diameter of the

EDM wire. Furthermore, due to the circular profile of the wire, it is almost impossible to machine some sharp edges and internal corners in the work piece. However, it is able to produce an excellent surface finish by carefully controlling the discharge current.

2.3.4 Deep Reactive Ion Etching (DRIE)

Deep Reactive Ion Etching (DRIE) is a highly anisotropic etching process used to create deep, steep-sided holes and trenches in wafers, with aspect ratios of 20:1 or more. It involves the use of sulphur hexafluoride (SF_6) which supplies highly reactive fluorine radicals to etch silicon wafer in an isotropic manner. Fluorocarbon plasma is subsequently introduced to deposit a layer of fluorocarbon polymer on the substrate before the next etching step proceeds. Thus, by alternating between the stages of etching and deposition, deep, vertical micro features can be formed. It was developed for MEMS, which require these features, but is also used to excavate trenches for high-density capacitors for DRAM.

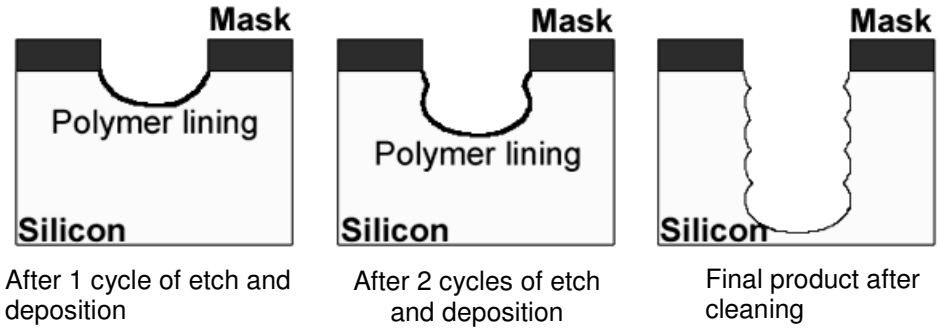

Fig. 2.16: Deep reactive ion etching (DRIE) process

Fig. 2.16 illustrates how the DRIE process can cause ripples (or scallops) in the vertical walls of the substrate. Since the degree of scalloping depends on the duration and number of etching and deposition cycles, the smoothness and texture of the side walls is

inevitably affected. Also, this process is dependent on the etching rate on the aspect ratio of the microfeatures, as the etching rate is controlled by the flux of the fluorine radicals which decreases significantly when high aspect ratio micro features are being formed. This slows down the etching process to less than 1μm per minute [40], thereby increasing the time-to-market.

2.3.5 LIGA

LIGA is a German acronym which stands for Lithographie (lithography), Galvanoformung (electroplating), Abformung (moulding). The LIGA process was developed in the 1980s and it combined X-ray lithography with electroforming to create moulds which was then used to mass produce plastic, metal [50] and ceramic parts. Repeatability can be achieved by LIGA [51].

In this lithography technique, extreme shortwave length (therefore very dangerous) X-rays replaced UV laser to pass through the transparent region of x-ray lithographic mask and penetrate a polymer layer which is subsequently removed by a developing chemical. This leaves behind a template that can be electroplated and used as a mould insert for injection moulding.

LIGA is capable of producing high aspect ratio micron-scale structures. Heights of hundreds of micron to millimeters (mm) can be achieved while the diameter is kept at a submicron level. This is only made possible with the use of X-ray as the energy source but the high cost (special photomask is needed for x-ray wavelength) and lack of

synchrotrons to produce X-rays make the process unattractive and uneconomical [52]. Furthermore, LIGA is not a true 3D process and is effectively only 2.5D. Although theoretically, 3D micron-scale structures can still be formed by curing multiple layers of photoresists using different photomasks, but this introduces additional problems like mask alignment, thereby increasing the difficulty of the overall process. Recently research on LIGA can be found in [53].

2.3.6 UV-LIGA

To resolve the limitations mentioned earlier, the original "LIGA" concept has since been modified, using another cheaper energy source such as UV laser to replace X-ray. Hence, the UV-LIGA process is also known as poor man's LIGA and was developed to use UV-rays to cure photosensitive resists, such as SU8 photoresists, and produce the template to be electroplated. This new process is able to reduce the cost of fabrication while retaining the capability to produce micron-scale structures of high aspect ratio.

2.3.7 Electrochemical fabrication (EFAB)

EFAB is a unique and patented microfabrication technology, EFAB™, which can create complex 3D micron precision metal structures with unprecedented flexibility. It is owned by Microfabrica, which is a private company founded to commercialize work that began with DARPA (Defense Advanced Research Projects Agency) at the University of Southern California (USC).

The EFAB technology, like the RP process, is an additive microfabrication process based on multi-layer selective electrodeposition of metals and its selective process generates micron-scale structures quickly and makes it possible to rapidly deposit an unlimited number of independently patterned layers. Together, these form virtually arbitrarily, complex 3D shapes, overcoming the geometrical limitations of conventional microfabrication. As a result, new Radio Frequency (RF), optical, and inertial microdevices can be created in less time, have greater functionality, and are far easier to design than previously possible. Hence this technology allows a designer to go from idea and CAD design to production of a 3D microdevice in a very direct and rapid fashion. See Fig. 2.17 below for some examples.

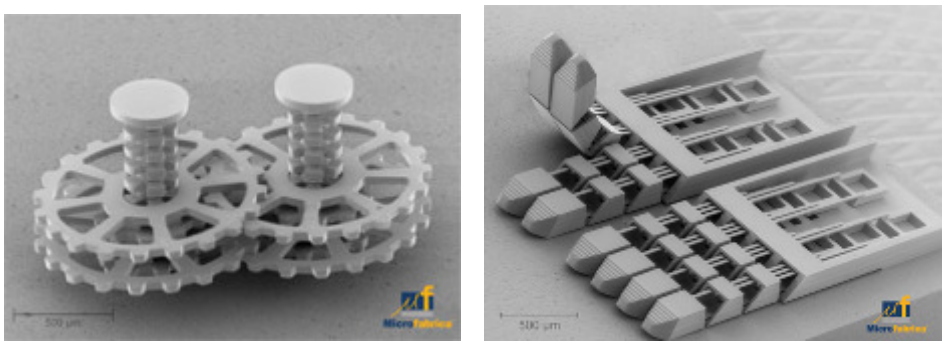

Fig. 2.17: Microdevices fabricated by EFAB

Although EFAB is the first microfabrication technology that relies on quick, successive deposition of tens of precision metal layers to create 3D micromachines which are robust and require little-to-no assembly, it is interesting to note that not many research projects using this technique have been reported in journals. More information and illustrations can be found in [43] and [54].

2.3.8 Electrodeposition

Electrodeposition is the process of using electrical current to coat an electrically conductive object with a relatively thin layer of metal (nanometers to a few micrometers thick). The primary application of electroplating was to deposit a layer of a metal on a metal surface having some desired improved property (e.g., wear resistance, corrosion protection etc.) onto a surface lacking that property. It can also be used to fabricate micromoulds [45].

Many micromoulds created by various lithography methods (except for LIGA) use non-conductive material such as silicon wafer as substrates. Since silicon is a semiconductor, it cannot be electroplated as easily as a metal substrate. Therefore, a thin metallic seed layer needs to be deposited onto the wafer surface first before the structure is built. After the structure is created, another conductive layer has to be deposited over the surface of the structure to make it conductive for electrodeposition to take place.

When the electrodeposition has covered the entire structure, the micromould has to be separated from the substrate through dissolution of the seed layer (Fig. 2.18). This requires additional steps of mechanically tooling and polishing in order to insert the micromould into the injection-moulding frame [68]. If a metal substrate is used directly instead of silicon, several steps such as depositing and dissolution of the seed layer can be eliminated. Although LIGA uses metal as its substrate, the cost for a synchrotron radiation makes commercial applications unfeasible.

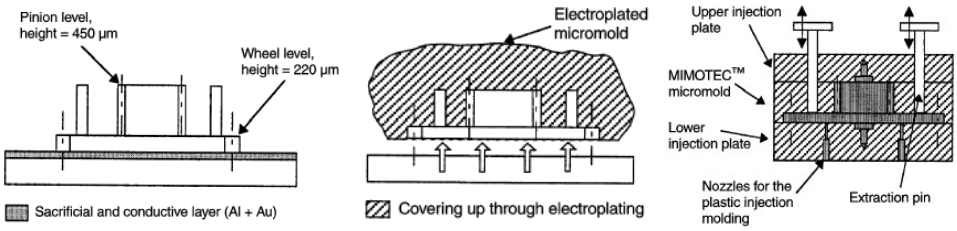

Fig. 2.18: Seed layer deposit needed on non metal substrate for electrodeposition to take place

Using pulse electroplating current on a diamond turned brass substrate, instead of the typical silicon wafer, a nickel micromould (Fig. 2.19) was directly fabricated on a brass substrate [55].

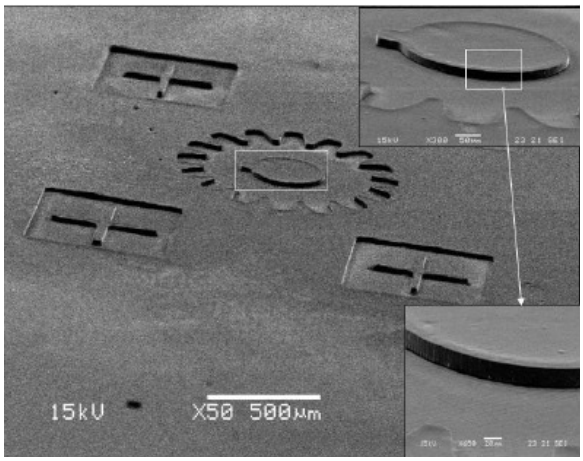

Fig. 2.19: Nickel micromould by pulse electrodeposition on diamond turned brass substrate

2.3.9 Vacuum Casting

Vacuum casting is a copying technique characterised by the use of a vacuum during the processes of mould fabrication. It is currently one of the most popular and flexible forms of rapid tooling for consumer products [56] when combined with a silicone rubber mould.

As this technique requires a master pattern before a mould tooling can be formed, and the fact that a silicone rubber mould is soft and can only support castings in small batches before breaking down [56], it is known as indirect soft tooling. Using vacuum casting has the following advantages over existing microfabrication techniques described in the previous sections with regard to the production of microparts:

- Silicone rubber moulds can be fabricated directly from the master pattern, whereas most existing micromoulding methods require the additional step of producing the micromould insert first before integrating into a mould base.
- Very fine geometrical details of the master pattern can be faithfully reproduced in the micromould cavities [57].
- The master patterns can thus be fabricated using the most cost effective method.
- Silicone rubber possesses high chemical resistance due to the low interfacial energy of its surface [58]. This property allows a wide range of resins, including wax, plastic and metals, to be cast, without any possible reaction with the surface of the silicone rubber mould.

- Vacuum casting uses cheaper tools, materials and is simpler to implement and allows the possibility of harnessing the potential of silicone rubber moulds in the batch production of functional prototypes.
- The flexibility and elasticity of silicone rubber, along with the potential to replicate 3D parts by vacuum casting gives silicone rubber tooling a competitive edge over hard tooling. The elastomeric moulds can be flexed to release the parts (Figure 2.20).

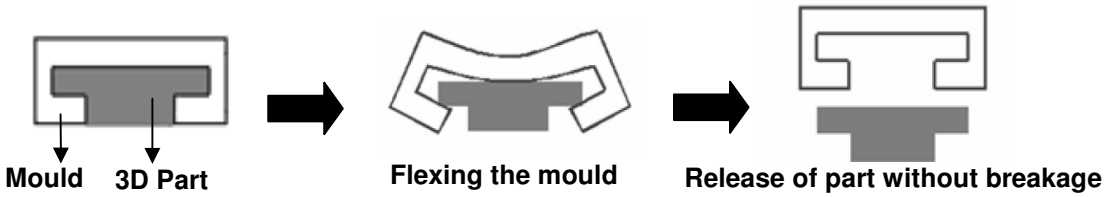

Fig. 2.20: Flexibility of elastomeric silicone rubber mould

The two most popular materials that vacuum casting use are Poly(dimethylsiloxane) (PDMS) and silicone rubber. M Denoual *et. al.* uses PDMS [59, 60] while Sungil Chung *et. al.* use silicone rubber [61, 62, 63].

The drawback of PDMS is that it is generally incompatible with non-polar solvents such as toluene and hexane [64] which leads to swelling of PDMS. The deformation and distortion of the elastomeric stamp/mould during soft lithography has yet to be fully understood and controlled. For example, PDMS shrinks by 1% upon curing due to fabrication processes leading to dimensional inaccuracies of the part [60]. Hence, the properties of the elastomer would have to be optimised to make pattern transfer reproducible.

The flexibility and elasticity of silicone rubber, along with the potential to replicate 3D parts by vacuum casting, gives silicone rubber tooling a competitive edge over hard tooling as these elastomeric moulds can be flexed to release the parts without damaging the parts.

Recently, Chung *et. al.* [61] have evaluated silicone rubber transferability while Denoual *et. al.* [59, 60] demonstrated the use of vacuum casting as an alternative method for bio-microsystems. In addition, vacuum casting has also been shown to be capable to cast 3D micro helical gear with bismuth [62] and epoxy-aluminum [63]. Furthermore, silicone rubber mould has recently been used to electroplate micro patterned tools [45] and as a mould for low-pressure injection moulding process in fabrication of ceramic micro components [65].

2.3.10 Soft lithography

Soft lithography refers to a set of methods for fabricating or replicating structures using elastomeric stamps, moulds, and conformable masks. Because it uses elastomeric materials, it is therefore called "soft". It includes the technologies of Micro Contact Printing (μCP), replica moulding (REM), microtransfer moulding (μTM), micromoulding in capillaries (MIMIC) and solvent-assisted micromoulding (SAMIM). However, these soft lithography techniques will not be discussed in this thesis.

2.3.11 Hot Embossing

Micro hot embossing is a method for reproducing high quality micron-scale structures. It is essentially a process that involves pressing a mould tool into a semi-finished polymer material that is held above its glass transition temperature.

Depend on the size and geometry of the micron-scale structures, the mould tool can be fabricated in a number of ways. From machining of stainless steel for micron-scale structures with dimensions in hundred micrometer range to LIGA technologies for micron-scale structures with dimensions in few micrometers range and high aspect ratios. Nickel and silicon are the most commonly used for mould insert.

The advantages of hot embossing are low material flow, avoiding internal stress which induces e.g. scattering centers infavorable for optical applications, and low flow rates. Hence, more delicate structures such as free standing thin columns or narrow oblong walls can be fabricated. Another advantage is the simple setup of the machine, which results in very short setup times due to the easy exchangeability of the mould insert or polymer material.

It is often applied to the Bio-MEMS for fabrication of microfluidic chip. Micro optical components such as LIGA-micro spectrometer, micro lens arrays and optical wave guides are just some examples that can be produced by hot embossing. Many prototypical micron-scale structures have been fabricated by this technique in laboratories but not in industries because it is believed to be too slow and to be associated with too much

manual work. Yet in [66], it was shown that hot embossing has more potential than merely for use in the laboratory.

2.4 SU8 Photoresists

SU8 is a negative, epoxy type, near-UV photoresists developed and patented by IBM [67]. It has been used widely in MEMS applications and for mould making [68, 38]. SU8 can also be exposed by various energy sources such as X-ray, e-beam sources [69], infrared laser [70, 71], and ion beam [72]. The excellent thermal and chemical properties of SU8 make it very suitable for micromould making. However, removing the well cross-linked SU8 structure after electrodeposition is extremely difficult as it is insoluble to most chemicals. Hence, extracting the cavity is a challenge, often requiring special and expensive equipment. Methods such as using high-pressure water jet, excimer laser ablation [38], O_2/SF_6 plasma etching [73], and chemical removal such as reactive ion etching (RIE) have all been reported [74]. Each method is effective in its own case and all of them require a significant amount of specialized costly equipment to do the removal. Various techniques have been reported in numerous journals [70, 72, 76 – 78] ever since it was invented by IBM. A PhD research on SU8 photoresists can be found in [75].

SU8 is very sensitive to its process parameters in a practical way and much research was conducted to find out which of its parameters is the most important. The interesting thing to note is that the key parameters involved to fabricate perfect micron-scale structure differ from paper to paper. [79, 80, 81] reported that prebake is the most important parameter while [82] reported that cooling rate is the most critical parameter. Ronald A.

Lawes investigates the variation of the key parameters that affect the tolerances which lead to the reproducibility [83].

A. Mata *et. al.* [89] fabricated multi-layer (up to six layers) SU8 micron-scale structures by using multiple coating and exposure steps but in a single developing step. The multiple SU8 layers create patterned micron-scale structures with overall thicknesses of up to 500 μm and minimum lateral feature size of 10 μm. However, closed structures are hard or impossible to achieve directly achievable in such multi-layer lithography because the irradiation of the top film induces cross linking of the layer [90]. Single-step 3D lithography and single-step electroplating was reported in [91].

2.4.1 New SU8 Formulation

Recently, a Swiss company, Gersteltec Engineering Solutions, formulated a new SU8 photoresists. Using nanomaterial added into SU8 photoresists, conductive SU8 was invented and the result was published in [92]. Low stress SU8 for microfabrication application was reported in [93]. Even colours such as Black, Red, Blue, Yellow, Violet, and Green have also been formulated by them. More details can be found in the company website [94].

2.5 Application of 3D microstructures

Complex 3D micron-scale structures have recently received a significant amount of attention within, as well as beyond the scientific community, because of the promise they

hold for exciting new applications in a variety of areas especially in photonics. Since photonic crystals can manipulate the flow of light, this makes them attractive materials for new types of optical components.

These 3D micron-scale structures may serve as mechanical or optical microdevices (e.g. waveguides) in micro environments or even nano environments. For example, diagnosis or surgery inside the human body may become more efficient because of micromovers and pumps that can interact on the cellular level. In addition to mechanical characteristics, these structures can be fabricated to have interesting optical properties and can be used as photonic devices [95 - 98] in applications such as telecommunications [99] and optical information processing.

Combining biology with MEMS (BioMEMS) is targeted to have the fastest growth rate within the MEMS market, particularly for drug discovery and delivery, diagnostics, biotelemetry, and genomics [100]. However, manufacturing of BioMEMS devices differs from IC manufacture because the market requires a diversity of materials, physical structures, input/output methods, products, and initially lower volumes per product [101].

3. EXPERIMENTAL EQUIPMENT, SETUP AND PROCEDURES

There are two types of setup used in this work: one for the lithography and the other, for the vacuum casting machine, which uses silicone rubber to fabricate micromoulds. Hence, there are also two sets of equipment and materials used in each setup.

3.1 Materials and Equipment Used

3.1.1 Materials and Equipment used for Lithography

Materials used:

- Norland optical adhesive, NOA 60 photopolymer,
- Vantico SL5510 photopolymer and
- Microchem SU8 photoresists.

Solvents used:

- Microchem SU8 developer
- Acetone
- Alcohol

Equipment used:

- Lambda Physik COMPex 205 multigas (KrF) excimer laser (λ = 248 nm)
- Laser filter
- UV reflecting mirrors
- 3 inch and 4 inch quartz photomask

- Machined fixture to hold the photomask
- Newport XY linear micropositioner and a rotation stage
- XYZ micropositioner stage
- Laurell single wafer spin coater (WS-400A-6NPP)
- LabTech Hotplate (LSM-2003D)
- Machine vision system consists of PC, CCD camera (JAI CV-A11) and LCD monitor.
- Microscope rectangle glass slide and diamond turned brass substrates

Figures of these equipments can be seen in Appendix A. Some of the descriptions can be found in following section 3.2.

3.1.2 Materials and Equipment used for Micromoulds via Vacuum Casting

Materials used :

- VTV 750 Silicone Rubber
- CAT 750 Catalyst

Equipment used :

- MCP 5/01 Vacuum casting system
- Shel Lab 1330FX Oven

Figures of these equipment and details regarding the interface controls during degassing are covered in Appendix B.

3.2 Experimental Setup

3.2.1 Lithography Experimental Setup

There are two types of setup; single layer and multi-layers setup. It is vital that the air gap between photomask and substrate is kept to a minimum so as to reduce the diffraction effect.

A *single layer* lithography experimental setup is shown in Fig. 3.1. An excimer laser mirror was used to reflect the energy of the laser beam downward onto the photomask with the coated substrate placed below it. The substrate would be spin coated with the material (photopolymer or photoresists) using the Laurell coater.

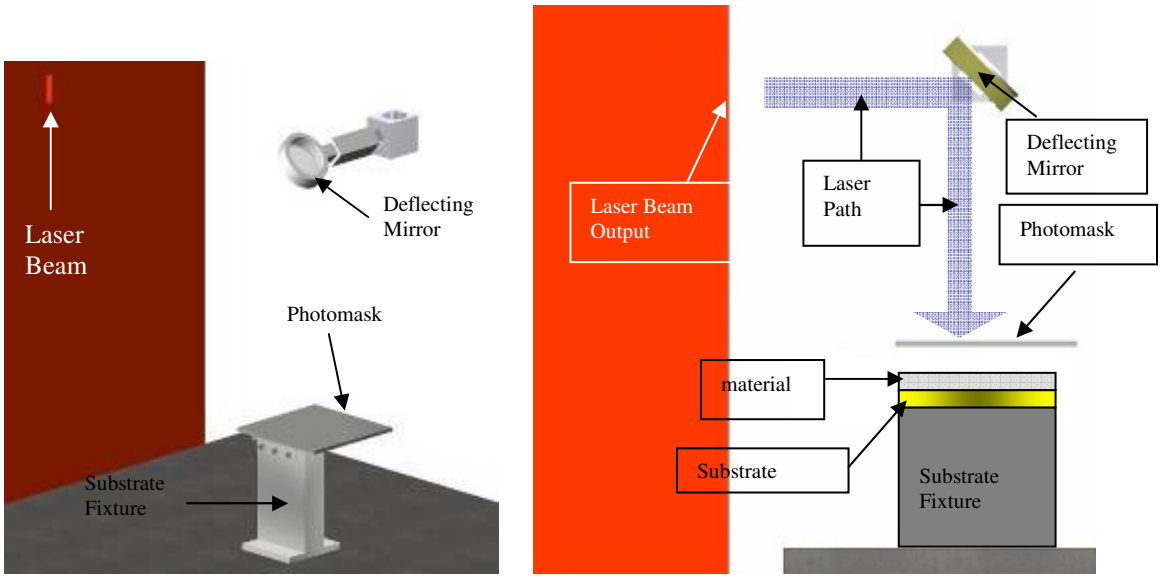

Fig. 3.1: Setup for single layer lithography a) 3D view b) Side view.

A *multi-layer* lithography experimental setup is shown in Fig. 3.2. Two linear (*xy* axis) and one rotating stage positioner within the fixture, were used to align the substrate to the photomask. The difference between a single and multi-layers setup is the addition of a mask translation stage (not shown), a CCD (Charge-coupled devices) camera and two additional deflecting mirrors for alignment purposes.

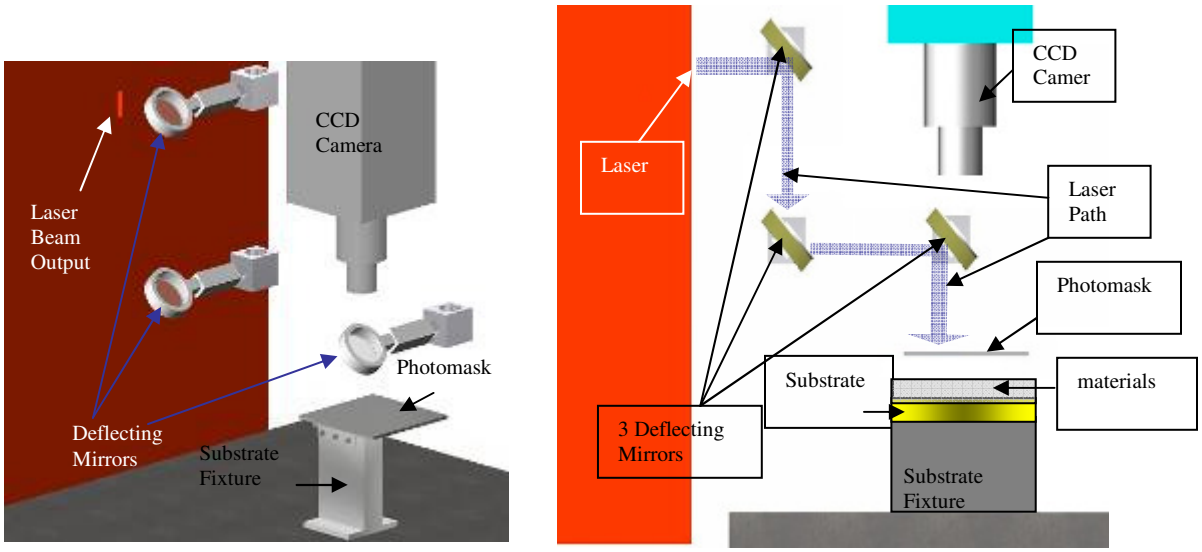

Fig. 3.2: Setup for multi-layers lithography a) 3D view b) Side view.

3.2.2 Light source

A Lambda Physik COMPex 205 multigas (KrF) excimer laser was used for the experiment. The wavelength of the laser is 248 nm, which is in the deep UV range. This laser is usually used for precision machining, producing features down to 40 nm in resolution with virtually no heat-affected zone [102]. Therefore, medical doctors make use of this property to correct myopia in refractive eye surgery, such as LASIK (*La*ser in *s*itu *K*eratomileusis). In principle, a shorter wavelength allows the beam to be focused to

smaller spots and thus, excimer lasers have also been used in high-resolution material processing and surface modification [103].

The maximum energy output of this laser is 600 mJ per pulse with pulse duration of 25 nanoseconds (ns). Hence the peak power can reach as high as 24 MW. With a rectangular beam of 24 × 6 mm, the power density achievable is 16.7 MW/cm^2. This level of energy is powerful enough to induce photopolymerisation for most commercial UV liquid photopolymers.

3.2.3 Photomask

A 3 inch and a 4 inch quartz square photomask were made (by IGI) for this project. The photomask had to be made of quartz instead of soda lime glass (commonly used for UV light lithography) because soda lime glass does not have high transmitted ability at 248 nm. The only difference between these two photomasks is the diameter of the microgear, in which the 3 inch photomask is 1mm in diameter while the 4 inch photomask is 0.5 mm. Basic information on the fabrication of photomasks can be found in Appendix C.

Fig. 3.3a shows the 4 inch square photomask of a microgear. The whole photomask consists of two positive (darker portion of the photomask) and two negative (top portion of the photomask) columns of 30 patterns; each 5 rows by 6 columns. There is a rotating angle of 0.5 degrees between each pattern of microgear. Therefore, the whole microgear has a rotating angle of 15 degrees for the total of 30 layers.

The enlarged view of one pattern is shown in Fig. 3.3b. The pattern is a 0.5 mm diameter (measured from tooth to tooth) gear with 16 teeth and 4 alignment marks at its corners. The alignment marks are to assist in the alignments with the previous layers. The width of each tooth is 30 µm. The quality and accuracy of the photomask is extremely important, as the outcome of the developed pattern depends on it.

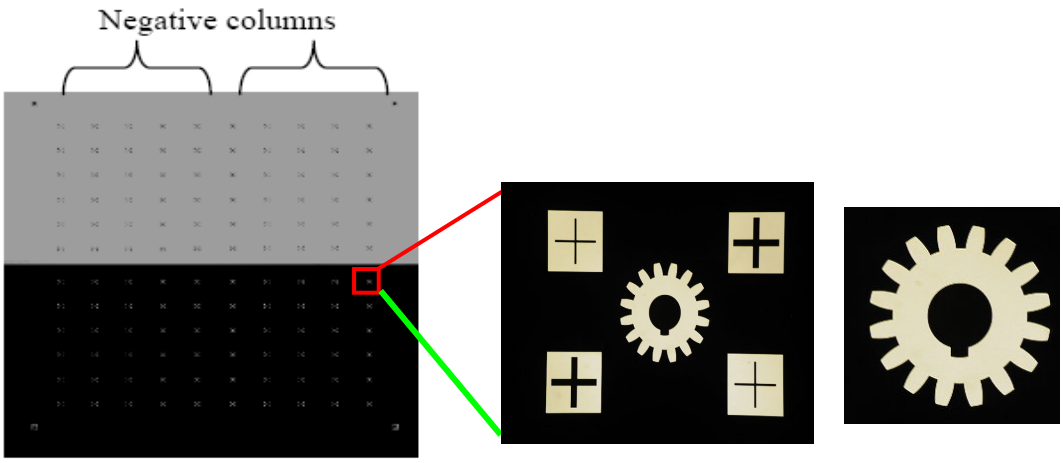

Fig. 3.3: Quartz photomask a) 4 inch quartz photomask b) enlarge view of a microgear pattern with alignment marks c) 500 µm microgear.

3.2.4 Manual micrometer positioner

A manually actuated linear micro-positioner of 3 µm resolutions was used to position the substrate in the *xy* axis for alignment to the photomask. An additional rotation positioner was placed on top of the linear positioner to correct any misalignment due to rotation. The whole process of the alignment was monitored by the machine vision system.

3.2.5 Machine Vision

Semiconductor industries use either expensive automatic alignment systems or split-field microscopes to carry out the alignment. Automatic alignment systems are expensive and meant for large volume of production, while using the microscope will strain the eyes

even for low-volume productions. A machine vision system compromising a CCD camera and a LCD monitor screen for display was used for this research. This method is compact, low cost, and comfortable to the eyes.

3.2.6 Vacuum Casting Experimental Setup

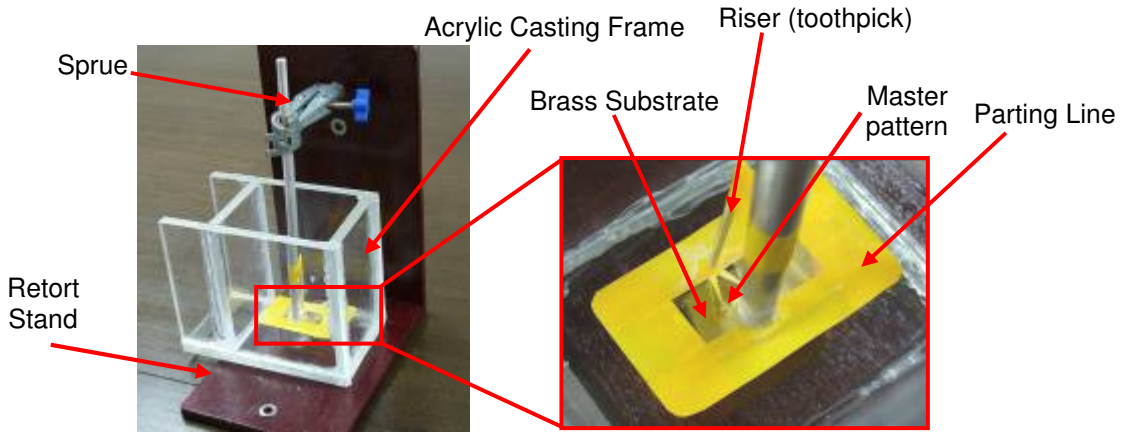

Fig. 3.4: Micromould experimental setup

It is first necessary to assemble an acrylic casting frame (Fig. 3.4) to contain the liquid silicone rubber. The master pattern to be copied was fabricated onto a substrate (brass or glass) and carefully glued to a metal rod and toothpick, which was used to create the sprue and the risers in the mould respectively. The master pattern was then suspended in the casting frame by means of a retort stand so that silicone rubber can be poured around the pattern to embed it. A parting line has to be formed by a tape along the perimeter of the substrate so as to facilitate the splitting of the micromould into two halves after the silicone rubber was taken out of the oven during the curing process. To secure the master pattern in place during subsequent degassing and curing operations, the retort stand was custom made to fit into the small vacuum chamber (Fig. 3.5).

Fig. 3.5: Degassing process in MCP 5/01 system

3.3 Procedure for Lithography

The experiments included both single layer and multi-layer lithography. The single layer lithography experiments were conducted to test the material suitability. The parameters for the single layer lithography were also optimised by a series of experiments, which were aimed for multi-layer lithography. Two kinds of materials were tested. Two photopolymers : Norland optical adhesive; NOA 60 and Vantico SL5510, and one photoresists namely SU8. The flow chart (Fig. 3.6) illustrates the difference of the *single layer* procedure between photopolymer and photoresists:

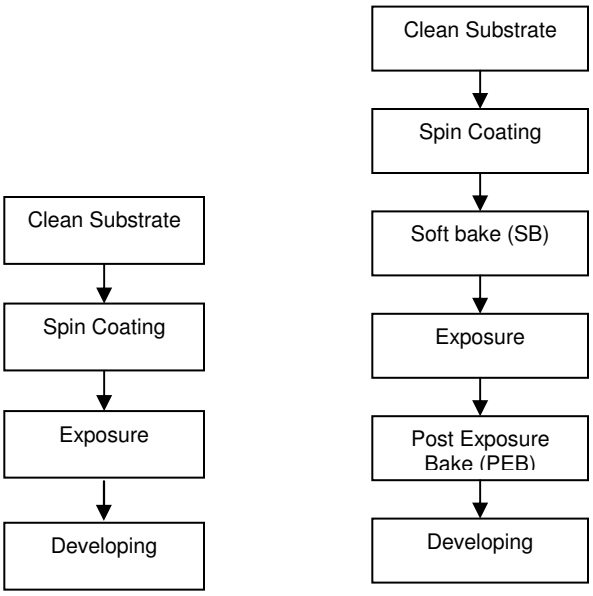

Fig. 3.6: Flow chart for *single layer* between photopolymer and photoresists

3.3.1 Procedure for Single Layer Lithography

This procedure is the same for both NOA 60 and SL5510, since both materials are liquid photopolymer. The only significant differences are their viscosity and wavelength absorption graph. The developing solvent for photoresists was the SU8 developer while alcohol was suitable for the selected photopolymers (SL5510 and NOA 60). See Appendix D for more information on these two materials.

The substrate was first cleaned under ultrasonic bath and baked, if necessary, to dehydrate the substrate before dispensing the liquid photopolymer onto the substrate. After that, it was spin coated to a thin layer by the spin-coating machine. Various thicknesses throughout the whole substrate can be obtained, as thickness of the layer is dependent on the viscosity of the material and speed of the rotation. The coated substrate

was then placed under the photomask and exposed to different energy levels of the excimer laser. After the layer was exposed, the glass slide (substrate) was put into a suitable solvent for developing. The unsolidified (unexposed) material would then be dissolved by the alcohol, leaving the solidified pattern stuck to the substrate. The solid pattern was then observed and analysed by using an optical microscope. Results and discussion can be found in section 4.1.

3.3.2 Procedure for Single Layer of SU8 Lithography

The difference between photopolymers and photoresist is that the former can be polymerised without the need of any baking process. Hence two additional baking steps were required for photoresists: Soft bake (SB) was carried out immediately after spin-coating and post exposure baking (PEB) was only carried out after the laser exposure.

Similar to the photopolymer material, the substrate has to undergo ultrasonic cleaning to ensure it was free from contaminates before the dehydrate baking. The SU8 was dispensed onto a substrate and spin coated at certain rpm to achieve a certain thickness according to the given graph in Appendix E. The next step was to SB the substrate at 65^0C for 1 min (time varies with thickness). The spin coated substrate was then affixed onto a fixture via contact printing with the quartz photomask placed over it. The excimer laser was then activated to pass through the mask and expose the SU8 that was coated onto the substrate.

After the exposure, photopolymerisation occurred in the photoresists and the pattern on the photomask was transferred onto the photoresist. A second baking PEB was required at 95^0C for 1 min. The substrate was then dipped into a developing solvent to wash away unexposed SU8 (under yellow light), leaving the pattern of the exposed SU8 on the substrate. The substrate was then blown with nitrogen to prevent staining from the solvent. Ultrasonic vibration could be used to speed up the development but care had to be taken not to agitate it too much to avoid delamination (peeling). The developed single layer was then analysed under an optical microscope and scanning electronic microscope (SEM), if necessary. Results can be seen and discussed in section 4.1.3.

A detailed map of the experiment process with required parameters are mapped in a flowchart under Appendix F.

3.4 Procedure for Multi-layer Lithography

NOA 60 was not chosen for multi-layer~~s~~ experiments as the alcohol used in its development stage did not give a satisfactory outcome. See the results shown in section 4.1.1.

The multi-layer photolithography process basically consists of repeated single level photolithography process. Based on the optimised parameters obtained from single layers, the obtained parameters will be used in the multi-layers. The flow chart below illustrates the procedure for multi-layers of SL5510 photopolymer and SU8 photoresists:

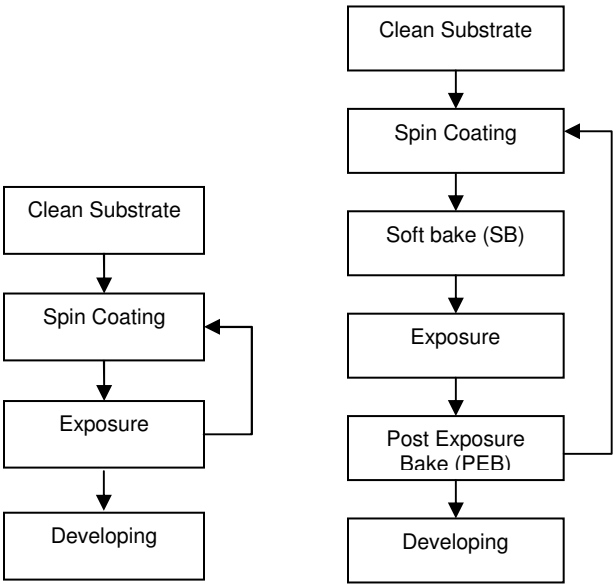

Fig. 3.7: Flow chart of multi-layers of photopolymer (left side) and SU8 (right side)

3.4.1 Procedure for Multi-layer of SL5510 Photopolymer

In this part of the work, the *same particular microgear pattern* on the photomask was used throughout, in other words, there is no need to shift the substrate to the next precedent pattern for the next layer exposure.

The substrate was spin coated with the first layer of SL5510 followed by exposure to the excimer laser using the optimum parameters. After ensuring that the first layer of photopolymer was well solidified and stuck to the glass slide, the substrate was spin coated again with the second layer of liquid photopolymer without developing at this stage. The substrate was then exposed to the laser again and the second solidified layer would be obtained. The process was repeated until a 3D microgear was created, layer by layer, in the liquid photopolymer. Finally, the substrate was put into the alcohol for

developing, where the uncured liquid photopolymer was dissolved, displaying a solidified 3D micropart. The results can be seen and discussed in section 4.2.1.

3.4.2 Procedure for Multi-layers of SU8 Photoresist

The procedure for performing a multi-layer lithography on SU8 photoresist is similar to the single layer lithography. The process is repeated after each PEB (See Fig. 3.7).

After the first layer of photoresists was exposed through the photomask, another layer was spin coated onto the substrate. However, before the next exposure take place, an alignment of the first pattern to the next pattern needs to take place. Thus, an additional xyz stage was used to align the successive required gear pattern on the photomask to the precedent mask pattern, with the use of CCD camera system. Development was only carried out after the required numbers of layers have been achieved. Results can be seen and discussed in section 4.2.2.

3.5 Procedure for Fabricating Micromould via Vacuum Casting

The procedure for fabricating micromoulds is divided into four main steps:

1) Analysis of master pattern,
2) Cleanliness of master pattern,
3) Preparation of silicone rubber mixture, and
4) Fabrication of micromould.

Step by step illustrations can be found in Appendix G.

3.5.1 Analysis of the Master Pattern

The master pattern was first checked under an optical microscope for any form of contamination and presence of defects in the microgear. Then, the dimensions were measured by the white light interferometer (WLI), where a 3D profile can be generated, showing all the critical dimension of the master pattern. Fig. 3.8 shows an example of the 3D data generated by WLI. This data will be used to compare with the dimensions of the micromould later. Details of WLI can be found in [104].

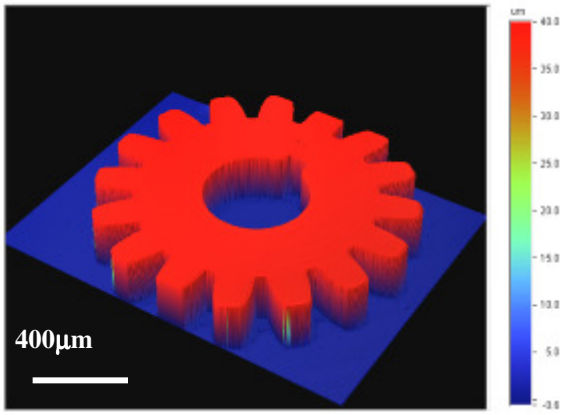

Fig. 3.8: 3D profile of master microgear by WLI

3.5.2 Cleanliness of Master Pattern

Because the vacuum casting technique is capable of reproducing every detail on the master pattern, it is vital that the surface of the master pattern and substrate are free from any contamination. If there are any contaminates, cleaning without damage to the master pattern can be achieved by dipping into Isopropyl Alcohol (IPA) for glass substrate, or

dilute hydrochloric acid (HCL) for brass substrate. Care has to be taken during the cleaning process so as not to damage the master pattern as well as affecting the adhesion of the master pattern to the substrate. Ultrasonic cleaning should only be used if there are any stubborn contaminates.

3.5.3 Preparation of Silicone Rubber Mixture

The amount of silicone rubber required was calculated by multiplying the desired volume of the micromould to be made by the density of the silicone rubber (1.09kg/dm^3 at 23°C). This calculated amount was then mixed with a catalyst having 10 percent the weight of the silicone rubber used for 2 to 5 minutes. After the mixing was completed, the silicone rubber mixture was degassed (see Appendix B) to remove any air bubbles. The duration of the degassing process could last from 10 to 15 minutes, depending on the extent of air bubbles in the mixture. After the degassing, the silicone rubber mixture was poured into the casting frame (Fig. 3.4) to embed the master pattern.

3.5.4 Fabrication of Micromould

After pouring the silicone rubber mixture into the casting frame, the setup undergoes another degassing step, since air may be introduced into the mould during the pouring process. This second degassing process typically takes longer than the first degassing, around 25 to 35 minutes. After degassing, the entire setup was transferred to the oven for

the curing process, where the silicone rubber is heated from 40^0C to 45^0C for a duration of 10 to 12 hours, for maximum dimensional accuracy. After the curing process, the whole setup was removed from the oven, and the casting frame was disassembled. The silicone rubber mould was separated into the core and cavity halves by cutting along the parting line (Fig. 3.9) with a scalpel. The parting line should be cut in zigzag form (instead of a straight line) so that the original orientation of the core half relative to the cavity half upon closing can be preserved easily. Hence, the micromould of the master pattern was obtained (Fig 3.9) after removing the master pattern.

Fig. 3.9: Core and cavity of silicone rubber mould

3.6 Difficulties Encountered

- The energy level of excimer laser only becomes consistent at high frequency. Every laser pulse generated yielded a different energy reading at low frequency. This issue was minimized by using a UV laser filter at high frequency.
- The air gap between the photomask and the coated substrate has to be maintained at a very small distance (in tens of micrometer or less), so as to reduce diffraction effects.

- An UV lamp was used to replace the excimer laser to fabricate a thicker master pattern, as there is very high absorption of SU8 photoresists at 248 nm wavelength. High UV absorption of the material cannot lead to thick structures.

- The current alignment method is not automated and as advanced like those being used in the semiconductor industry. Using the alignment marks, manual translation stages and vision equipment on hand are the best that I can do to get accurate alignment of the layers.

4. EXPERIMENTAL RESULTS AND DISCUSSIONS

4.1 Analysis of Single Layer

The first material tested was the Norland optical adhesive NOA 60 photopolymer followed by Vantico liquid photopolymer SL 5510 and then the microchem SU8 photoresists. For all the materials, the experiments started off with single layer formation and followed by multi-layers experiments if promising results were obtained from the single layer experiments.

4.1.1 Single Layer of NOA 60 Photopolymer

Fig. 4.1a shows the micron-scale structure pattern on the photomask under a microscope. This pattern was a typical alignment mark, used in a stepper machine for auto alignment. The whole pattern was made up of four squares: two squares made up of vertical lines and two squares made up of horizontal lines, placed diagonally to each other. The width of each line was 23 μm.

After exposing the photomask pattern to a range of different energy levels and pulses onto coated glass substrate, the best combination of parameters found was: 18KV, 10 shots, 100-110 mJ. The thin solid layer was formed and the substrate was developed in alcohol solution. After the development, the amplified micron-scale structure of the solid layer is shown in Fig. 4.1b.

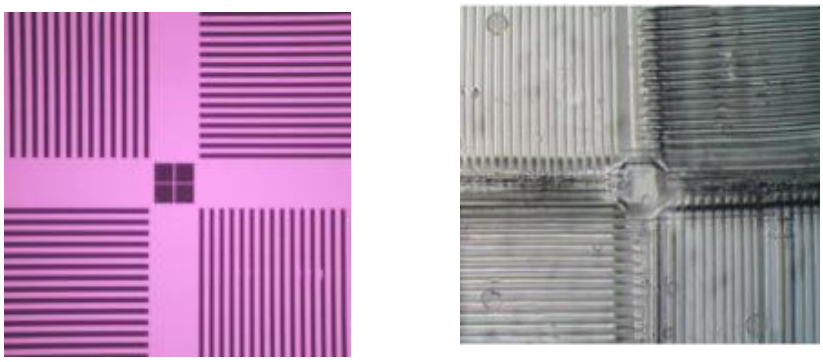

Fig. 4.1: Pattern for NOA 60 a) Alignment mark on a photomask b) Single layer of NOA on glass substrate.

From Fig 4.1, it can be seen that the NOA 60 was photopolymerised under the irradiation of excimer laser and a solid micron-scale structure was formed. The dimensions of the solid lines were close to 23 μm (measured by optical microscope). However, the solid structure was not sharp and clear, as there were still some uncured photopolymer left, covering the solid structure. Since the structure could not be developed cleanly, experiments to form multi-layers was not continued.

4.1.2 Single Layer of SL5510 Photopolymer

This SL5510 liquid photopolymer was designed for RP processes, i.e., stereolithography apparatus (SLA). To determine the optimal energy level for SL5510, it was exposed to a series of different levels of energy as well as a number of shots using the 3 inch photomask (microgear diameter of 1mm).

Figures 4.2 to 4.8 show the series of outcomes that correspond to the various combinations of energy levels (64 to 180 mJ) and number of shots (1 to 10 shots). From the figures, all the various energy combinations were able to solidify the photopolymer coated on the glass substrate. The results indicated that a lower energy level and a low

number of shots produce better sharpness (Fig. 4.2), whereas higher energy levels and higher number of shots resulted in an over-reaction of the photopolymer and the shape of the solid layer became fuzzy (Fig. 4.3 ~ 4.8).

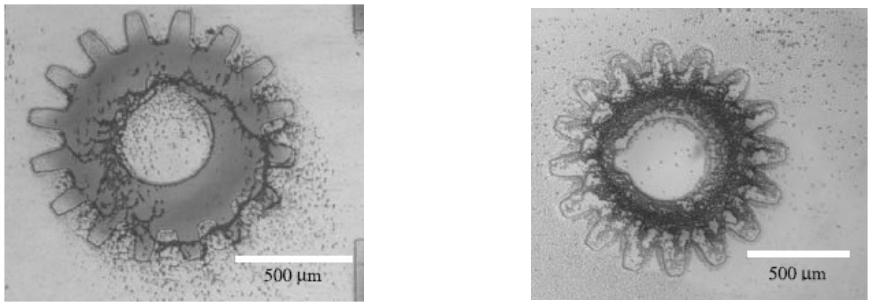

Fig. 4.2: Single layer of 1 shot at a) 64mJ b) 112 mJ

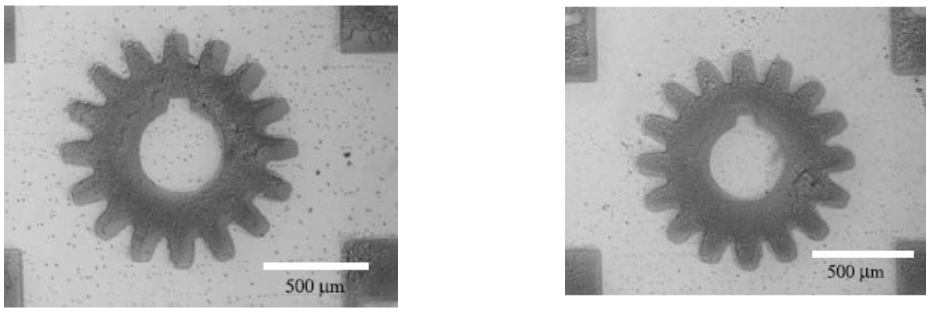

Fig. 4.3: Single layer of 1 shot at c) 144mJ d) 168 mJ

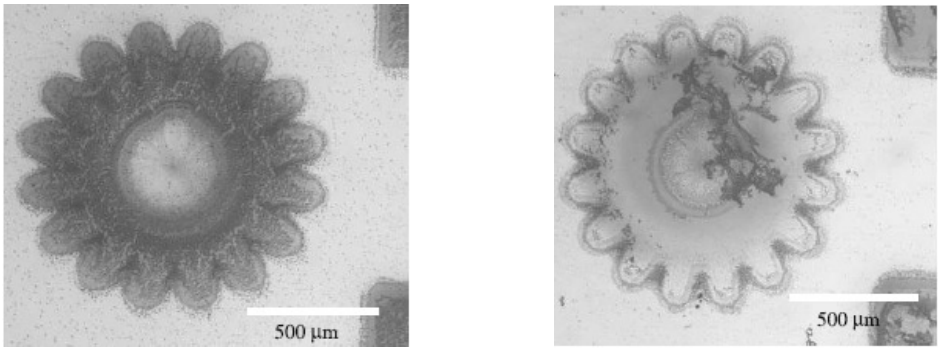

Fig. 4.4: Single layer of 2 shots at e) 120mJ f) 170 mJ

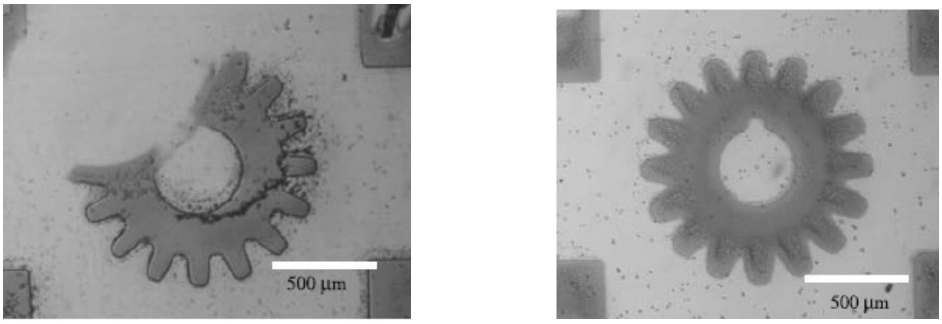

Fig. 4.5: Single layer of 3 shots at g) 120mJ h) 170 mJ

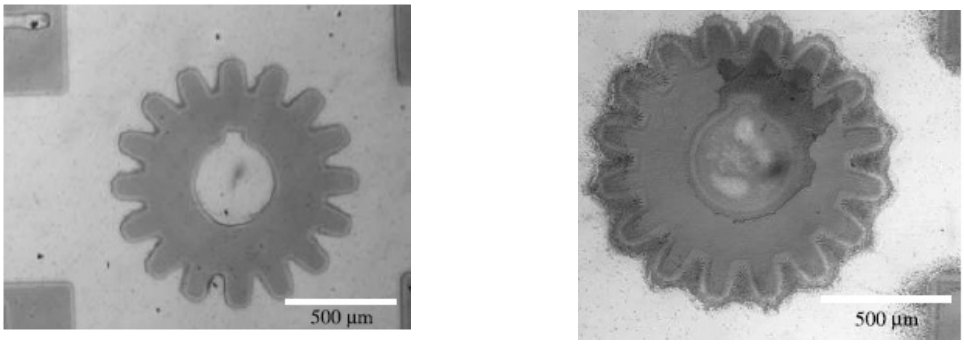

Fig. 4.6: Single layer of 4 shots at i) 130mJ j) 170 mJ

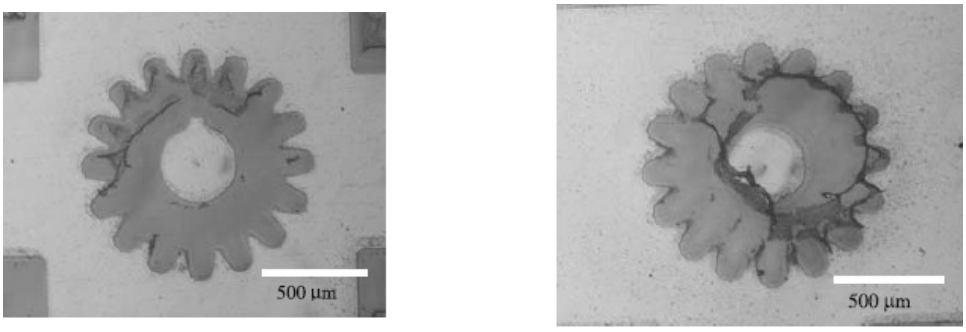

Fig. 4.7: Single layer of 5 shots at k) 130mJ L) 180 mJ

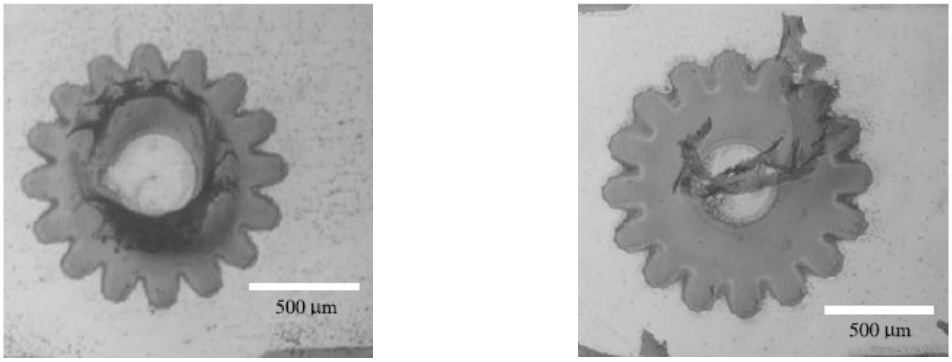

Fig. 4.8: Single layer of 10 shots at m) 160mJ n) 180 mJ

Hence, several attempts were made to expose the SL5510 at even lower energy levels (< 64 mJ) and the optimal combination obtained was two shots at 16 mJ, as shown in Fig. 4.9 below.

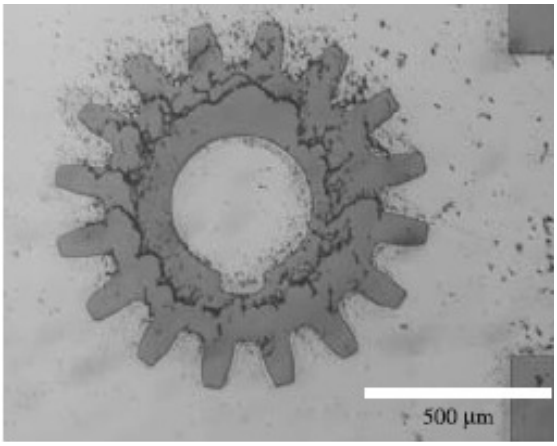

Fig. 4.9: Single layer of 2 shots at 16 mJ

Therefore, it was proven that SL5510 liquid photopolymer can be photopolymerised under excimer laser with the correct selection of energy level and number of laser shots.

4.1.3 Single Layer of SU8 Photoresists

The SU8-5 photoresists was spin-coated on a glass substrate at 5000 rpm to achieve a thickness of about 2µm and exposed to various energy levels with the 4 inch photomask. The SB and PEB were fixed at 65°C and 95°C for 2 and 5 min respectively. After several trials, the optimal parameter for a single SU8 layer was a single exposure of 72mJ. Fig. 4.10 shows the outcome. The teeth and alignment mark can be seen clearly after the development.

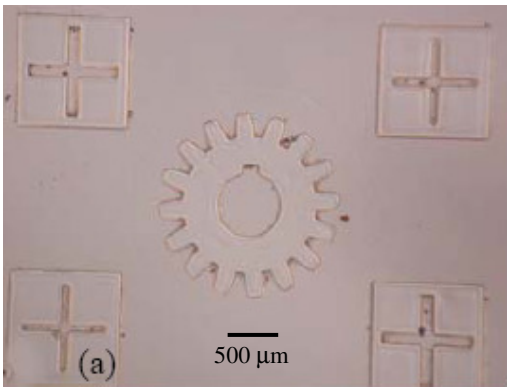

Fig. 4.10: Optical view of a developed SU8 after exposure to single shot of 72mJ.

4.1.4 Important Parameters of Single Layer Experiments

The important parameters for both photopolymer and photoresists are substrate cleanliness, exposure dosage, development duration and air gap (between the photomask and coated substrate).

Cleanliness would affect the adhesion of the coated material to the substrate. Higher exposure dosage would give better adhesion but resolution may be compromised, i.e. overexposed. See Fig 4.2 to 4.9.

Prolonged development and insufficient exposure may result in delamination or peeling of the thin layer from the substrate.

Air gap between the photomask and substrate would cause diffraction and hence, loss of resolution (sharpness) would result. Therefore, it was important to keep the air gap as small as possible to reduce the diffraction effect. Gaps that are greater than 100 µm

would cause loss of sharpness. Fig. 4.11 shows one example, captured by optical microscope. See Appendix H for more illustrations of the diffraction effect.

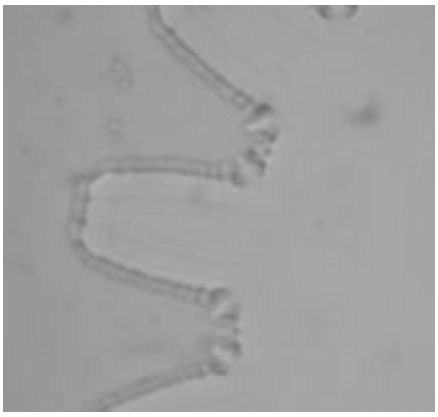

Fig. 4.11: SU8 on glass with 20mJ exposure of 500 μm gap

4.2 Analysis of Multi-layers

The parameters obtained from the single layer experiments were used in the multi-layered experiments. As the viscosity of SL5510 was lower than NOA 60, it was easier to spin-coat for multiple layers. Furthermore, lower viscosity makes development much easier than NOA 60. Therefore, SL5510 was selected as the material for the multiple-layer experiment.

4.2.1 Multi-layers of SL5510 Photopolymer

Based on the single layer experiments, the multiple-layer lithography was therefore conducted using the photopolymer SL5510 and the optimal parameters, obtained in section 4.1.2.

After the first layer was solidified by first exposure, the substrate was recoated with the second layer and placed into the *exact original position* under the photomask by using a special fixture, for another round of exposure. The process was repeated and a total of five layers were cured, resulting in a five layered microgear being fabricated. The SEM result is shown in Fig. 4.12.

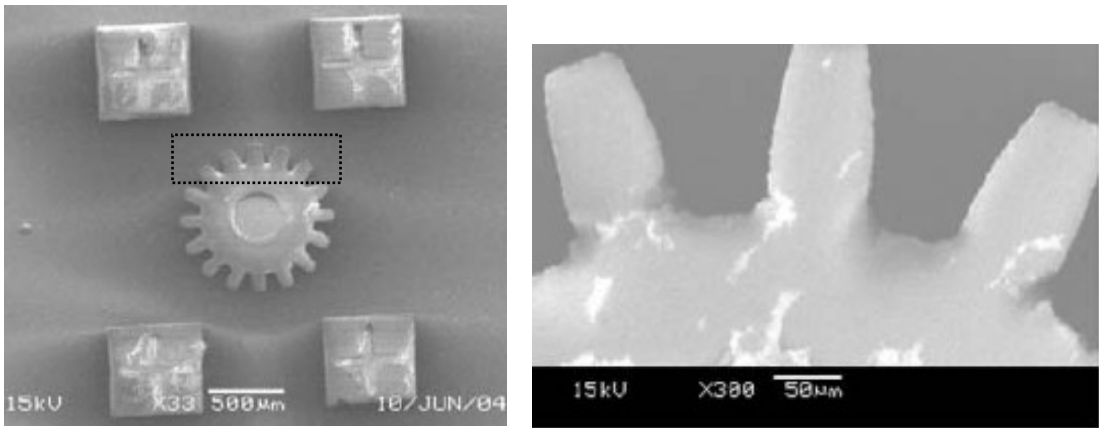

Fig. 4.12: SEM view of a 5 layered microgear a) overview b) 300x magnification of highlighted area.

The result showed that the 2.5D micron-scale structure of the microgear was rather good with sharp features, like the gear teeth. The alignment marks (in four corners) were also well formed in a 2.5D micron-scale structure, with a cross sign in the center (Fig. 4.12a). This result proved that the mask-based lithography for 3D layered microfabrication was feasible, although only a 2.5D object was fabricated in this case.

4.2.2 Multi-layers of SU8 Photoresists

In the earlier section, a 2.5D microgear was fabricated using the SL5510 photopolymer, as the same microgear pattern was used throughout the five layers. In an attempt to prove a complex 3D micron-scale structure could also be fabricated by this method, different

microgear patterns (0.5^0 differences between each microgear pattern as mentioned in section 3.2.3) on the photomask would be used.

Hence, it was necessary for the subsequent layer to be aligned to the previous layer in this multi-layer experiment. After the final layer was post baked, the substrate was put into the developing solvent for development, where the unexposed photoresists was dissolved, displaying a solidified 3D micropart. Fig. 4.13 show a three layered "twisted" 3D microgear on a glass substrate.

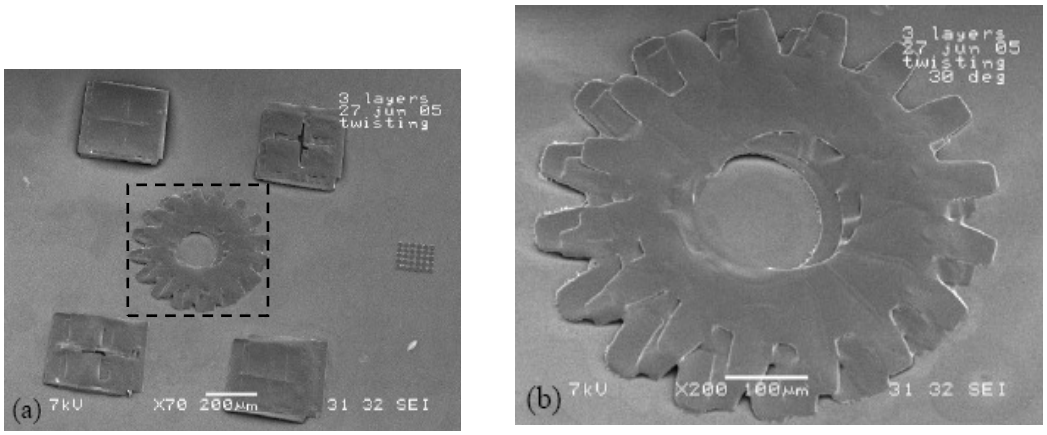

Fig. 4.13: SEM view of 3 layered SU8 microstructure a) overview b) magnification of microgear.

From Fig. 4.13b and Fig 4.14, we can see that the hub was not aligned to the previous layers. Although the three layers of SU8 were not aligned to each other, the three individual layers could be clearly seen in Fig 4.14b. This was due to the limitation of current alignment method and equipment (Refer to section 3.2.1 and 3.4.2). Therefore, with better alignment equipment, this misalignment issue can be overcome. The key difference between the commercial contact aligner and our current set up is the precision control. Detailed discussion of the misalignment would be discussed in section 4.2.4.2. After many experiments and analysis, the optimal exposure energy for each layer was

between 60 mJ to 80 mJ. A taller microgear could also be obtained by building up more layers.

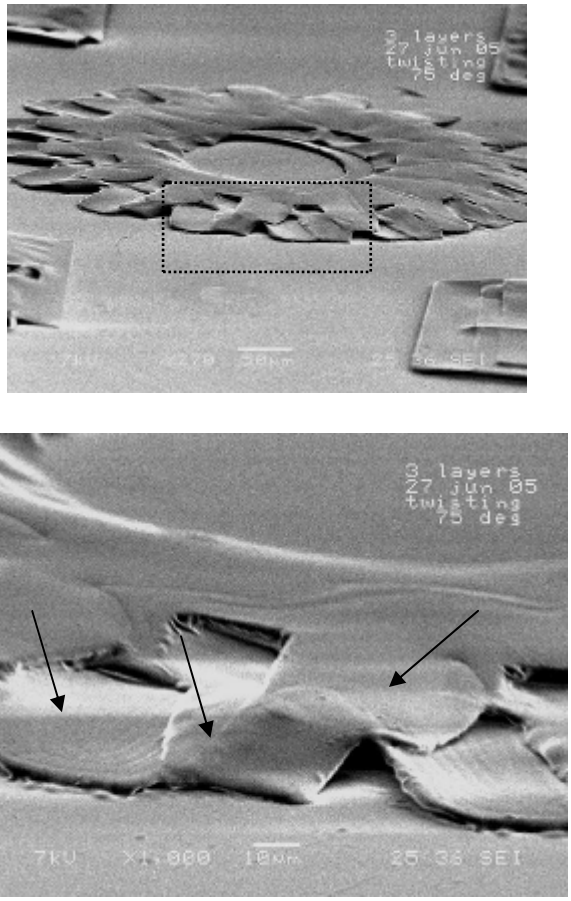

Fig. 4.14: 3D SEM view of a) 3 layered microgear b) 1000X magnification of highlighted area

4.2.3 Key Parameters for Multi-layers SU8

In a comparison of SU8 photoresists and SL5510 photopolymer, it was found that building the multi-layers of SU8 was more complicated and more time consuming, due to the fact that *each SU8 layer* needed to have two baking processes; SB before and PEB after each exposure.

The key parameters for SU8 photoresists was the same as those in single layer experiments, which was mentioned in section 4.1.4. i.e. substrate cleanliness, exposure dosage, duration of developing and air gap. However, in multi-layers of SU8, the baking parameter played a more critical part. Section 4.2.4.3 will explain in greater detail.

4.2.4 Defects in SU8 Photoresists

The following defects happened in both single and multi-layers SU8, except for misalignment which only occur in multi-layers.

4.2.4.1 Delamination

Fig. 4.15 below shows the edges of the teeth being delaminated from the substrate. Delamination can happen for the following four reasons:

- Substrate not clean properly
- Underexposure
- Prolong development especially in ultrasonic condition
- Uneven UV distribution of the lamp / laser

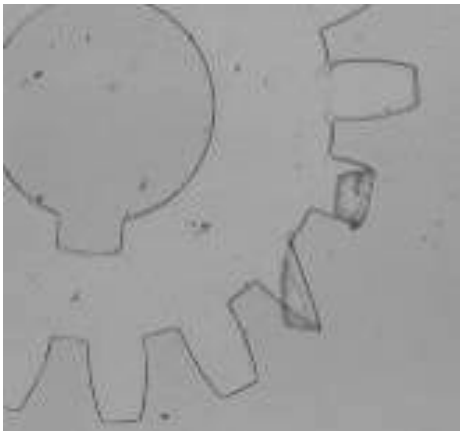

Fig. 4.15: Delamination of SU8 on glass substrate

4.2.4.2 Misalignment

The reason for the misalignment in multi-layers SU8 photoresists is explained below.

Fig. 4.16 below shows an example of the misalignment of the 2nd layer to the 1st layer at the key hub.

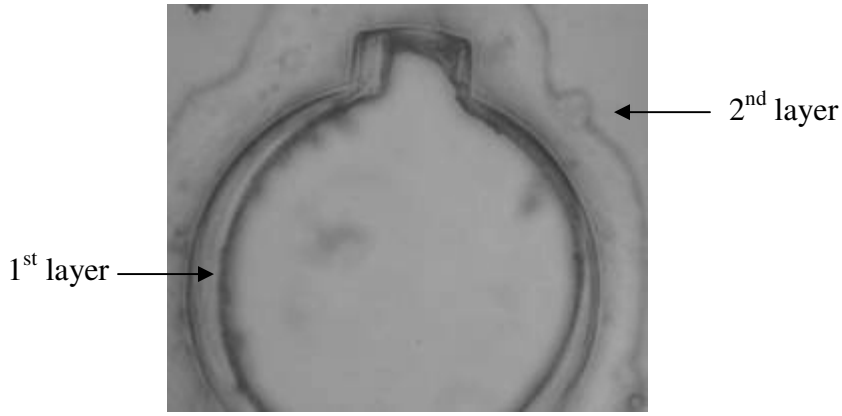

Fig. 4.16: Misalignment of the microgear keyway

Fig 4.17a shows the blurriness of alignment marks after the second layer of SU8 was spin coated onto the first layer, while Fig. 4.17b shows sharp features of the marks on the photomask.

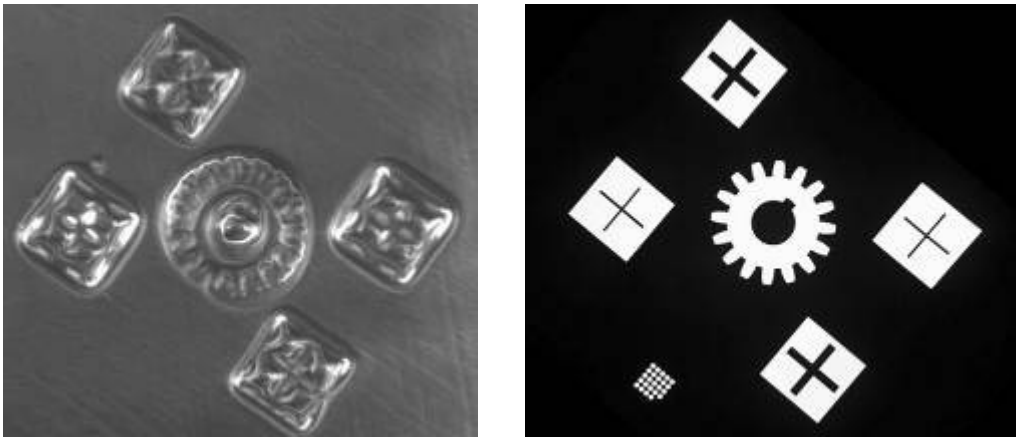

Fig. 4.17: Alignment marks a) on brass substrate after second layer b) on the photomask

When the photomask (Fig 4.17b) is moved over the coated substrate (Fig. 4.17a) for alignment, it will appear like Fig. 4.18.

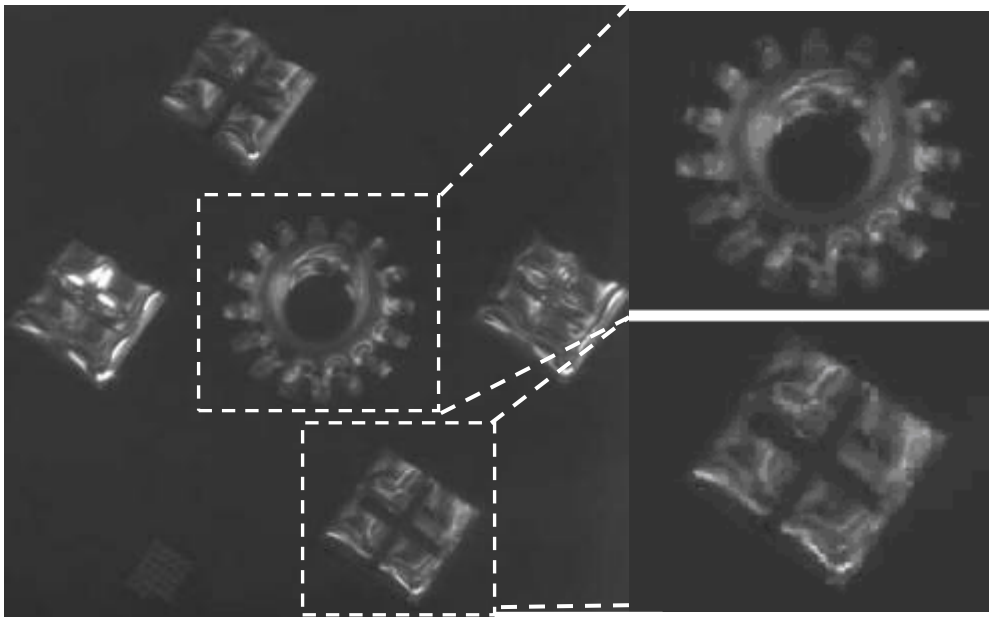

Fig. 4.18: Visibility of alignment marks for aligning process

Hence, it was difficult to get an accurate alignment of the photomask to the coated substrate which thereby resulted in the misalignment. This was due to the slight difference in the reflective index of the uncured and cured SU-8, which makes the "bending" light too minimal for us to see two separate mediums.

4.2.4.3 Loss of Resolution

Baking parameters (SB and PEB) play an important role in the resolution. To learn the effect of baking, all parameters were kept the same except for the parameter of SB and PEB. The results are shown in the Fig. 4.19 to 4.22.

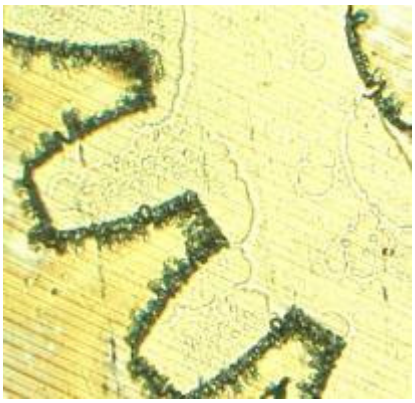

Fig. 4.19: Effect of *under SB* on SU8 on brass

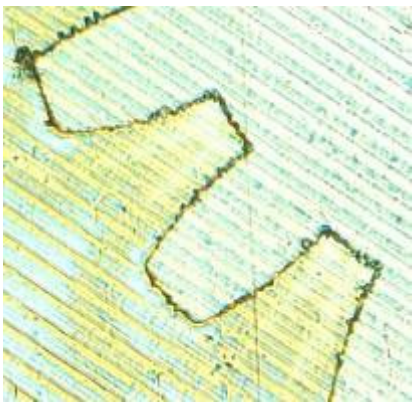

Fig. 4.20: Effect of *over SB* on SU8 on brass

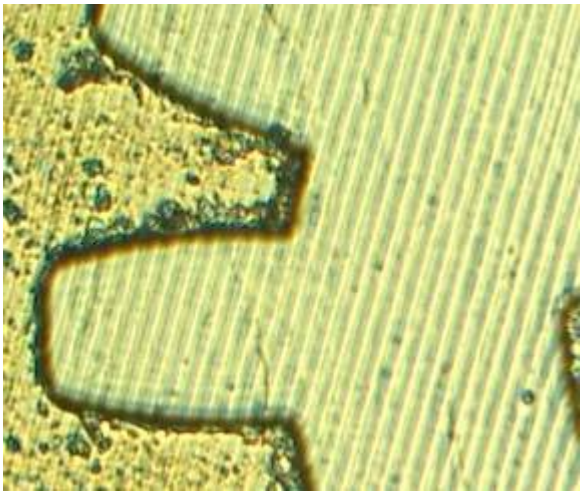

Fig. 4.21: Effect of *under PEB* of SU8 on brass

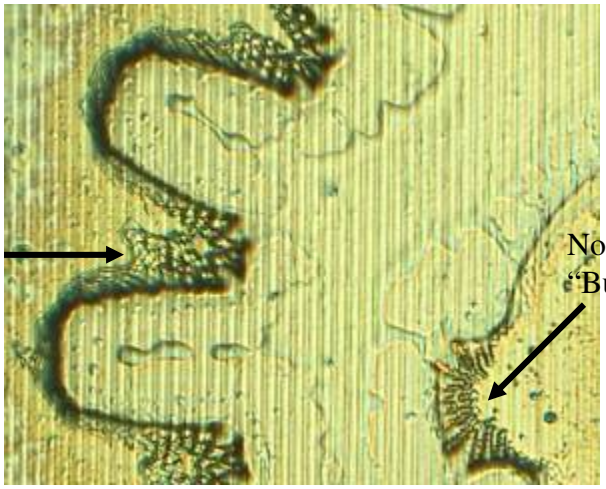

Fig. 4.22: Effect of *over PEB* of SU8 on brass

The duration of SB and PEB were determined by the layer thickness. Hence, accurate baking duration was difficult unless the thickness of the layers could be measured accurately.

Therefore, both these baking requirements and the blurriness (Fig 4.18) made SU8 multi-layers difficult to achieve.

4.3 Analysis of Micromoulds

In order to determine if the micromould fabricated by vacuum casting was repeatable, a total of ten silicone rubber micromoulds were fabricated from a single master SU8 microgear. This master microgear (38 μm thick) is shown in Fig. 4.23. However, it was fabricated by UV lamp lithography instead of excimer laser since the number of layers to build a thick microgear via excimer laser would be too tedious.

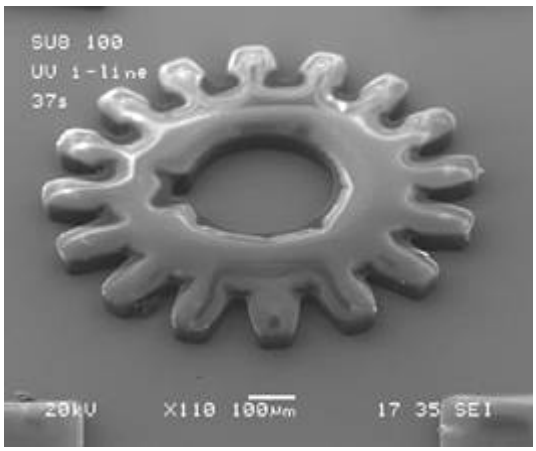

Fig. 4.23: Master microgear by UV lamp lithography

White light interferometry (WLI) was used to analyse the dimensional accuracy and repeatability of both the micromoulds and master microgear. Full details of WLI can be found in [104].

A set of measurements has been defined for the measurement of master microgear and micromould. Fig. 4.24 below illustrates the definition:

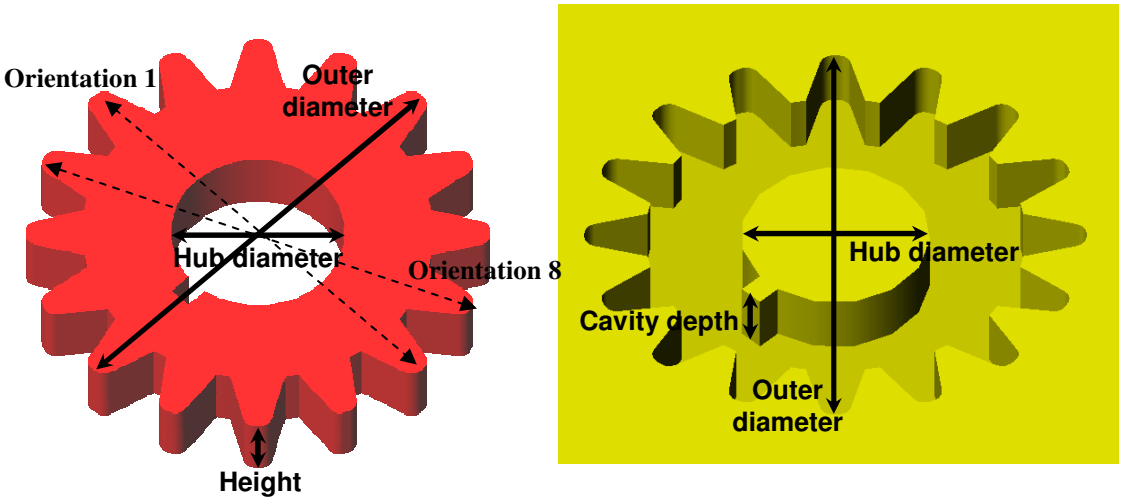

Fig. 4.24: Defined measurement for master microgear and micromould

4.3.1 Methods of Determining the Dimensions

Many possible errors (by machine or operator) could occur during measurement. In order to capture consistent and accurate dimensions by the WLI, the temperature was fixed at 25°C in a clean room environment, as any dirt particles may affect the readings.

4.3.1.1 Measurement of Outer Diameter

From Fig. 4.24, the outer diameter for both the microgears and micromoulds was defined as the average tooth-to-tooth distance of two oppositely-facing gear teeth. Fig. 4.25 shows the sample image of the dimension of the master microgear outer diameter for *orientation 1* by WLI. The outer diameter is 1.013 mm as highlighted.

Since this was a microgear with 16 teeth, there were therefore, *eight possible orientations* which the tooth-to-tooth distance can be measured. Measurements were taken from these eight orientations to account for any non-uniformity or roundness in the gear. The measurement at each orientation was repeated a second time to reduce the operator's error and the error imposed by the equipment tolerance. To maintain consistency, the microgear diameter was measured with reference to the top surface of the microgear specimen. The tabulated results of the master microgear is shown in section 4.3.2.

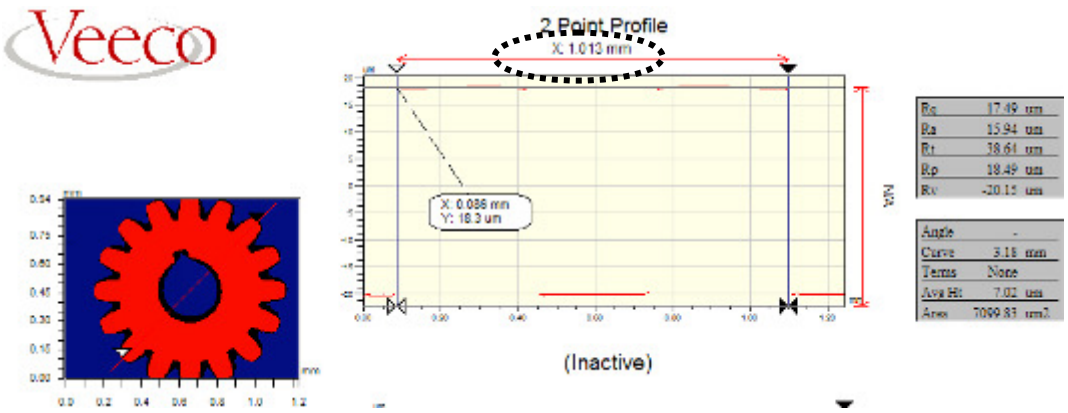

Fig. 4.25: Outer diameter of the master microgear in orientation 1

4.3.1.2 Measurement of Hub Diameter

Similarly, the hub diameter for both the micromould and microgears was defined as the average of sixteen diameter values taken from eight orientations. Measurements were again, taken from the eight possible orientations to account for any non-uniformity in the hub. A second measurement at each orientation was also conducted so as to reduce the operator's error and the error imposed by the equipment tolerance.

4.3.1.3 Measurement of Microgear Height / Micromould Depth

The average dimension for the microgear height and micromould depth was calculated automatically by the software. Details on how this data was capture by WLI can be found in Appendix I.

4.3.2 Master Pattern SU8 Microgear

The calculated average dimension of the outer diameter SU8 master microgear captured by WLI is shown below:

Table 1: Average calculation of outer diameter dimension of master SU8 microgear

Orientation	Reading 1/µm	Reading 2/µm	Average/µm
1	1013	1011	1012.0
2	1011	1011	1011.0
3	1012	1013	1012.5
4	1014	1013	1013.5
5	1014	1014	1014.0
6	1015	1016	1015.5
7	1012	1013	1012.5
8	1012	1012	1012.0
		Average outer diameter	1012.875

Using the same method to calculate the hub diameter of the master microgear, it was determined that the average hub diameter was 333.375µm,

Table 2: Average calculation of hub diameter dimension of master SU8 microgear

Orientation	Reading 1/µm	Reading 2/µm	Average/µm
1	331	330	330.5
2	335	336	335.5
3	335	333	334.0
4	334	334	334.0
5	334	333	333.5
6	332	331	331.5
7	337	336	336.5
8	331	332	331.5
		Average hub diameter	333.375

Using the software in the WLI to generate the average microgear height, the average for the master microgear is 38.46µm, as shown in Fig. 4.26 below.

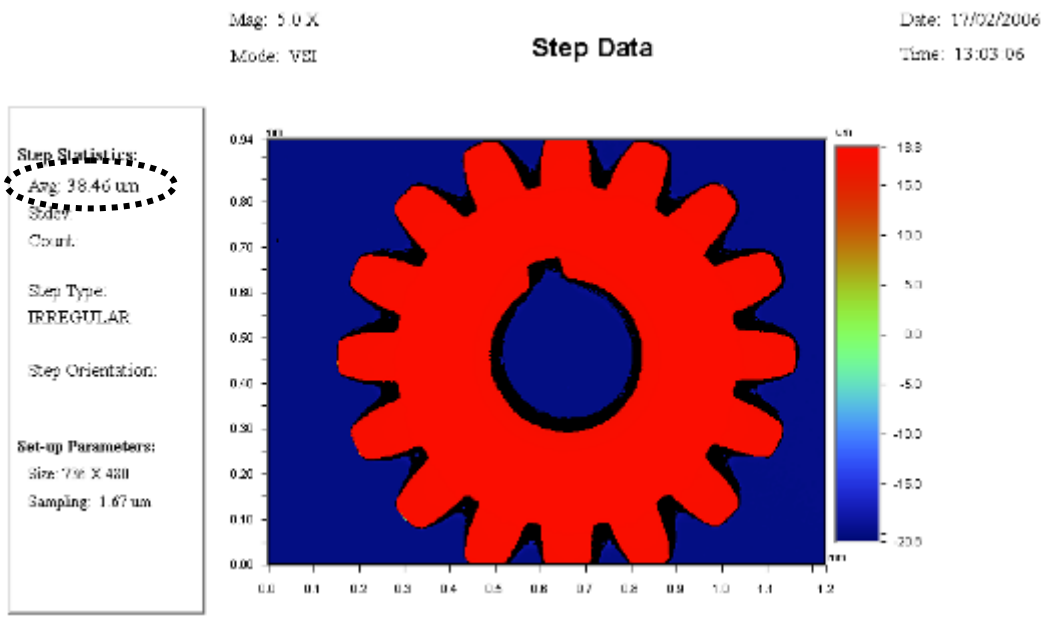

Fig. 4.26: Average height of SU8 master microgear

Hence, the final average dimension of the master microgear is :

Table 3: Average dimension of master SU8 microgear

	Outer Diameter (µm)	**Hub Diameter (µm)**	**Gear Height/Cavity Depth (µm)**
Master microgear	1012.87	333.38	38.46

4.3.3 Silicone Rubber Micromould

Using the definition set in section 4.3.1 and method illustrated in section 4.3.1.1 to measure the respective dimension for the micromoulds, the overview results of the ten

silicone rubber micromoulds (specimen A to J) is shown in the form of a graph (Fig. 4.27).

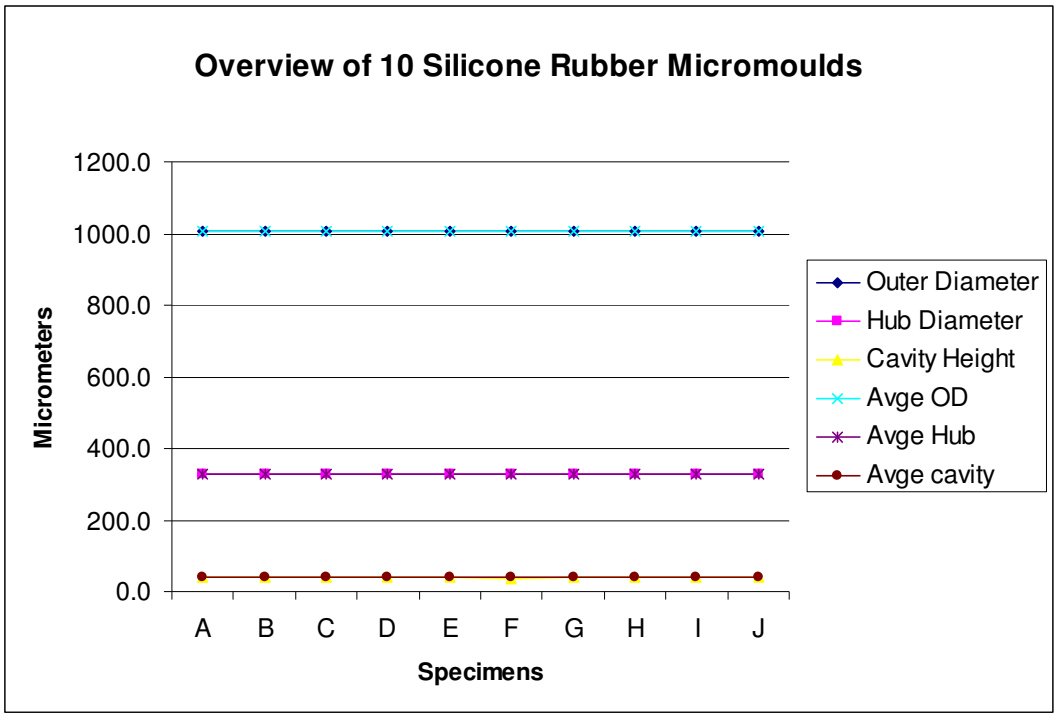

Fig. 4.27: Overview of the dimension of 10 micromoulds

The reproducibility of the micromoulds via vacuum casting can be described by plotting the ten specimen values for a particular dimension, such as the outer diameter, on a graph and calculating their standard deviation. By calculating their standard deviation, which is a standard measure of spread, reproducibility would be demonstrated. The smaller the value, the higher the level of dimensional consistency in the microcavities produced, and hence the greater the reproducibility of the microcavity dimensions. When examined closely into each of the specific dimensions, the following graphs for outer diameter (Fig.4.28), hub diameter (Fig. 4.29) and depth of the micromould (Fig.4.30) were obtained.

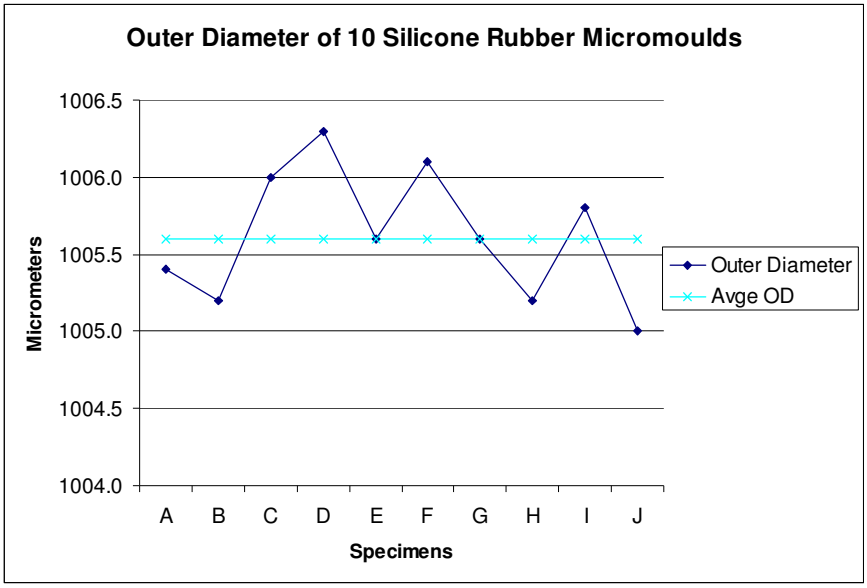

Fig. 4.28: Comparison between actual and average dimension of outer diameter

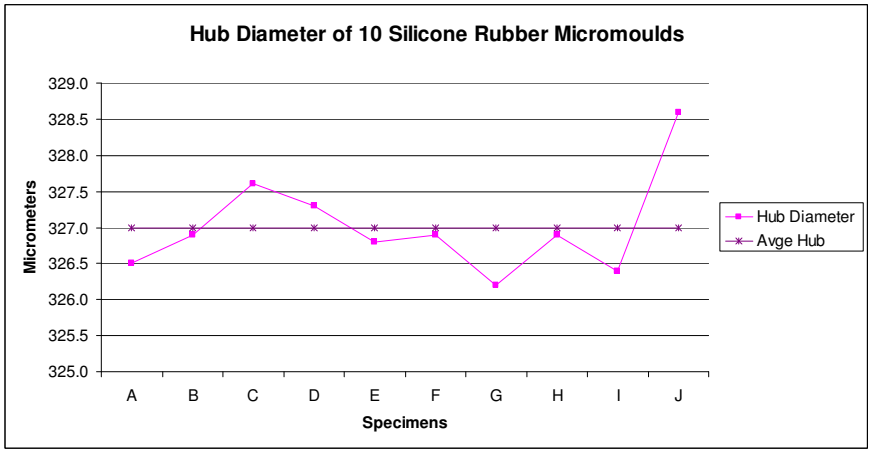

Fig. 4.29: Comparison between actual and average dimension of hub diameter

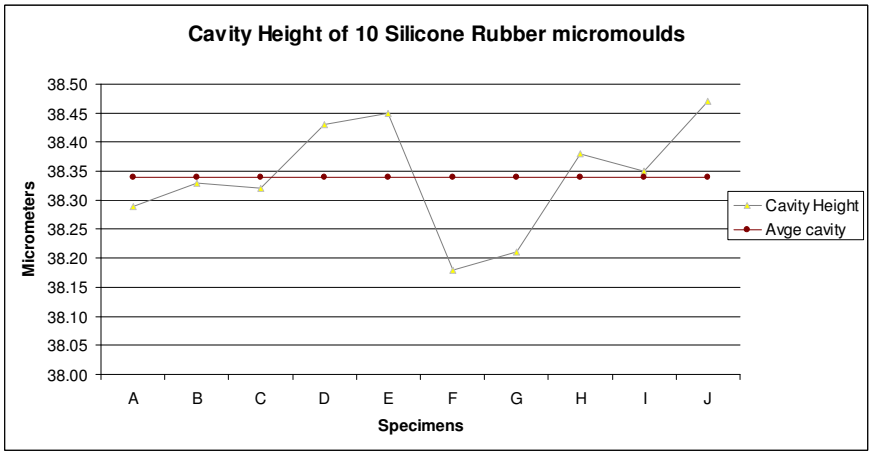

Fig. 4.30: Comparison between actual and average dimension of cavity height

From Fig. 4.28 to Fig. 4.30, although the actual specific dimension (outer diameter, hub diameter, depth of micromould) appears to deviate alot from their average line, the largest difference is only 1.6 µm for the hub diameter while the smallest difference is 0.1 µm for hub diameter. The standard deviation works out as 0.421, 0.693 and 0.0968 for outer diameter, hub diameter and cavity depth respectively. Hence this proved that the vacuum casting is capable of producing repeatable micromoulds (standard deviation < 1). Some SEM images of the micromould are shown in Fig. 4.31. The data table used to generate the above graphs can be found in Appendix J.

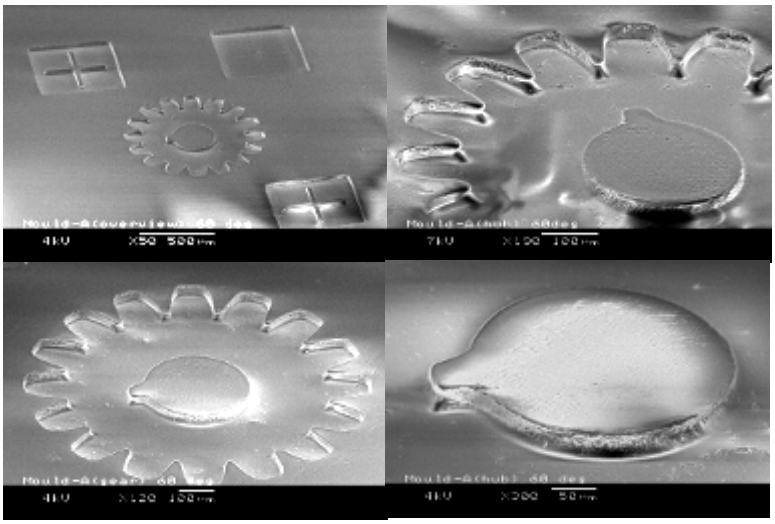

Fig. 4.31: SEM images of silicone rubber micromould

4.3.4. Comparison of Master Microgear with Micromoulds

After knowing that there was good consistency among the 10 micromoulds, it would be pointless if the dimension of the micromoulds were not close to the master pattern microgear, since moulds are meant to reproduce many specimens that are dimensionally close to the master.

The results below show the respective micromould dimension against the dimension of the master microgear. The calculation of the average micromould specimens can be found in Appendix J.

Table 4: Comparison between master microgear and ten specimens

	Outer Diameter (μm)	**Hub Diameter (μm)**	**Gear Height/Cavity Depth (μm)**
Master SU8 Microgear	1012.9	333.4	38.46
Average Micromoulds Specimens	1005.6	327.0	38.34
Deviation (%)	0.72	1.92	0.31

Table 4 gives a comparison between the master microgear and the micromoulds produced in the ten specimens. Generally, the results showed that the micromould cavities are physically smaller than the master gear used to fabricate them, with average dimensions smaller than that of the master gear. This result confirmed the occurrence of mould shrinkage due to a drop in mould temperature which comes from the curing temperature of around 40^0C to the room temperature of around 25^0C where micromoulds were measured and stored.

From Table 4, it shows that the average micromould diameter differs from that of the master microgear by 0.72%, while the average hub diameter differs by 1.92%. The average micromould depth is comparable to the master microgear height, deviating by only 0.31%. These highlight the dimensional accuracy of the microcavities in relation to the master gear.

It should be noted that since the micromould cavities had experienced some form of shrinkage when the measurements were taken, it was possible that the actual dimensions of the micromoulds produced may be even closer to the corresponding dimensions of the master microgear if the micromoulds were preheated to 40°C before the measurements were performed.

4.4. Key Parameters for Micromould Fabrication

4.4.1 Amount of Catalyst

The recommended catalyst (for VTV 750) dosage was ten percent the weight of the silicone rubber used. After many extensive tests, it was observed that a slightly heavier dosage of up to fifteen percent was still acceptable without compromising the mould quality. However, excessive use of catalyst would shorten the mould life and make it susceptible to tearing [105]. On the other hand, partial curing would occur should there be an inadequate dosage. This was evident from the stickiness and softness of the catalyst-deficient regions on the mould surface as shown in Fig 4.32.

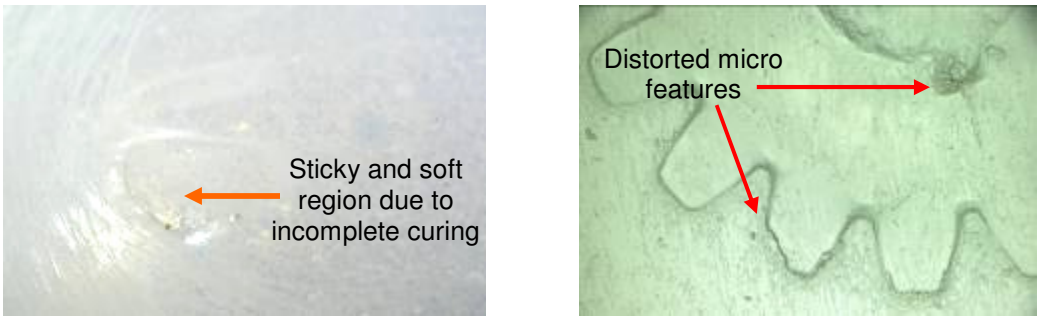

Fig. 4.32: Partial curing at mould surface (left) and micro gear cavity (right)

The features of the micromould would be distorted, thereby rendering the micromould defective where the vicinity of the micromould was not fully cured. Another factor was the poor mixing of the silicone rubber and the catalyst, causing catalyst-deficient regions to be form and leading to incomplete curing of the silicone rubber, similar to the case in which insufficient catalyst was added to the silicone rubber.

4.4.2 Mixing and Degassing Duration

The bulk of the micromould fabrication time consisted of the mixing and degassing duration. This duration had to be controlled carefully to ensure that the total processing time does not exceed the pot life of the silicone rubber. Pot life is defined as the time that it remains fluid [106]. If the pot life is exceeded during degassing, formation of voids would occur in the micromould. This is because the silicone rubber would start to cross-link and harden at the same time when air was being removed from the silicone rubber mixture. The hardening silicone rubber would trap the remaining air bubbles inside and cure around them to form voids permanently in the mould (Fig 4.33b). These voids would distort the features of the micromould.

Furthermore, the hardening silicone will cure around the air bubbles that collect on the top surface of the silicone rubber in the casting frame during degassing. This will result in a permanently rough mould surface upon curing as shown in Fig 4.33a.

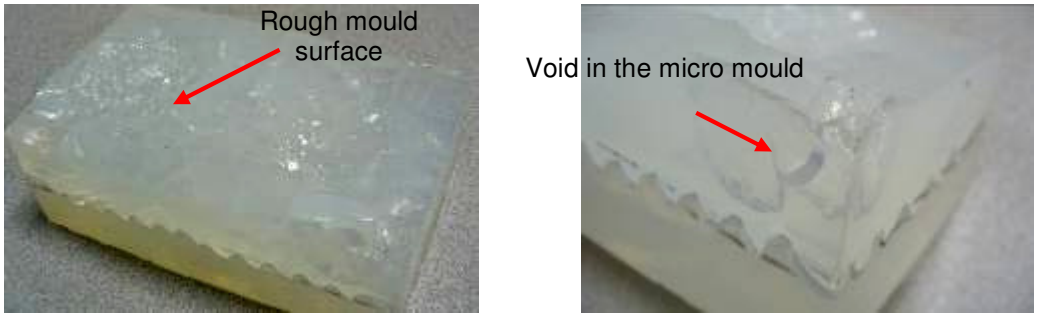

Fig. 4.33: Void formation in mould due to degassing beyond silicone pot life

Therefore, the solution to produce a void-free micromould with smooth surface was to ensure that the degassing process was completed before the pot life of silicone rubber was exceeded. The mixing time must be kept to a minimum yet a thorough mix must be ensured between the silicone rubber and catalyst.

From the experiments, it was generally observed that a duration of 2 to 5 minutes of mixing using a high speed mixer was good enough to ensure the thorough mixing and complete curing of the silicone rubber. It was also empirically found that a duration of 10 to 15 minutes for the first degassing process was able to remove most of the air in the silicone rubber while ensuring that it was still fluid enough to be poured into the casting frame to make the micromould. For the second degassing process, a maximum degassing time of 25 to 35 minutes was found to be permissible before silicone rubber started to show signs of hardening.

4.4.3 Curing Duration and Temperature

The curing temperature was found to have an influence over the curing time of the silicone rubber. In the moulding industry, higher temperatures are used to cure the silicone rubber in order to reduce the curing time [105, 106]. For VTV 750 silicone

rubber, the experimental curing temperatures and their approximate curing times are shown in Table 5. These experimental results proved to be consistent with the general observation that a higher curing temperature leads to a shorter curing time.

Table 5: Experimental cure times/temperatures for VTV 750 silicone rubber

Cure Temperature (^{0}C)	25	40	55	70
Approximate Cure Time (hours)	24	10-12	4-6	2-3

By convention, it has been recommended that the silicone rubber mould be cured at 40^{0}C to achieve "extreme dimensional accuracy in the castings" [107]. Since dimensional accuracy was crucial, experiments were done to ascertain any relationship between the curing temperature and the dimensions of the micromould in the silicone rubber mould.

Table 6: Micromould cavity under different cure temperatures

Cure Temperature (^{0}C)	**Outer Diameter (μm)**	**Hub Diameter (μm)**	**Cavity Depth (μm)**
25	1005.7	326.4	38.39
40	1005.6	326.1	38.20
55	1005.4	326.4	38.47
70	1005.7	326.9	38.41

From Table 6, we can see that there was no obvious relationship between the curing temperature and the dimensions. Hence, this implied that curing temperature was not a major factor and that micromoulds are producible from a wide range of curing temperatures without compromising the dimensional quality. Nevertheless, it would be good to conduct more tests to check for any relationship between the cure temperature and other properties, like the material properties of the micromoulds made. Taking other

factors like lead time savings into consideration, the cure temperature was fixed at between 40^0C to 45^0C, so that a micromould can be produced within a day.

5. CONCLUSIONS

The objective of this research is to develop a novel method to fabricate 3D micron-scale structures as well as to develop an alternative moulding method that is simple to implement, has fewer processing steps, and reduces cost and lead time compared to many existing moulding methods. In order to demonstrate that this vacuum casting (with silicone rubber) method is a viable alternative to existing moulding techniques, a total of ten silicone rubber micromoulds were fabricated from a single master SU8 photoresists microgear (38μm thick).

For single layer lithography, the optimum process parameters to fabricate single layer microgear for all three materials (NOA 60, SL5510 and SU8) were realised. The optimum parameters for NOA 60 is 10 shots of 100 to 110mJ range (See section 4.1.1), while the optimum parameters for SL5510 is 2 shots of 16mJ (See section 4.1.2). As an additional step of baking is needed for SU8 photoresists, the optimum parameter is a single shot of 72mJ, with SB baking of 65^0C and PEB at 95^0C, for 2 and 5 min respectively (See section 4.1.3).

In the case of NOA 60, multi-layer experiments were not performed because of the residual photopolymer that still remained after developing with alcohol. However, NOA 60 may still be suitable for multi-layer fabrication if a better solvent is found to fully develop the microgear cleanly.

Based on the RP principle of building layer-by-layer, a novel method was proposed to create a 3D micron-scale structure via the multi-layered lithography. The process can be used for creating 3D microparts or even metal micromould via electroforming [55].

An experimental setup was constructed successfully according to the principle of the process, and a photomask which carries multiple layers patterns was built and used in the experiment. The single and multi-layers lithography experiments of SL5510 photopolymers demonstrated that the mask-based lithography for 3D layered micro-fabrication is feasible. A five layered microgear of 1 mm in diameter with 60 μm features has also been fabricated successfully using the proposed method. The results can be seen in Fig. 4.12.

We have also shown that liquid SU8 photoresists can be photopolymerised by excimer laser (248nm) instead of the usual UV lamp. A series of single layer lithography has been tested, and multi-layer fabrication via the RP principle has also been demonstrated. Although the 3-layered 500 μm diameter micron-scale structure created was not aligned accurately due to the current alignment method, nevertheless, it still demonstrated that it is possible to create 3D micron-scale structures with the RP principle combined with 3D lithography. With better equipment and alignment method, an accurate 3D micron-scale structure with more layers is certainly possible.

The important parameters for both photopolymer and photoresists are substrate cleanliness, exposure dosage, development duration and diffraction caused by the air gap

between the photomask and coated substrate. In the case of SU8 photoresists, additional baking parameters (SB and PEB) are paramount to obtain a good resolution, since the baking process is needed during the microfabrication process.

We have also successfully demonstrated the use of the vacuum casting technique in fabricating micromoulds. The small deviations between the master pattern and the ten micropart specimens have proven that the proposed method is capable of consistently producing microparts that are dimensionally accurate with respect to the master pattern. In addition, this technique is much faster and cheaper than many existing micromoulding techniques. Therefore, we believe that the simplicity of this vacuum casting technique would encourage its wider use in microfabrication and is more suitable than current moulding methods for casting 3D microparts (since the mould is flexible).

Hence, the objective of this project has been achieved since a novel method has been setup and successfully fabricated two micron-scale structures (1mm with SL5510 photopolymer and 3-layered 500 μm diameter with SU8 photoresists) while the silicone rubber micromoulds fabricated by the vacuum casting technique has shown very small standard deviation (0.1% to 0.7%) among itself and are very close to the dimension of the master pattern.

6. RECOMMENDATIONS

To overcome the misalignment of the 3-layered (SU8 photoresists) micron-scale structure, better equipment for alignment such as a commercial aligner should be used. This should be possible since alignment to previous layers using photomask via aligner is already very established in the semi-conductor industries.

The current master pattern (SU8 microgear) used is not sufficiently complex and since vacuum casting is able to cast complex 3D microparts, the master pattern can be a complex 3D part. This will demonstrate the power of the method.

To prove metal micron-scale structure can also be cast with the silicone rubber micromould, a low melting metal such as bismuth can be used and with the subsequent specimen compared with the master pattern.

Since shrinkage of PDMS has been investigated by several researchers [59 – 60], shrinkage of silicone rubber should be investigated, so that comparison can be done between PDMS and silicone rubber, in terms of accuracy.

Lastly, it would be ideal if the experiments are conducted in clean room environment to ensure that particles do not contaminate the parts.

References

[1] Patri K. Venuvinod and Weiyin Ma, "Rapid Prototyping – Laser-based and other technologies," USA: Kluwer Academic Publishers, 2004.

[2] Vijay K. Varadan, Xiaoning Jiang and Vasundara V. Varadan, "Microstereolithography and other fabrication techniques for 3D MEMS," New York: Wiley, 2001, pp. 121-123

[3] Maruo S, Nakamura O, Kawata S "Three-dimensional microfabrication with two-photon-absorbed photo-polymerization", Optics Letters, Vol 22, 1997, pp 132–134.

[4] http://www.ni.com/images/csma/us/cs_microphotonics_fig2.jpg

[5] LZH website http://www.laser-zentrum-hannover.de/de/publikationen/pressemitteilungen/2006/20060421-Small_smaller_smallest.php

[6] Martin Heule, Sibylle Vuillemin and Ludwig J Gauckler "Powder based ceramic meso- and microscale fabrication processes", Advanced material, No. 15, 5 Aug 2003, pp 1237.

[7] Jennifer A. Lewis and Gregory M. Gratson, "Direct writing in three dimension", Materials today July/August 2004, page 32, Elsevier Ltd 2004

[8] Loose, K., Nakagawa, T. and Niino, T. (1997), ``Concept modelling using multiple LED photographic curing'', Proceedings of 13th Rapid Prototyping Symposium, Yokohama, November, pp. 35-40.

[9] A. Bertsch, H. Lorenz and P. Renaud "3D microfabrication by combining microstereolithography and thick resist UV lithography", Sensors and Actuators A: Physical Volume 73, Issues 1-2, 9 March 1999, pp 14-23.

[10] Central Microstructure Facility website http://www.cmf.rl.ac.uk/latest/msl.html

[11] Bertsch, Arnaud-Jiguet, Sébastien - Renaud, Philippe, "Microfabrication of ceramic components by microstereolithography", J.Micromech Microeng, 14, 2004, pp 197 – 203.

[12] LZH website http://www.laser-zentrum-hannover.de/en/fields_of_work/material_processing/microtechnology/msl/index.php

[13] Arcam website http://www.arcam.se/technology/tech_ebm.asp

[14] MCP Group website http://www.mcp-group.com/rpt/rpttslm.html

[15] Website of Centre for Ion Beam Applications (CIBA), Department of Physics, National University of Singapore http://www.ciba.nus.edu.sg/pbw_publications.html

[16] Jonathan Wood, "Writing structures in Silicon", Materialstoday, July/August 2004, p 21.

[17] P.Calvert, Chem Mater 13, 2001, pp 3299.

[18] Satoshi Kawata and Hong-Bo Sun et al. "Finer features for functional microdevices", Nature 412, 2001, pp 697-698.

[19] Satoshi Kawata and Hong-Bo Sun "Two-photopolymerization as a tool for making micro-devices" Applied surface Sci, 208, 2003, pp 153.

[20] Fraunhofer Technology Development Group TEG website http://www.teg.fraunhofer.de/ueberuns/en

[21] J.Serbin, A.Egbert, A.Ostendorf et al "Femtoseconds laser-induced two-photon polymerization of inorganic-organic hybrid materials for applications in photonics", Optics letters vol 28, no.5, 1 march 2003, pp 301.

[22] Fraunhofer-Gesellschaft zur Förderung der angewandten Forschung e.V. München Website http://www.ormocer.de/EN/

[23] http://www.heise.de/bilder/69971/0/0

[24] Marius Albota, David Beljonne, Jean-Lic Bredas et al "Design of Organic Molecules with large Two-Photon Absorption Cross sections" Science Vol 281, 11 Sep 1998, pp 1653.

[25] Brian H.Cumpston, Sundaravel P.A, Stephen Barlow et al "Two-photon polymerization initiators for three-dimensional optical data storage and microfabrication", Nature, Vol 398, 4 MARCH 1999

[26] Irene Wang, Michel Bouriau and P.L.Baldeck "Three-dimensional microfabrication by two-photon initiated polymerization with a low-cost microlaser", Optics letters, Vol 27, no. 15, Aug 2002, pp1348

[27] C.Martineau, G. Lemercier, C.Andraud et al "New initiator for two-photon absorption induced polymerization with a microlaser at 1.60µm" Synthetic metals Vol 138, 2003, pp 353.

[28] C.Martineau, R.Anemian, C.Andraud et al "Efficient initiator for two-photon induced polymerization in the visible range" Chemical physics letters, 362, 2002, pp 291.

[29] J.H. Strickler, W.W. Webb, "Three-dimensional optical data storage in refractive media by two-photon point excitation" Opt. Lett., Vol 16 , Issue 22, 1991,pp 1780.

[30] M.M. Wang, S.C. Esener, "Three-Dimensional Optical Data Storage in a Fluorescent Dye-Doped Photopolymer", Appl. Opt. Vol. 39, Issue 11, 2000, pp 1826.

[31] Min Gu and Daniel Day, "Use of continuous-wave illumination for two-photon three-dimensional optical bit data storage in a photobleaching polymer" Optics Letters, Vol 24, Issue 5, 1999, pp 288.

[32] A. H. Buist, M. Müller, J. Squier and G. J. Brakenhoff "Real time two-photon absorption microscopy using multipoint excitation" Journal of Microscopy, Vol. 192, Pt 2, November 1998, pp. 217–226.

[33] Reza Salem "Characterization of two-photon absorption detectors for applications in high-speed optical systems" M.Sc thesis, 2003, Graduate School of the University of Maryland, College Park.

[34] Hong-Bo Sun and Satoshi Kawata "Two-photon laser precision microfabrication and its applications to micro-nano devices and systems" Journals of lightwave technology, vol 21, no.3, march 2003, pp 624.

[35] Katherine J. Schafer, Joel M. Hales, Mihaela Balu, Kevin D. Belfield, "Two-photon absorption cross-sections of common photoinitiators" Journal of Photochemistry and Photobiology A: Chemistry , 162, 2004, pp 497–502.

[36] N. H. Loh, S. B. Tor , B. Y. Tay Y. Murakoshi R. Maeda "Fabrication of micro gear by micro powder injection molding" Microsyst Technol, 14, 2007, pp 43–50.

[37] Rudolf Zauner, "Micro powder injection moulding", Microelectronic Eng, Vol 83, Issues 4-9, 2006, pp 1442-1444.

[38] Muralidhar K. Ghantasala, Jason P. Hayes, Erol C. Harvey, and Dinesh K. Sood, "Patterning, electroplating and removal of SU-8 moulds by excimer laser micromachining", J. Micromech. Microeng, Vol. 11, 2001, pp. 133 – 139.

[39] Eckart Uhlmann, Sascha Piltz and Ulrich Doll, "Machining of micro/miniature dies and moulds by electrical discharge machining—Recent development", Journal of Materials Processing Technology, Vol 167, Issues 2-3, 30 August 2005, pp 488-493

[40] Ayón, A. A., et al., "Etching Characteristics and Profile Control in a Time Multiplexed Inductively Coupled Plasma Etcher", Tech. Digest Solid-State Sensor and Actuator Workshop, Hilton Head Island, SC, June 8 - 11, 1998, pp. 41 – 44.

[41] Kupka, R. K., Bouamrane, F., Cremers, C., and Megtert, S., "Microfabrication: LIGA-X and applications", Applied Surface Science, Vol. 16, No. 1, 2000, pp. 97 – 110.

[42] Kim, S-H., Lee, S-H., and Kim, Y-K., "A high-aspect-ratio comb actuator using UV-LIGA surface micromachining and (110) silicon bulk micromachining", J. Micromech. Microeng, Vol. 12, 2002, pp. 128 – 135.

[43] EFAB website http://www.microfabrica.com/

[44] J.C Mcdonald and G.M Whitesides Poly(dimethysiloxane) as a Material for Fabricating Microfluidic Devices, Acc Chem Res, 35, 2002, pp 491-499.

[45] J. Lorenz, G. Schanz , N. Holstein , J. Konys "Electroplating of micro-patterned tools via replication of silicone rubber forms" Microsyst Technol , 12, 2006 pp 870.

[46] W P fleging, T Hanemann, M Torge and W Bernauer "Rapid fabrication and replication of metal, ceramic and plastic mould inserts for application in microsystem Technologies" Proc. Instn Mech. Engrs Vol. 217 Part C: J. Mechanical Engineering Science, pp 53.

[47] Malcolm C. Gower; Henry Helvajian; Koji Sugioka Laser Applications in Microelectronic and Optoelectronic Manufacturing VI Proc. SPIE Vol. 4274, p. 331-345; Jan J. Dubowski; Eds.

[48] Liu, X., Du, D., and Mourou, G., "Laser Ablation and Micromachining with Ultrashort Laser Pulses", IEEE Journal of Quantum Electronics, Vol.33, No. 10, 1997, pp. 1706 – 1716.

[49] Liwei Lin, Chun-Jung Chiu et al., "Microfabrication Using Silicon Mold Inserts and Hot Embossing", Seventh International Symposium on Micro Machine and Human Science 1996, pp 67.

[50] D. M. Cao, D. Guidry, W. J. Meng, K. W. Kelly "Molding of Pb and Zn with microscale mold inserts", Microsystem Technologies, Vol 9, 2003, pp 559–566.

[51] J. Schulz, K. Bade, M. Guttmann, L. Hahn, A. Janssen et al "Ensuring repeatability in LIGA mold insert fabrication" Microsystem Technologies, Vol 10, 2004, pp 419–422.

[52] Chen, R.-H., Chang, C.-C., and Cheng, C.-M., **"**Fabricating a micromould insert using a novel process", Int. Adv. Manuf. Technol, Vol. 25, 2005, pp. 678 – 684.

[53] The International LIGA-HARMST Commercialisation Group Website http://www.mancef.org/liga.htm

[54] Said Emre Alper, Ilker Ender Ocak, and Tayfun Akin, "Ultrathick and High-Aspect-Ratio Nickel Microgyroscope Using EFAB Multilayer Additive Electroforming", Journal of Microelectromechanical Systems, Vol. 16, No. 5, Oct 2007.

[55] S Thian, Y Tang, J Y H Fuh, Y S Wong, H T Loh, L Lu, and D Z S Tee, "Formation of micromoulds via UV lithography of SU8 photoresist and nickel electrodeposition", Proc. IMechE Vol. 220 Part B: J. Engineering Manufacture, pp 329

[56] Chua C.K., Leong K.F., and Lim C.S., "Rapid Prototyping: Principles and Applications", 2nd edition, World Scientific Publishing Co. Pte Ltd, 2003, pp. 306 – 310.

[57] Chung, S., Im, Y., Kim, H., Jeong, H., and Dornfeld, D. A., "Evaluation of micro replication technology using silicone rubber molds and its applications", International Journal of Machine Tools and Manufacture, Vol. 43, No. 13, 2003, pp. 1337 – 1345.

[58] Chung, S., Park, S., Lee, I., Jeong, H., and Cho, D., "Replication techniques for a metal microcomponent having real 3D shape by microcasting process", Microsystem Technologies, Vol. 11, 2005, pp. 424 – 428.

[59] M. Denoual, Y. Mace, B.L. Pioufle, P. Mognol, D. Castel and X. Gidrol, "Vacuum casting to manufacture a plastic biochip for highly parallel cell transfection", Measurement Science Technology, 17, 2006, pp 3134-3140.

[60] M. Denoual, P. Mognol, B. Lepioufle, "Vacuum casting, a new answer for manufacturing biosystems", Proc.IMechE part B: J. Eng. Manuf. 219, 2005, pp 697-701.

[61] S. Chung, Y. Im, H. Kim , H. Jeong, D.A Dornfeld, "Evaluation of micro-replication technology using silicone rubber molds and its applications", Int J. Machine tool & Manuf, 43, 2003, pp 1337-1345.

[62] S. Chung, S Park , I. Lee , H. Jeong , D. Cho, "Replication techniques for a metal microcomponent having real 3D shape by microcasting process", Microsystem Technology, 11 ,2005, pp 424-428.

[63] S. Chung, Y. Im , H. Kim, S. Park , H. Jeong, "Evaluation for micro scale structure fabricated using epoxy-aluminum particle composite and its application", J. Matererial Processing Technology, 160, 2005, pp 168-173.

[64] N.L Jessamine, P. Cheolmin, G.M Whitesides, "Solvent Compatibility of Poly(dimethylsiloxane)-Based Microfluidic Devices", Anal. Chem., 75, 2003, pp 6544-6554.

[65] R. Knitter, W. Bauer, D. GÖhring, P. Risthaus, "RP process chain for ceramic microcomponents", Rapid Prototyping 8, 2002, pp 76-82.

[66] M. Heckele, W. Bacher, K.D. MÜller "Hot embossing - The molding technique for plastic microstructures" Microsystem Technologies 4, 1998, pp 122-124

[67] Guerin, L. J., SU8 homepage., http://www.geocities.com/guerinlj/

[68] Lorenz, H., Despont, M., Vettiger, P., and Renaud, P. "Fabrication of photoplastic high aspect ratio microparts and micromolds using SU-8 UV resist". Microsystem. Technologies, Vol 4, Issue 3,1998, pp 143–146.

[69] Microchem website. http://www.microchem.com/products/pdf/SU8 2-25.pdf

[70] Teh, W. H., Du¨rig, U., Salis, G., Harbers, R.,Drechsler, U., and Mahrt, R. F. et al."SU-8 for real three-dimensional subdiffraction-limit two-photon microfabrication", Applied. Physics. Letters, Vol 84, Issue 20, 2004, pp 4095–4097.

[71] Teh, W. H., Du¨rig, U., Drechsler, U., Smith, C. G., and Gu¨ntherodt, H.-J. "Effect of low numerical-aperture femtosecond two-photon absorption on (SU-8) resist for ultrahigh-aspect ratio microsterolithography". J. Appl. Phys., 97, 2005, pp 054907 (on line).

[72] Van Kan, J. A., Sanchez, J. L., Xu, B., Osipowicz, T., and Watt, F. "Micromachining using focused high energy ion beams: deep ion beam lithography", Nuclear Instrument and Meth. in Phys. Res. B, 148, 1999, pp1085–1089.

[73] Hong, G., Holmes, A. S., and Heaton, M. E. "SU8 resist plasma etching and its optimization. DTIP 2003", Mandelieu – La Napoule, France, 5–7 May 2003, pp. 268–271.

[74] Dentinger, P. M., Miles Clift, W., and Goods, S. H. "Removal of SU-8 photoresist for thick film application." Microelectronic Engineering, 61–62, 2002, pp 993–1000.

[75] Grégoire Genolet **"**New photoplastic fabrication techniques and devices based on high aspect ratio photoresist" PhD thesis**,** Lausanne, EPFL 2001.

[76] A. del. Campo and C.Greiner "SU-8: a photoresist for high aspect-ratio and 3D submicron lithography" J.Micromech. Microeng, 17, 2007 pp R81.

[77] Z. Ling, K. Lian "SU-8 3D microoptic components fabricate by inclined UV lithography in water" Microsyst Technolo 13, 2007, pp 245

[78] Biao Li, Aurelien Gueit and Andre Sharon "Thickness management in three-dimensional laser manufacturing of suspended structures in a single SU-8 layer", Rev Sci instruments 77, 2006, pp 065103.

[79] Peng Jin, Kyle Jiang and Nianjun Sun "Ultrathick SU-8 fabrication for microreciprocating engines", Microstructures J. Microlith., Microfab., Microsyst., Vol. 3 No. 4, October 2004 pp 571

[80] J Zhang, KL Tan, GD Hong et al "Polymerization optimization of SU-8 photoresist and its applications in microfluidic systems and MEMS" J.Micromech Microeng 11, 2001, pp 20.

[81] K Jiang M J Lancaster et al "SU-8 Ka-band filter and its microfabrication" J.Micromech Microeng, Vol 15, 2005 pp 1522.

[82] John D.Williams, Wanjun Wang "Study on the postbaking process and the effects on UV lithography of high aspect ratio SU-8 microstructures", J. Microlith., Microfab., Microsyst., Vol. 3 No. 4, Oct 2004, pp 563.

[83] Ronald A.Lawes "Manufacturing tolerances for UV LIGA using SU-8 resist" J.Micromech Microeng Vol 15, 2005, pp 2198

[84] M. Despont, H. Lorenz, N.Fahrni, J. Brugger. P. Renaud, and P. Vettiger, "High aspect ratio ultrathick, negative-tone near-UV photoresist for MEMS applications," MEMS'97, IEEE, Nagoya, 1997, pp. 518-522.

[85] K. Lee, N. LaBianca, S. Rishton, and S. Zohlgharnain, "Micromachining applications for a high resolution ultra-thick photoresist," J. Vac. Scien. Technol. B, 13 , 1995, pp. 3012-3016.

[86] Man Hee Han, Woon Seob Lee, Sung Keun Lee, Seung S Lee, "3D micro-fabrication with rotated/inclined UV lithography", Sensors and Actuators A, Volume 111, Issue 1, March 2004, pp 14-20

[87] Che-Hsin Lin, Gwo-Bin Lee, Bao-Wen Chang and Guan-Liang Chang, "A new fabrication process for ultra-thick microfluidic microstructures utilizing SU-8 photoresist", Journal of Micromechanics and Microengineering, 12, 2002, pp 590-597.

[88] P.M. Dentinger et al, "High aspect ratio patterning with a proximity ultraviolet source", Microelectronic Engineering, 61-62, 2002, pp 1001-1007.

[89] Alvaro Mata, Aaron J Fleischnman and Shuvo Roy "Fabrication of mulit-layer SU-8 microstructures", Journal of Micromechanics and Microengineering Vol 16, 2006, pp 276

[90] P Abgrall et al. "A novel fabrication method of flexible andmonolithic 3D microfluidic structures using lamination of SU-8 films", J. Micromech. Microeng. 16, 2006, pp 113–121.

[91] J.B Yoon et al. "Multilevel microstructure fabrication using single-step 3D Photolithography and single-step electroplating" SPIE Vol. 3512 · 0277-786X/98/ 358-366

[92] S. Jiguet, A. Bertsch, H. Hofmann, P. Renaud, "Conductive SU8 Photoresist for Microfabrication**",** Advanced Functional Materials, Vol 15, Issue 9, 2005, pp 1511.

[93] Sébastien Jiguet, Arnaud Bertsch, Moshe Judelewicz, Heinrich Hofmann and Philippe Renaud, "SU-8 nanocomposite photoresist with low stress properties for microfabrication applications", Microelectronic Engineering, Vol. 83, 2006, pp 1966-1979.

[94] Gersteltec Engineering Solutions website http://www.gersteltec.ch/

[95] Richard De La Rue and Chris Smith "On the threshold of success" Nature, Vol 408, 7 Dec 2000, pp 653.

[96] Alfred Forchel "Switching light with light" Nature Materials, Vol 2, Jan 2003, pp 13

[97] Martin Maldovan and Edwin L. Thomas,"Diamond-structured photonic crystals", Natural Materials , Vol 3, Issue 9, Sep 2004, pp 593.

[98] David J. Norris, "Photonic crystals : A view of the future", Nature Materials, Vol 6, Issue 3, March 2007, pp 177.

[99] Markus Deubel, Georg Von Freymann et al "Direct laser writing of three-dimensional photonic-crystal templates for telecommunications" Nature Materials, Vol 3, July 2004, pp 444.

[100] Schneider A, Yang T. H. J, Reuben R. I, Stevens R, Huq S. E, Mcneill S. A., "Microstereolithography for microdevice packaging in biomedical applications - : A urology catheter for minimally invasive endoscopy", Proc. 2004 European micro and nano systems. Conference, Noisy le Grand , France, pp. 289-292.

[101] Publication: Advances in R&D for the Commercialization of Small Fuel Cells http://www.knowledgefoundation.com/biomemsbook.html

[102] TWI World Centre for Material Joining Technology website http://www.twi.co.uk/j32k/protected/band_3/ksdwt001.html

[103] Lambda Physik (2000) Industrial Report. Standardized Characterization of Excimer Laser Radiation April:11

[104] Tee Koon Heng "Dimensional metrology in microcomponents", BEng Thesis, National University of Singapore, 2005/6.

[105] Glen J. Kuban, "Making Silicone Rubber Molds © 1991-2004", retrieved from World Wide Web, http://paleo.cc/casting/silsum.htm

[106] Jim Leonard, "Silicone Molds for Urethane Castings, POLYJET finishing guide – Silicone Rubber Molding", retrieved from World Wide Web, http://www.stratasys.com/pdfs/EDEN_silicone_molding.pdf

[107] MCP-HEK Tooling, "Operating manual for type MCP 5/01 Vacuum Casting Machine", MCP-HEK Tooling Gmbh, Germany, 2005

[108] S.B.Ippolito, B.B.Goldberg and M.S.Ünlü, "Theoretical analysis of numerical aperture increasing lens microscopy", Journal Applied Physics, 97, 2005, pp 053105.

[109] S.B.Ippolito, B.B.Goldberg and M.S.Ünlü, "High spatial resolution subsurface microscopy", Applied Physics Letters, Vol 78, No. 26, 2001, pp 4071.

[110] US Patent 6,6687,058 B1 "Numnerical Aperture increasing Lens (NAILS) techniques for high resolution sub-surface imaging".

Publications

Journals

[1] S C H Thian , Y X Tang, J Y H Fuh, Y S Wong, L Lu and H T Loh, "Micro-rapid-prototyping via multi-layered photo-lithography". International Journal of Advanced Manufacturing Technology, 29, no. 9-10 (2006): 1026-1032. (United Kingdom).

[2] S Thian, Y Tang, J Y H Fuh, Y S Wong, H T Loh, L Lu, and D Z S Tee, "Formation of micromoulds via UV lithography of SU8 photoresist and nickel electrodeposition", Proc. IMechE Vol. 220 Part B: J. Engineering Manufacture, 2006, pp 329.

[3] S C H Thian, Y X Tang, Wee Kwang Tan, J Y H Fuh, Y S Wong, H T Loh and L Lu, "Manufacture of Micromould and Microparts by Vacuum Casting". International Journal of Advanced Manufacturing Technology, (2007). (United Kingdom).

[4] Tang, Y X, W. K. Tan, J Y H Fuh, H T Loh, Y S Wong, S C H Thian and L Lu, "Micro-mould fabrication for a micro-gear via Vacuum casting". Journal of Materials Processing Technology, 192-193, no. Special Issue (2007): 334-339. (Netherlands).

Conference Paper

[1] S C H Thian, Y X Tang, J Y H Fuh, Y S Wong, L Lu and H T Loh, "Three-dimensional microfabrication by photolithography and electroforming". Proceedings of the ICMA 2004, ed. Shao X Y and Deng C (2004): 795-802. PEP, UK: PEP. (International Conference on Manufacturing Automation, ICMA 2004, 26 - 29 Oct 2004, Lake View Garden Hotel, Wuhan, China

[2] Thian, S C H, J Y H Fuh, Y X Tang, Y S Wong, H T Loh and L Lu, "Creating microstructure using rapid prototyping with 3D lithography". Proceedings of ICMM (2006). Kuala Lumpur: UTM. (International Conference Manufacturing and Materials (ICMM), 14 - 15 Mar 2006, Kuala Lumpur, Malaysia)

[3] S C H Thian, W Feng, K H Tee, Y S Wong, J Y H Fuh, H T Loh, Y X Tang and L Lu, "Dimensional measurement of 3D microstructure based on white light interferometer". Proceedings of The 4th International Symposium on Instrumentation Science and Technology (2006): 580-590. Harbin: HIT. (The 4th International Symposium on Instrumentation Science and Technology, 8 - 12 Aug 2006, Harbin, China)

[4] Y.Tang, W.K. Tan, J.Y.H. Fuh, H.T. Loh, Y.S. Wong, S.C.H. Thian, and L. Lu, “Micro mould Fabrication via Vacuum Casting.” Proceeding of 7th Asia Pacific

Conference on Material Processing, APCMP 2006, 15 – 17 Dec 2006, NUS Guild House, Singapore

[5] S C H Thian, Y X Tang, J Y H Fuh, Y S Wong, H T Loh, K H Tee, W K Tan and L Lu, "Creating of micro-parts via lithography and Vacuum casting". International Conference on Product Design and Manufacturing Systems (Chongqing University, Chongqing, Chongqi, China)

.

Appendices

Appendix A

Materials used for lithography

NOA 60 photopolymer

SU8 Photoresists

Equipments used for lithography

Lambda Physik COMPex 205 multigas (KrF) excimer laser

UV reflecting mirrors

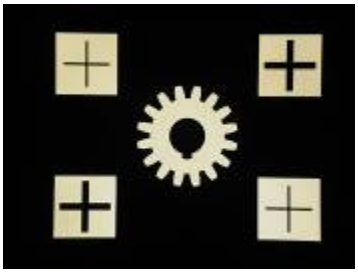

Quartz Photomask (left) and pattern on the photomask (right)

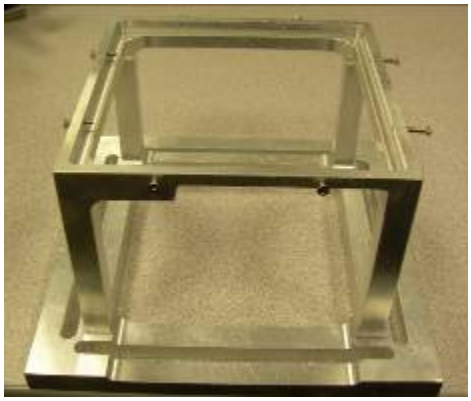

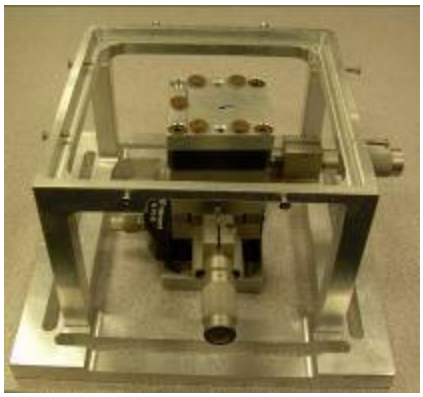

Fixture used to mount substrate and stage

Newport XY linear micropositioner and a rotation stage

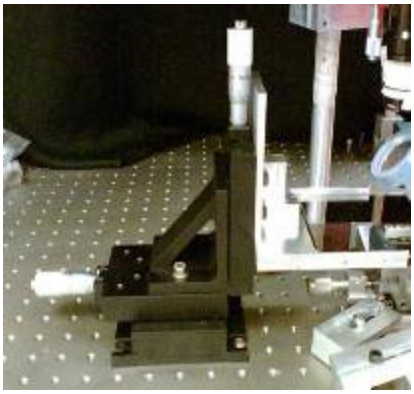

XYZ micropositioner stage

Laurell single wafer spin coater (WS-400A-6NPP)

LabTech Hotplate (LSM-2003D)

Machine vision : CCD camera

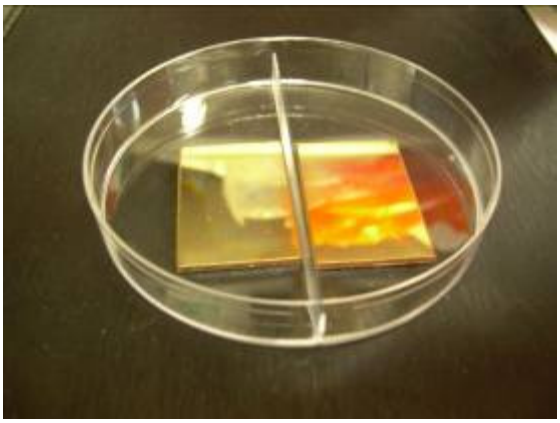

Diamond turned brass substrate kept in a petri dish

Appendix B

Materials used for micromould via vacuum casting

MCP VTV 750 Silicone Rubber. The RTV (Room Temperature Vulcanisation) silicone rubber is the mould material for all the micromoulds produced in this work.

VTV 750 silicone rubber

MCP CAT 750 Catalyst. This catalyst is used in conjunction with the VTV 750 silicone rubber to accelerate its curing during the micromould fabrication process.

CAT 750 silicone rubber catalyst

Equipment used for micromould via vacuum casting

MCP 5/01 Vacuum Casting System. The vacuum casting system generates a vacuum in its chamber by means of a mechanical pump. This allows it to execute the degassing operation during the mould fabrication and casting processes. It also controls the heating, mixing and casting of the resins under vacuum conditions.

MCP 5/01 vacuum casting system

Shel Lab 1330FX Oven. This oven provides temperature and timing controls, and is capable of controlling the curing conditions of silicone rubber and moulded parts. It

provides convection heating and an air valve at the top controls the amount of air intake.

Shel Lab 1330FX (left) and interior heating compartment (right)

Various tools for micromould fabrication

Degassing Process

The vacuum casting machine is operated during the degassing process of the micromould fabrication. The main controls on the vacuum casting machine are presented on the touch-screen panel to the right of the vacuum chamber.

Control panel during micro mould fabrication and casting

Important controls for micro mould fabrication

There are two degassing processes for micromould fabrication. Primary degassing is carried out after mixing the silicone rubber mixture in a container, while secondary degassing is carried out after pouring the mixture into the casting frame. Degassing is controlled manually, as indicated by the word “Manual” on top of the interface screen.

Description of interface buttons

Indicators/Buttons		Functions
1	'Pump'	Pressing this button will activate the pump to reduce the air pressure and achieve vacuum conditions in the vacuum chamber by pumping out air from the chamber.
2	Pressure bar	The pressure bar provides an indication of the air pressure in the vacuum chamber at any point in time. Zero bars represent vacuum conditions.
3	'Slow'/'Fast'	These two buttons determine the speed at which air is introduced into the vacuum chamber once vacuum conditions are no longer desired.
4	Timer	The timer provides an indication of the time that the degassing operation has gone through.

Degassing Procedures

1. Place the silicone rubber mixture into the vacuum chamber.

2. Activate the vacuum casting machine by turning the red 'power' knob at the side of the machine (figure C-3). Once activated, the introduction screen appears.

Red 'Power' knob on vacuum casting machine

Introduction screen (left) and main menu (right)

3. Tap the screen to skip the introduction screen and go to main menu.

4. Press the 'Manual' button on the main menu to go to the interface screen for degassing operations.

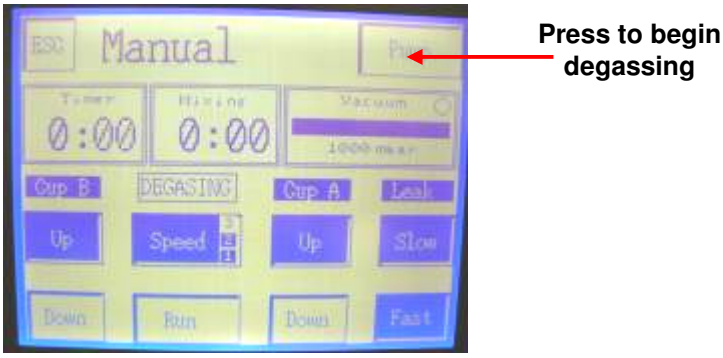

Interface screen for degassing operations

5. Press the 'Pump' button to begin the degassing process. The pressure in the vacuum chamber will begin to drop as air is pumped out of the vacuum chamber. This is indicated by the value on pressure bar which will drop from 1000 mbar (atmospheric) to 0 mbar (vacuum) as shown below.

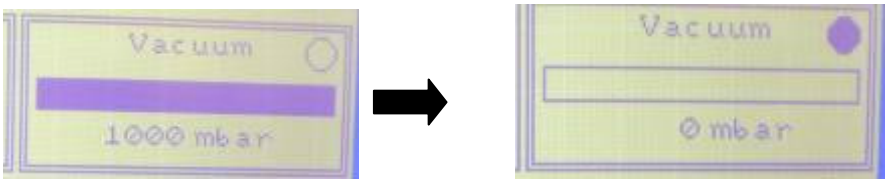

Reduction in air pressure during degassing

6. During degassing, the level of the silicone rubber mixture will rise due to the expansion of air in the mixture itself. Should the level of the silicone rubber mixture reach the top of the container or casting frame, press the 'Fast' button to let air leak into the vacuum chamber to reduce the level of the silicone rubber mixture in the container or casting frame. Once the level has dropped substantially, proceed with degassing by pressing the 'Fast' button again.
7. After degassing is complete, press the 'Pump' button to stop degassing and the 'Slow' button to reintroduce air into the vacuum chamber. The silicone rubber mixture can be removed from the vacuum chamber and placed in the oven after atmospheric pressure (1000 mbar) is achieved in the chamber. This is indicated by the pressure bar on the interface screen as shown below.

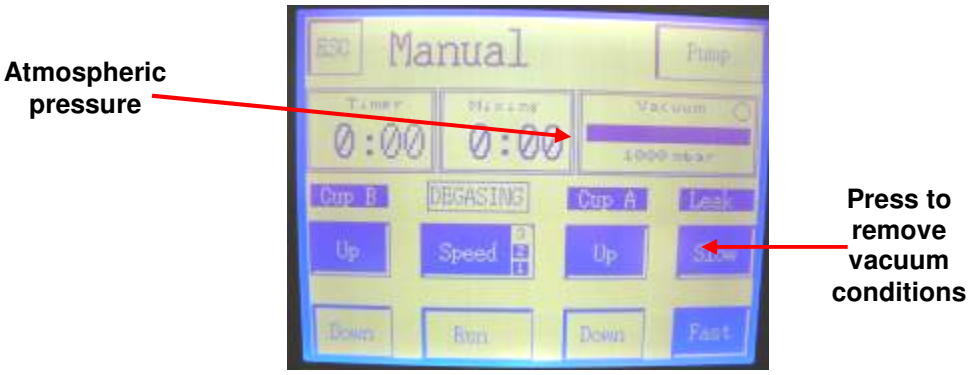

Removing vacuum conditions after completing degassing

Appendix C

(from www.photronics.com)

HOW PHOTOMASKS ARE MADE

CIRCUIT DESIGN:

The customer designs the circuit and digitizes the information. The customer then sends us the digitized data containing the design for each layer. The data can be sent on a floppy disk, magnetic tape, cassette or via modem.

DATA PREPARATION:

Photronics takes the customer's data and formats it for the write (lithography) tools or systems. This includes **fracturing** the data, sizing the data if needed, rotating the data if needed, adding fiducials and internal reference marks, and making a **jobdeck** (instructions for the placement of all the different patterns on the mask).

Fracturing the data means translating the customer data into a language the write tool can understand. The write system uses rectangles and trapezoids - so the customer data is divided up (fractured) into these shapes.

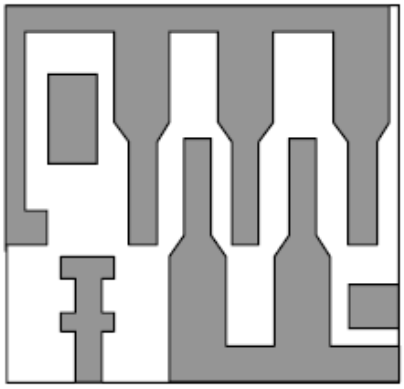

CUSTOMER DATA

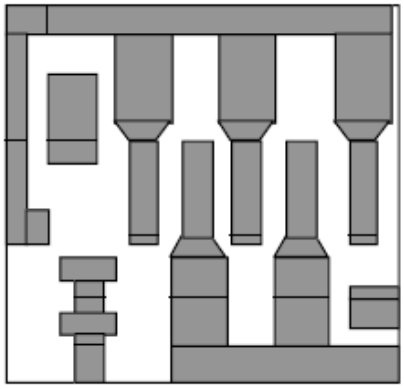

FRACTURED DATA

The jobdeck with the fractured data is put on a magnetic tape and sent to the write area or pulled directly to the machines using network software.

MATERIAL USED TO MAKE PHOTOMASKS:

There are four types of material used to make photomasks; quartz (the most commonly used and most expensive), LE, soda lime, and white crown. The mask sizes can range from 3 inches square to 7 inches square and 7.25 inches round. The thickness of the masks ranges from 60 mils to 250 mils. Currently the most common sizes of masks used are 5 inches square 90 mils thick and 6 inches square 250 mils thick.

The quartz or glass (or **substrate**) has a layer of chrome on one side. The chrome is covered with an **AR** (anti-reflective) coating and a photosensitive **resist**. The substrate with chrome, AR, and resist is known as a **blank.**

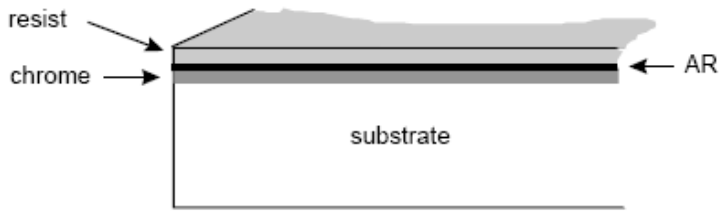

BLANK

LITHOGRAPHY:

Lithography is the process of writing the circuit design (geometry) onto the mask. The lithography or write equipment (E-beam or Core) writes the geometry onto the plate by exposing the resist with an electron beam or laser. This exposure changes the molecular composition of the resist. During the **developing** process any resist that has been exposed will be removed.

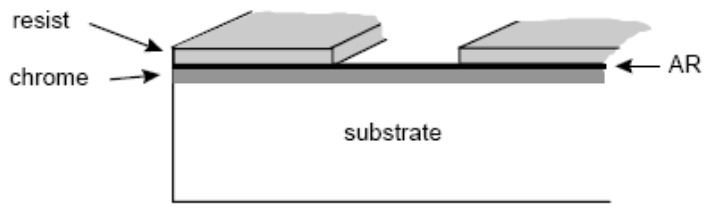

AFTER EXPOSURE AND DEVELOP

The mask is now **etched**. Etching removes the chrome and AR wherever the resist has been removed.

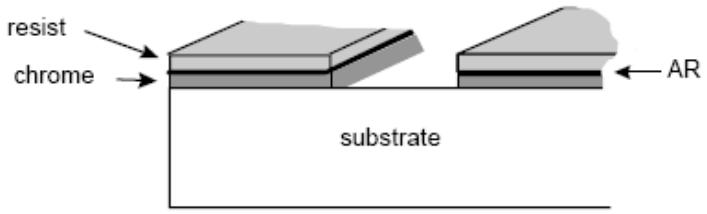

AFTER ETCH

Strip, the final step in making a photomask, removes all the resist from the mask.

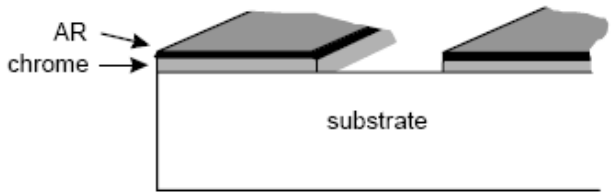

RESIST REMOVED

Note: Areas where the chrome has been removed are referred to as **clear** or **glass.** Areas where the chrome and AR remain are referred to as **chrome**, **dark** or **opaque**.

Appendix D

NOA 60 and SL5510 photopolymer information

Typical Properties of NOA 60	
Solids	100%
Viscosity at 25° C	300 cps
Refractive Index of Cured Polymer	1.56
Elongation at Failure	35%
Modulus of Elasticity (psi)	135,000
Tensile Strength (psi)	2,800
Hardness - Shore D	81
Water Absorption	0.15%

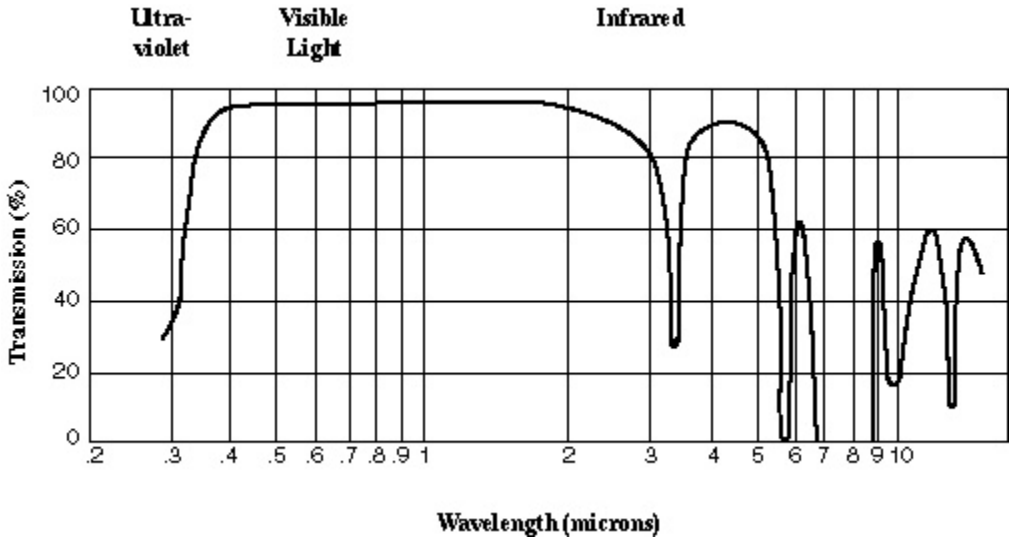

NOA 60 transmission graph

Stereolithography Materials

SL DIRECT

for use on

RenShape™ SL 5510

SLA® 350/3500/5000 system

Highest Accuracy Stereolithography Material

- Ultimate accuracy
- Excellent sidewall quality
- Humidity resistant
- Low viscosity
- Ideal for master patterns
- Ideal for QuickCast™ applications

Liquid Material

MEASUREMENT	CONDITION	VALUE
Appearance		Clear Amber
Density	@ 25°C (77°F)	1.13 g/cm³
Viscosity	@ 28°C (82°F)	230 cps
Viscosity	@ 30°C (86°F)	180 cps
Penetration depth (Dp)		4.1 mils (4.3 mils on SLA 5000 system)
Critical exposure (Ec)		11.4 mJ/cm² (11.2 mJ/cm² SLA 5000 system)
Part building layer thickness*		0.05 mm (0.002 in) 0.10 mm (0.004 in) 0.15 mm (0.006 in)

*Dependent upon part geometry and build parameters.

Post-Cured Material

MEASUREMENT	TEST METHOD	VALUE	VALUE
		90-minute UV post-cure	90-minute UV + 2 hours @ 80° thermal post-cure
Hardness, Shore D	ASTM D 2240	86	
Flexural modulus	ASTM D 790	3,054 MPa (443 KSI)	
Flexural strength	ASTM D 790	99 MPa (14,400 PSI)	
Tensile modulus	ASTM D 638	3,296 MPa (478 KSI)	
Tensile strength	ASTM D 638	77 MPa (11,100 PSI)	
Elongation at break	ASTM D 638	5.4%	
Impact strength, notched Izod	ASTM D 256	27 J/m (0.5 ft - lbs/in)	
Heat deflection temperature	ASTM D 648 @ 66 PSI @ 264 PSI	62°C (144°F) 53°C (127°F)	87°C (189°F) 76°C (169°F)
Glass transition, Tg	DMA, E" peak	68°C (154°F)	
Coefficient of thermal expansion	TMA (T<Tg) TMA (T>Tg)	84 x 10^{-6}/°C 182 x 10^{-6}/°C	79 x 10^{-6}/°C 184 x 10^{-6}/°C
Thermal conductivity		0.181 W/m °K 4.33 x 10^{-4} cal/sec cm °C	
Density		1.23 g/cm³	

Protected by one or more of the following patents: US 5,476,748; US 6,100,007; US 6,136,497; US 5,972,563

For SL Technical Support: Tel: 866-288-3554 (Toll Free), Fax: 517-324-1416. Email: slmaterials@vantico.com

www.renshape.com

Vantico A&T US, Inc. 4917 Dawn Ave, E. Lansing, MI 48823 USA Tel: 800-285-4784 Fax: 517-351-6255

RenShape® solutions vantico

Appendix E

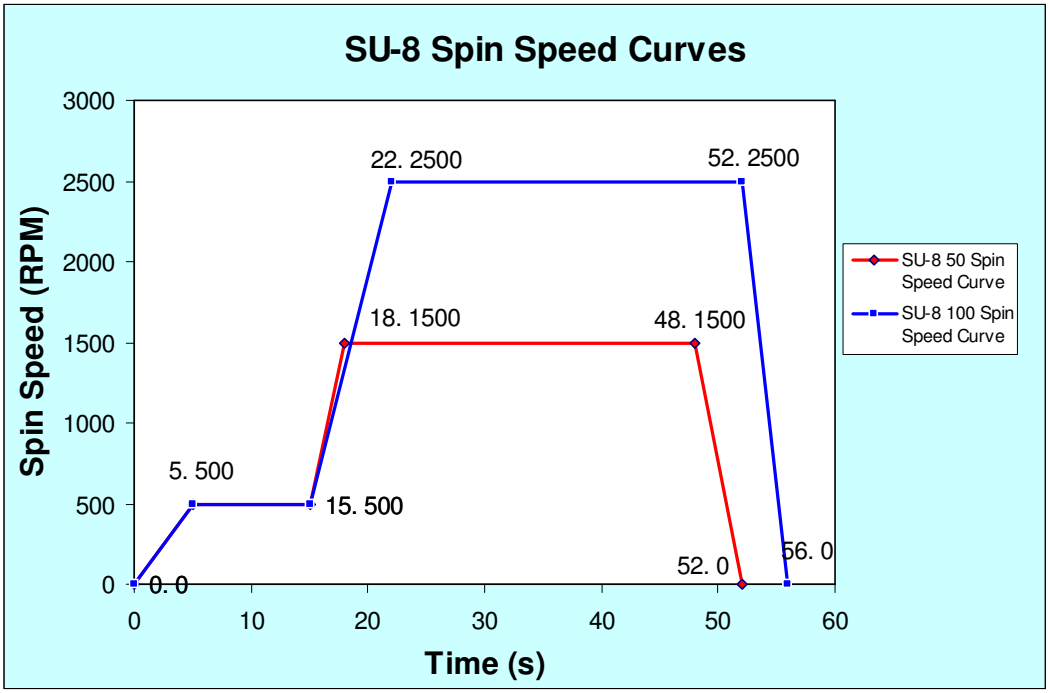
SU-8 Spin Speed Curves
Spin Speed (RPM)
Time (s)
3000
2500
2000
1500
1000
500
0
0
10
20
30
40
50
60
22. 2500
52. 2500
18. 1500
48. 1500
5. 500
15. 500
52. 0
56. 0
0. 0
SU-8 50 Spin Speed Curve
SU-8 100 Spin Speed Curve

Appendix F

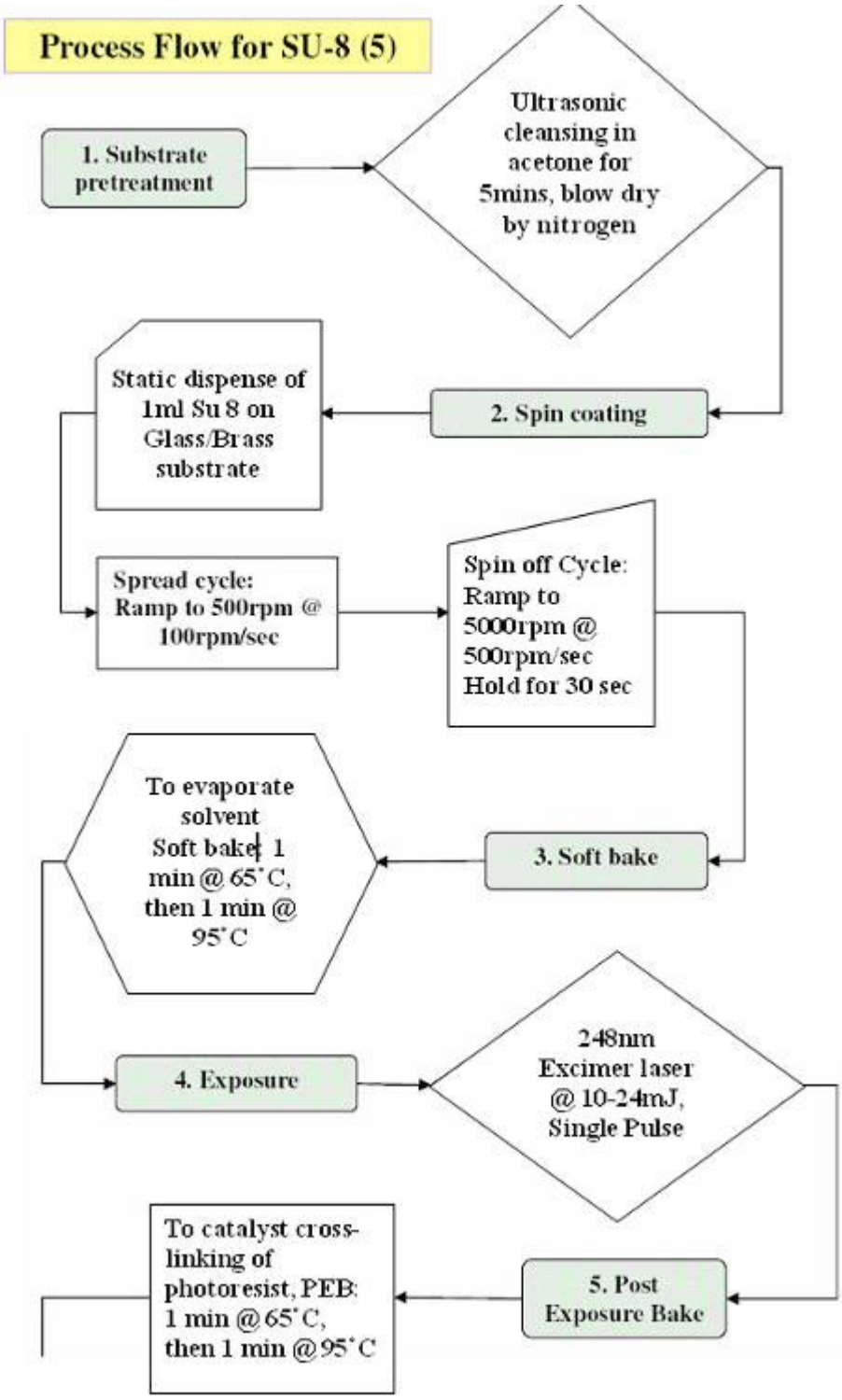
Process Flow for SU-8 (5)
1. Substrate pretreatment
Ultrasonic cleansing in acetone for 5mins, blow dry by nitrogen
2. Spin coating
Static dispense of 1ml Su 8 on Glass/Brass substrate
Spread cycle: Ramp to 500rpm @ 100rpm/sec
Spin off Cycle: Ramp to 5000rpm @ 500rpm/sec Hold for 30 sec
3. Soft bake
To evaporate solvent Soft bake 1 min @ 65°C, then 1 min @ 95°C
4. Exposure
248nm Excimer laser @ 10-24mJ, Single Pulse
5. Post Exposure Bake
To catalyst cross-linking of photoresist, PEB: 1 min @ 65°C, then 1 min @ 95°C

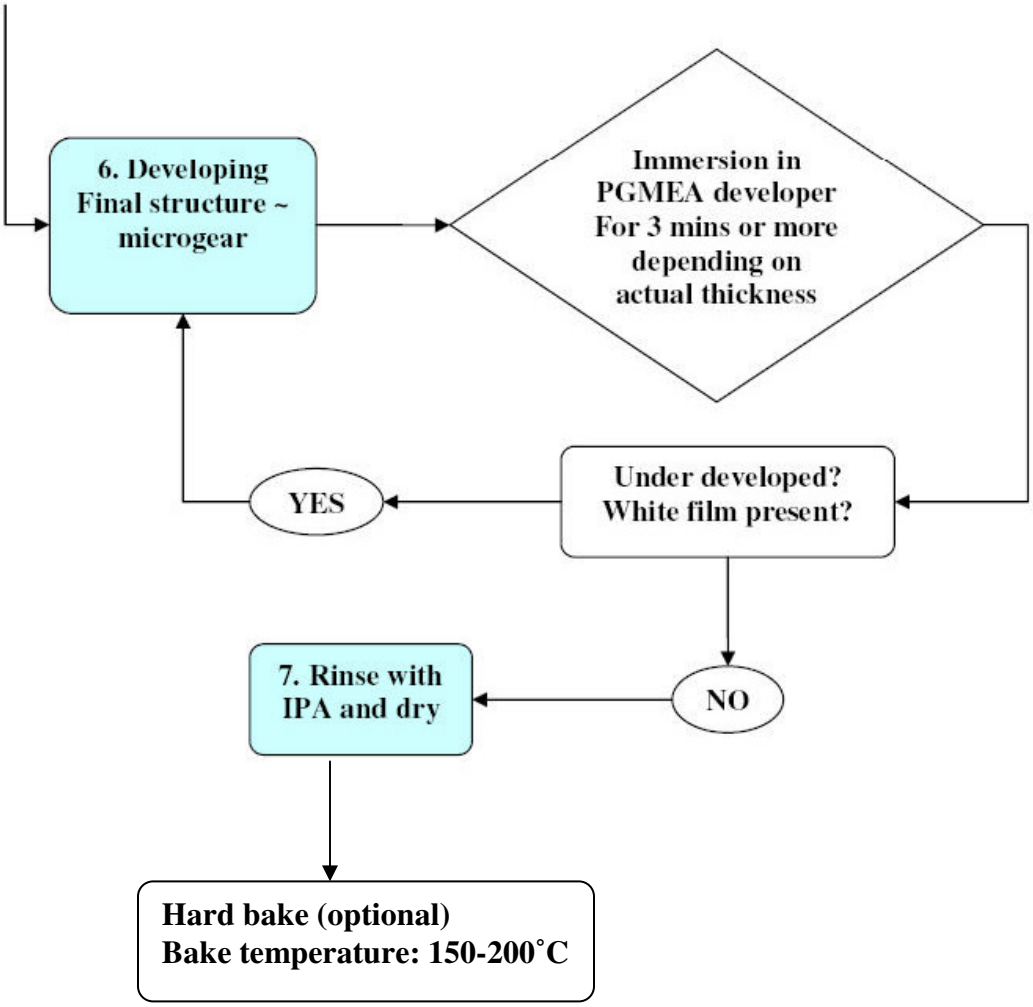
6. Developing
Final structure ~
microgear
Immersion in
PGMEA developer
For 3 mins or more
depending on
actual thickness
Under developed?
White film present?
YES
NO
7. Rinse with
IPA and dry
Hard bake (optional)
Bake temperature: 150-200˚C

Appendix G

Steps for Micromould Fabrication

Step 1 (Prepare mould-making setup)

Step 2 (Weigh the silicone rubber)

Step 3 (Add the catalyst to the silicone rubber)

Step 4 (Mix the silicone rubber and the catalyst)

Step 5 (Degas the silicone rubber mixture)

Step 6 (Pour the silicone rubber mixture into the casting frame)

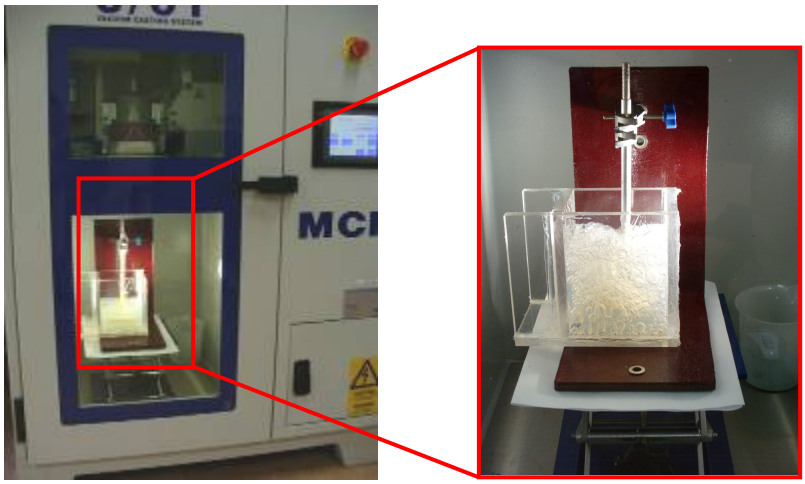

Step 7 (Degas the silicone rubber mixture in the vacuum chamber)

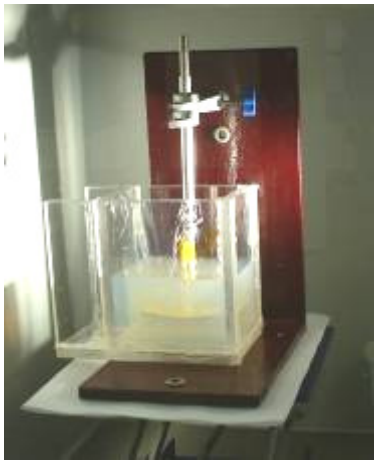

Step 8 (Reintroduce air into the vacuum chamber)

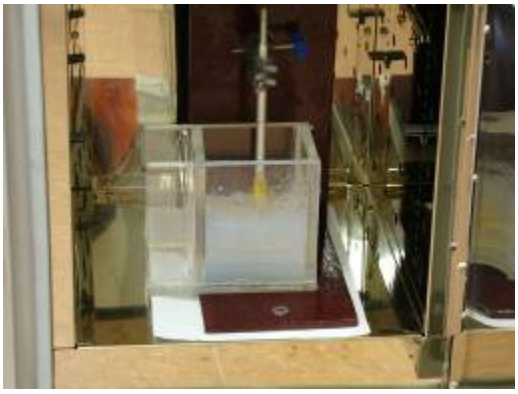

Step 9 (Cure the silicone rubber mixture in the oven)

Step 10 (Remove the mould from the casting frame)

Step 11 (Separate the mould into the core and cavity halves)

Appendix H

Diffraction Effects

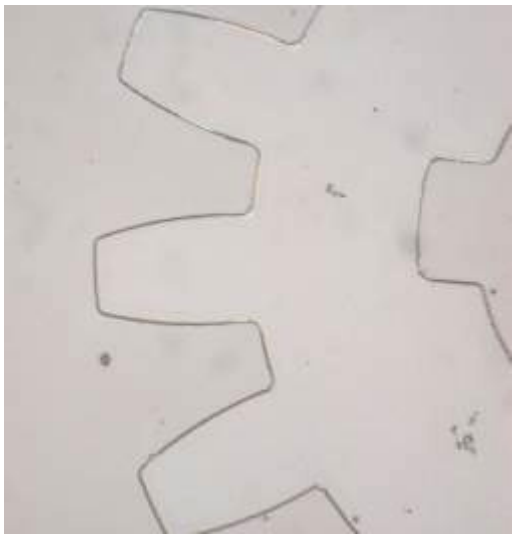

SU-8 on glass, 8mJ, 100-200 µm gap

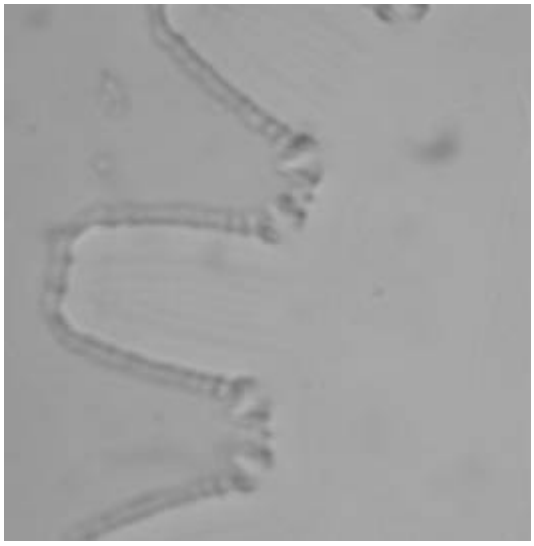

SU-8 on glass, 20 mJ, below 500 µm gap

SU-8 on glass, 20 mJ, below 1000 µm gap

SU-8 on glass, 8 mJ, and 1000-2000 µm gap

Appendix I

Basically the average gear height can be defined as the average distance of the top surface of the gear with respect to the base region immediate to the micro gear. Using the Vision 32 software designed for the Veeco white light interferometer, numerous data points are taken from the top surface of the gear and a histogram analysis is performed by categorising all the points taken into equally spaced intervals called bins.

Figure H1 shows the histogram generated for the SU8 master microgear. The vertical axis represents the number of data points contained within the equally spaced intervals (bins), while the horizontal axis represents the surface height. Using this information, the gear height can be derived by drawing a distribution curve. For the measurements done throughout the course of this research, 200 bins, the default value for the field of view of the white light interferometer are used.

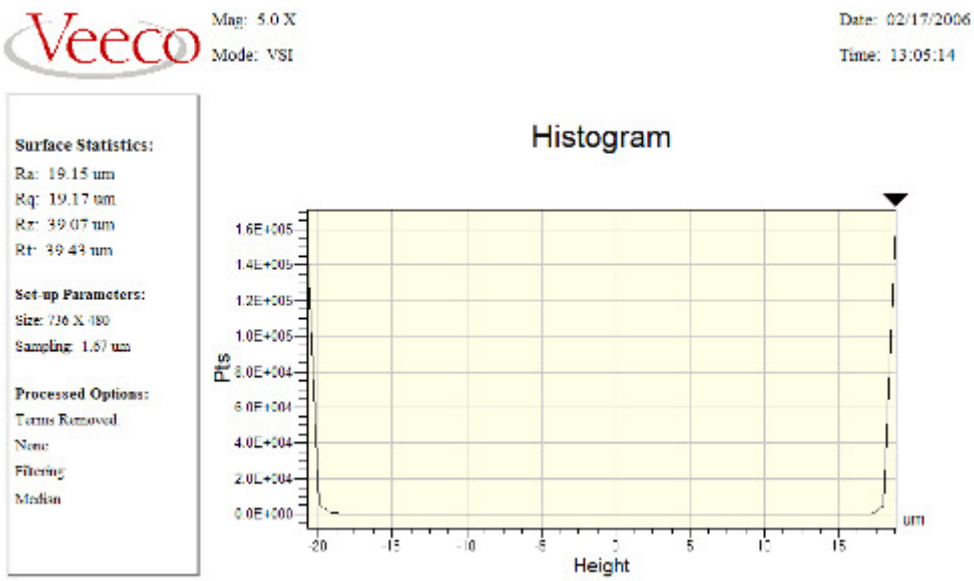

Figure H1: Histogram to characterise surface data points of SU-8 gear

In the same way, the depth of the gear cavity of a micromould can be generated by taking numerous random data points from the top surface of the region immediate to the cavity and measuring the average distance of the top surface from the bottom of the cavity surface.

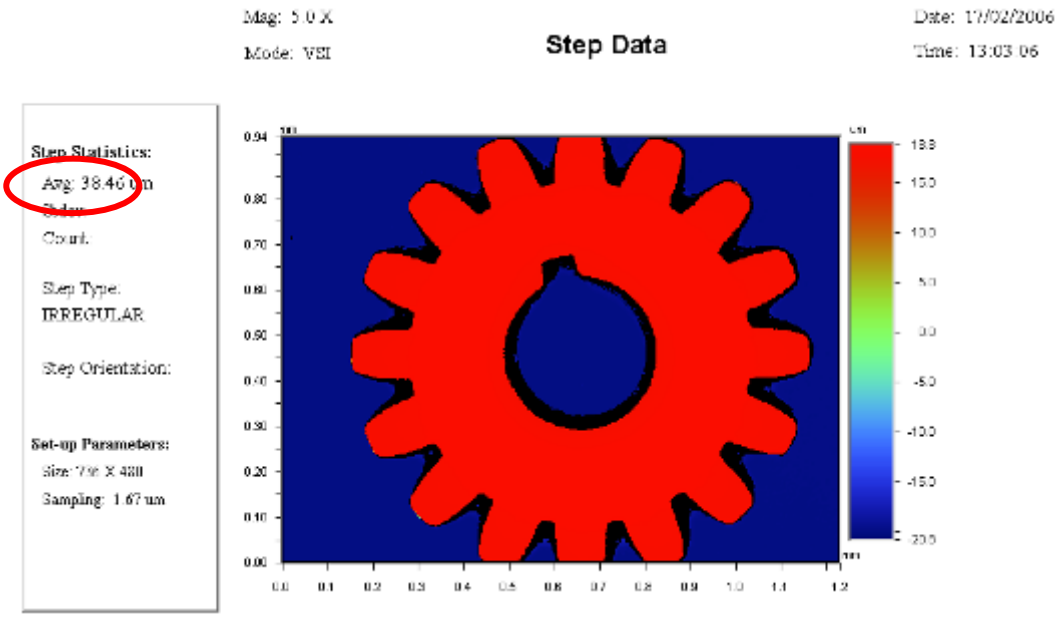

Figure H2: Measurements to determine average height of SU8 microgear

As shown in Figure H2, the circled value gives the average height of the SU8 microgear, which is 38.46µm. This represents the average distance of the red region (top surface) of the gear with respect to the blue (base) regions immediate to the gear.

Appendix J

Average dimensions of ten silicone rubber micromould cavities

Specimen	Outer Diameter (μm)	Hub Diameter (μm)	Cavity Depth (μm)
A	1005.4	326.5	38.29
B	1005.2	326.9	38.33
C	1006.0	327.6	38.32
D	1006.3	327.3	38.43
E	1005.6	326.8	38.45
F	1006.1	326.9	38.18
G	1005.6	326.2	38.21
H	1005.2	326.9	38.38
I	1005.8	326.4	38.35
J	1005.0	328.6	38.47
Average	1005.6	327.0	38.34
Std Dev	0.421	0.693	9.68×10^{-02}